(NASA-CR-174246) AN IMPROVED COMPUTER MODEL FOR PREDICTION OF AXIAL GAS TURBINE PERFORMANCE LOSSES Final Report (Tuskegee Inst.) 119 p HC A03/MF A01 CSCL 21E
N85-15724
Unclas
G3/07 13038

Final Report

AN IMPROVED COMPUTER MODEL FOR PREDICTION OF AXIAL GAS TURBINE PERFORMANCE LOSSES

By

R. M. Jenkins

August 1984

School of Engineering & Architecture
Tuskegee Institute
Tuskegee Institute, AL 36088

Prepared For

NATIONAL AERONAUTICS AND SPACE ADMINISTRATION
NASA LEWIS RESEARCH CENTER
Grant NSG 3295

Final Report

AN IMPROVED COMPUTER MODEL FOR PREDICTION OF AXIAL GAS TURBINE PERFORMANCE LOSSES

By

R. M. Jenkins

August 1984

School of Engineering & Architecture
Tuskegee Institute
Tuskegee Institute, AL 36088

Prepared For

NATIONAL AERONAUTICS AND SPACE ADMINISTRATION
NASA LEWIS RESEARCH CENTER
Grant NSG 3295

TABLE OF CONTENTS

ABSTRACT

The calculation model performs a rapid preliminary pitchline optimization of axial gas turbine annular flowpath geometry, as well as an initial estimate of blade profile shapes, given only a minimum of thermodynamic cycle requirements. No geometric parameters need be specified. The following preliminary design data are determined:

(1) the optimum flowpath geometry, within mechanical stress limits;

(2) initial estimates of cascade blade shapes;

(3) predictions of expected turbine performance.

The model uses an inverse calculation technique whereby blade profiles are generated by designing channels to yield a specified velocity distribution on the two walls. Velocity distributions are then used to calculate the cascade loss parameters. Calculated blade shapes are used primarily to determine whether the assumed velocity loadings are physically realistic. Model verification is accomplished by comparison of predicted turbine geometry and performance with an array of seven NASA single-stage axial gas turbine configurations, ranging in size from 0.6 kg/s to 63.8 kg/s mass flow and in specific work output from 153 J/g to 558 J/g at design (hot) conditions; stage loading factor ranges from 1.15 to 4.66.

LIST OF TABLES

LIST OF FIGURES

NOMENCLATURE

a_{cr} = critical sound speed, m/s

C_L = lift coefficient

D = diffusion coefficient

g = gravity constant, m/s^2

h = channel or blade height, m

Δh = rotor tip clearance gap, m

ℓ = velocity loading parameter defined by Eq. (23)

m = distance along axial direction, m

M = mean chord length in axial direction, m

p = static pressure, n/m^2

Δp = difference between blade pressure-surface static pressure and suction-surface static pressure, n/m^2

P = total or stagnation pressure, n/m^2

R = radius coordinate, measured from turbine axis of rotation, m

$\mathcal{R}$ = acceleration parameter, defined by Eq. (21)

s = blade pitch or spacing, m

t = blade thickness, m

U = rotor speed, m/s

V = velocity measured relative to non-rotating reference frame, m/s

$\mathcal{V}$ = blade loading velocity defined by Eqs. (24a-b)

W = velocity measured relative to rotating reference frame, m/s

W_f = mass flow rate, kg/s

T = total or stagnation temperature, °K

Y = loss coefficient (pressure)

Z = number of blades

α = flow angle measured with respect to absolute (non-rotating) velocities

β = flow angle measured with respect to relative (rotating) velocities

γ = ratio of gas specific heats

δ = pressure ratio referenced to standard conditions

ε = channel thickness parameter, defined by Eq. (18)

η = adiabatic efficiency

ϕ = angular coordinate

ρ = density, kg/m^3

$\mathcal{M}$ = distance along axial direction normalized by chord length M

θ = temperature ratio referenced to standard conditions

σ = cascade solidity

<u>Subscripts</u>

c = centerline

cg = clearance gap

e = cascade exit

i = cascade inlet

m = maximum

$\mathcal{M}$ = arbitrary location along axial direction

p = pressure surface

$p\ell$ = profile loss

s = suction surface

sf = secondary flow loss

std = standard conditions

tot = total

u = tangential

x = axial

<u>Superscripts</u>

' = absolute total or stagnation condition

" = relative total or stagnation condition

* = parameter normalized with respect to conditions at cascade inlet

INTRODUCTION

Axial gas turbine design can be described as a search for an optimum set of geometric parameters to satisfy certain general specifications such as work output and mass throughflow. Traditionally, the search procedure begins with computations which provide a quick estimate of optimum overall configuration for a given cycle data point. Such computations usually rely upon loss correlations that mainly depend on cascade inlet and exit conditions, without regard to specific cascade geometry. Use of such correlation models implicitly assumes that detailed blade geometry does not significantly influence flow losses, an assumption which is open to question.

The relationships between blade shape, loading, and flow losses are established in more detail later in the design procedure, a process which requires detailed knowledge of individual blade shapes. Since the overall design procedure is an iteration loop involving geometry and aerodynamic losses, however, these relationships should be established as early in the preliminary design procedure as possible. This should result in a more realistic final design in less overall time.

The present optimization technique seeks to provide an initial axial turbine stage design procedure which directly links overall stage performance and flowpath geometry with internally generated cascade loadings and blade shapes. Having such detailed geometry generated internally has a threefold advantage:

(i) excessive data preparation times are eliminated;

(ii) the loss model is provided flexibility in determining blade shapes (loadings) which optimize boundary layer (Reynolds number) effects;

(iii) relations between such factors as blade chord, blade camber-line, blade stagger, etc., and the specified velocity triangles are automatically accounted for without additional correlations.

The present design procedure is "preliminary" in that calculations are performed only for an average streamsheet surface (pitchline) location within the turbine stage. Pitchline radius may vary (linearly) within a blade row; however, radial velocity components are neglected and such variation should be small. The most basic assumption of the analysis is that velocity loadings on the blading are known. These loadings are used to calculate blade profile shapes and profile (friction) losses. The blade shapes are, in turn, examined to determine whether the assumed loading is physically realistic.

CALCULATION OF CHANNEL (BLADE) SHAPES

Cascade channel shapes (blade profiles) are generated using a simplified technique to provide solutions to the so-called indirect problem: that of the design of a channel to yield a specified velocity distribution on the two walls. Adjacent walls then become the suction and pressure surfaces, respectively, of the individual blades. The technique is similar to that utilized by J. D. Stanitz[1].

For given thermodynamic cycle requirements, wheel speed, and adiabatic efficiency, stage velocity triangles can easily be obtained along some representative pitch-line radius. If the channel velocity distribution is also known, the channel (blade) shape is generated as follows:

<u>Continuity</u>

$$W_f = \left(\frac{\rho V}{\rho' a'_{cr}}\right)_i \cos \alpha_i (2\pi R_i h_i) \frac{\delta_i}{\sqrt{\theta_i}} (\rho' a'_{cr})_{std} \tag{1}$$

<u>Moment of Momentum</u>

$$\frac{W_f}{gz} \frac{d}{dm} (RV_u) dm = (\Delta p) hR dm \tag{2}$$

Integration of Eq. (2) along the entire axial chord length of the blade results in the overall change in tangential (swirl) velocity across the cascade:

$$(RV_u)_e - (RV_u)_i = \frac{gz}{W_f} h_i R_i M \delta_i P_{std} \int_0^1 h^* R^* \frac{\Delta p}{P'_i} \, d\mathcal{M} \tag{3}$$

Note that "axial" chord is actually the vector sum of axial and radial displacements through the cascade, since the pitch-line radius may vary. Making use of the continuity equation (1), and the cascade solidity, σ, defined as the ratio of axial chord to blade spacing, Eq. (3) can be rearranged as

$$\sigma = \frac{\left(\frac{\rho V}{\rho' a'_{cr}}\right)_i \left(\frac{2\gamma}{\gamma + 1}\right) \cos \alpha_i \left[R^*_e \left(\frac{V_u}{a'_{cr}}\right)_e \sqrt{\frac{T'_e}{T'_i}} - \left(\frac{V_u}{a'_{cr}}\right)_i\right]}{\int_0^1 h^* R^* \frac{\Delta p}{P'_i} \, d\,m} \tag{4}$$

If the integration of Eq. (2) is carried out only to some arbitrary point m within the blade row, the result is

$$R^*_m \left(\frac{V_u}{a'_{cr}}\right)_m \sqrt{\frac{T'_m}{T'_i}} - \left(\frac{V_u}{a'_{cr}}\right)_i = \frac{\left(\frac{\gamma + 1}{2\gamma}\right)\sigma}{\left(\frac{\rho V}{\rho' a'_{cr}}\right)_i \cos \alpha_i} \int_0^m h^* R^* \frac{\Delta p}{P'_i} \, d\,m \tag{5}$$

from which the local absolute tangential velocity at that point, $(V_u/a'_{cr})_m$ can be obtained. A more useful relation is the tangential velocity distribution relative to a blade row moving at some wheel speed $(U/a'_{cr})_m$, defined by

$$\left(\frac{W_u}{a'_{cr}}\right)_m = \left(\frac{V_u}{a'_{cr}}\right)_m - \left(\frac{U}{a'_{cr}}\right)_m \tag{6}$$

where

$$\left(\frac{U}{a'_{cr}}\right)_m = \left(\frac{U}{a'_{cr}}\right)_i R^*_m \sqrt{\frac{T'_i}{T'_m}} \tag{7}$$

The term a'_{cr} is the local critical velocity defined with respect to absolute total temperature. Now, since critical velocity can also be defined with respect to relative total temperature, Eq. (6) can be rewritten as

$$\left(\frac{W_u}{a''_{cr}}\right)_{\mathcal{M}} = \left(\frac{W_u}{a'_{cr}}\right)_{\mathcal{M}} \sqrt{\frac{T'_{\mathcal{M}}}{T''_{\mathcal{M}}}} \tag{8}$$

or upon combining Eqs. (5), (6), (7), and (8),

$$\left(\frac{W_u}{a''_{cr}}\right)_{\mathcal{M}} = \sqrt{\frac{T'_{\mathcal{M}}}{T''_{\mathcal{M}}}} \left\{ \frac{1}{R^*_{\mathcal{M}} \sqrt{\frac{T'_{\mathcal{M}}}{T'_i}}} \left[\left(\frac{V_u}{a'_{cr}}\right)_i + \frac{\left(\frac{\gamma + 1}{2\gamma}\right)\sigma}{\left(\frac{\rho V}{\rho' a'_{cr}}\right)_i \cos \alpha_i} \int_0^{\mathcal{M}} h^* R^* \frac{\Delta p}{P'_i} \, d\mathcal{M} \right] - \left(\frac{U}{a'_{cr}}\right)_i R^*_{\mathcal{M}} \sqrt{\frac{T'_i}{T'_{\mathcal{M}}}} \right\} \tag{9}$$

Eq. (9) specifies the relative tangential velocity component at any location $\mathcal{M}$ within the cascade.

GENERATION OF BLADE CAMBERLINE DISTRIBUTION

At this point in the computation it is possible to analytically define a mean camberline distribution for the cascade. Let $W/a''_{cr,p}$ and $W/a''_{cr,s}$ represent the relative critical velocity ratios along the pressure and suction surfaces of the blade, respectively; note that both quantities are known since the velocity loading is presumed to be known. It is desired to calculate the average flow direction, $\beta_{\mathcal{M}}$, for any location $\mathcal{M}$ within the blade passage. In order to do this, an additional assumption is required. It might be assumed that the channel mean velocity is the arithmetic mean of the suction surface and the pressure surface velocities,

$$(W/a''_{cr})_{m} = 1/2[(W/a''_{cr})_p + (W/a''_{cr})_s]_{m} \tag{10}$$

in which case

$$\beta_{m} = \sin^{-1}\left\{\frac{W_u/a''_{cr}}{W/a''_{cr}}\right\}_{m} \tag{11}$$

On the other hand, one might assume, say, a linear variation of axial critical velocity ratio, W_x/a''_{cr}, through the blade passage, in which case

$$\beta_{m} = \tan^{-1}\left\{\frac{W_u/a''_{cr}}{W_x/a''_{cr}}\right\} \tag{12}$$

and $(W/a''_{cr})_{m}$ is approximated by

$$(W/a''_{cr})_{m} = \left\{\frac{W_x/a''_{cr}}{\cos\ \beta}\right\}_{m} \tag{13}$$

Even more flexibility can be provided by modifying the linear variation by a variable increment; the increment is zero at the cascade inlet and exit, and some specified maximum value at a given location within the cascade. The increment must then satisfy four boundary conditions and is defined by a third order polynomial. Experience has shown that either the linear or modified linear axial velocity distributions provide the most realistic blade shapes.

If the mean camberline is described by the cylindrical coordinates R, m, and ϕ, then the camberline is generated by the expression

$$\frac{d}{dm}(R\phi) = R\frac{d\phi}{dm} + \phi\frac{dR}{dm} = \tan\beta + \phi\frac{dR}{dm} \tag{14}$$

Equation (14) must be integrated point-by-point through the cascade.

GENERATION OF LOCAL BLADE THICKNESS

For any location $\mathscr{M}$ along the cascade passage the continuity equation can be written as

$$\frac{W_f}{z} = (\rho W \cos\beta)(h \times \text{channel width}) \tag{15}$$

Define a "channel width parameter," ε, by

$$\varepsilon = \frac{\text{channel width}}{\text{blade pitch}} = \frac{\text{channel width}}{\frac{2\pi R}{z}} \tag{16}$$

Equation (15) then becomes

$$W_f = (\rho W \cos\beta)(2\pi\varepsilon h R) \tag{17}$$

for a given position $\mathscr{M}$. Combination of Eqs. (1) and (17) yields, after rearrangement,

$$\varepsilon_{\mathscr{M}} = \frac{\left(\frac{\rho V}{\rho' a'_{cr}}\right)_i \cos\alpha_i \left(\frac{P'}{P''}\right)_i \sqrt{\frac{T''_i}{T'_i}} \left(\frac{P''_i}{P''_{\mathscr{M}}}\right) \sqrt{\frac{T''_{\mathscr{M}}}{T''_i}}}{\left(\frac{\rho W}{\rho'' a''_{cr}}\right)_{\mathscr{M}} (h^* R^* \cos\beta)_{\mathscr{M}}} \tag{18}$$

Now local blade thickness, $t_{\mathscr{M}}$, is the difference between local blade pitch and local channel width, so that Eq. (16) can be written as

$$t_{m} = \frac{2\pi R_{m}}{z}(1 - \varepsilon_{m}) = \frac{M}{\sigma} R^{*}_{m} (1 - \varepsilon_{m}) \tag{19}$$

Local blade thickness is then distributed equally about the camberline distribution defined by Eq. (14). Specification of the blade profile is thus complete. A representative blade section generated by this procedure is shown in Figure 1.

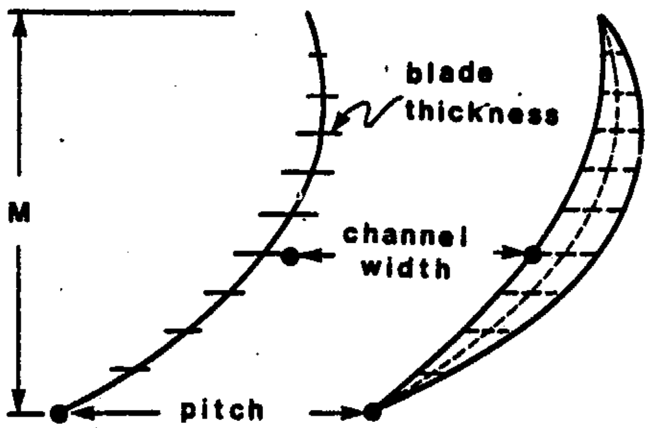

Figure 1: Representative Blade Section Generated by Inverse Method

CALCULATION OF BLADE LOADINGS

Of fundamental importance to the present optimization procedure is the selection of proper cascade blade loadings. These loadings are used to 1) calculate channel shapes (blade profiles), 2) meet required cascade solidity specifications, and 3) calculate profile (friction) losses. The loading model should be simple, yet flexible enough to accommodate a wide range of channel centerline accelerations, blade surface diffusion rates, and cascade loading requirements.

The loading model proceeds from the definition of a centerline velocity distribution, V_c, as

$$\frac{V_c}{V_e} = \frac{\mathcal{R}}{2}\left[\sin \pi(\mathcal{M} - \tfrac{1}{2}) - 1\right] + 1 \tag{20}$$

The parameters V_c and V_e represent (dimensionless) critical velocity ratios measured relative to the blade row, with V_e measured at the exit of the row. The parameter $\mathcal{R}$ is indicative of the channel centerline flow acceleration and is defined as

$$\mathcal{R} = 1 - \frac{V_i}{V_e} \tag{21}$$

where V_i is the critical velocity ratio relative to the blade row, measured at the inlet to the row. It should be noted that V_c is a fictitious parameter used only in the definition of blade loading and is not necessarily related to channel mean velocity, Eq. (13).

Suction Surface Velocity

It is assumed that the behavior of the velocity distribution on the blade suction surface is of primary importance to the overall optimization process. Although velocity diffusion occurs on both blade surfaces, the adverse effects of pressure-surface diffusion are to some degree obviated by the subsequent downstream re-acceleration of the flow along that surface; such re-acceleration does not usually occur on the suction side of the profile.

A fundamental characteristic of the suction-surface velocity distribution is deceleration of the boundary layer flow near the trailing edge of the blade row. Of interest is both the amount of such deceleration and the location along the suction surface at which such deceleration begins. If velocity "spike" effects near the leading edge of the blade are ignored, velocity diffusion on the suction surface becomes a simple question of where maximum velocity occurs and what its value is.

Following standard practice, a "diffusion coefficient" for the suction surface velocity is defined as

$$D_s = 1 - \frac{V_e}{V_m} \tag{22}$$

where V_m represents the maximum velocity occurring anywhere on the suction surface. Figure 2 illustrates each of the pertinent velocities employed in the model. As in Reference 2, the suction surface velocity is described by a simple piecewise parabolic curve fit; ℓ_m, the point of maximum velocity, is also the point where the two curve portions are matched. It has been suggested[2] that the location of ℓ_m is dependent on the value of the channel centerline flow acceleration $\mathcal{R}$ as

$$\ell_m = 0.5 + 0.3[1 - (1 - \mathcal{R})^2] \tag{23}$$

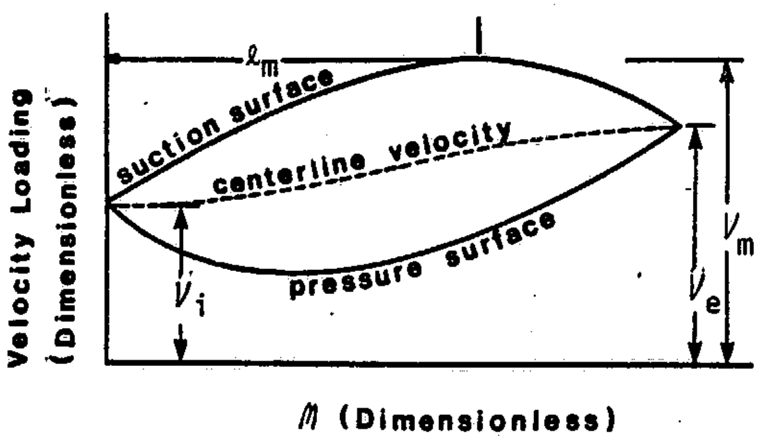

Figure 2: Blade Velocity Loading Model

Barring user input to the contrary, ℓ_m is calculated from Eq. (23). Should the user so desire, however, any value for ℓ_m can be specified.

The suction surface velocity distribution is defined by the following relations:

$$\mathcal{M} < \ell_m: \; V_s = (V_i - V_m)\left(\frac{\mathcal{M}}{\ell_m}\right)^2 - 2(V_i - V_m)\left(\frac{\mathcal{M}}{\ell_m}\right) + V_i \tag{24a}$$

$$\mathcal{M} > \ell_m: \; V_s = \frac{V_e - V_m}{(\ell_m - 1)^2}\,[\mathcal{M}^2 - 2\ell_m(\mathcal{M} - 1) - 1] + V_e \tag{24b}$$

It should be noted that it is, at least mathematically, possible to have negative values for the diffusion coefficient; in this case, $V_m < V_e$ and there is no real "maximum" velocity (other than V_e). For this situation, the piecewise curve fit degenerates to a single second-order curve of the form

$$V_s = \left[\frac{V_m - V_e}{\ell_m(\ell_m - 1)} - \frac{V_e - V_i}{\ell_m}\right]\mathcal{M}^2 + \left[(V_e - V_i)\,\frac{(\ell_m + 1)}{\ell_m} - \frac{V_m - V_e}{\ell_m(\ell_m - 1)}\right]\mathcal{M} + V_i \tag{25}$$

<u>Pressure Surface Velocity</u>

The pressure surface velocity distribution is obtained by assuming that the entire blade loading is distributed equally about the centerline velocity distribution V_c. The pressure surface distribution is then given by

$$V_p = 2V_c - V_s \tag{26}$$

where V_s is given by either Eq. (24) or Eq. (25). Though there is no mathematical constraint, negative (reverse direction) velocities are not desirable, and are not allowed by the model.

OPTIMIZATION OF THE DIFFUSION COEFFICIENT

The blade loading diagram, suction surface diffusion coefficient, and cascade solidity can be tied together through the Zweifel[3] loading coefficient. The Zweifel coefficient relates cascade solidity to flow angles at the cascade inlet and outlet, and, according to reference 3, tends to assume a certain narrow range of values for optimum cascade performance. Normal design practice utilizes Zweifel coefficients in the range of, say, 0.7 to 1.0. Thus, for specified flow angles and a given Zweifel coefficient within the "optimum" range, an optimum cascade solidity can be calculated. Now, solidity is related to the individual blade velocity loading through Eq. (4). Furthermore, for known cascade inlet and outlet conditions, the assumed velocity loading model possesses only one independent variable: the suction surface diffusion coefficient. Thus,

(1) specified thermodynamic cycle requirements establish cascade inlet and outlet conditions;

(2) these conditions, together with an input Zweifel coefficient will determine an optimum solidity;

(3) the present model then adjusts the suction surface diffusion coefficient so that the velocity loading, when integrated

in Eq. (4), yields a calculated solidity equal to the optimum solidity.

The final velocity loading is then used to calculate both blade shapes and blade profile losses.

CALCULATION OF CASCADE PERFORMANCE LOSS

Three aerothermodynamic loss mechanisms are accounted for in the present analysis: profile loss, secondary flow loss, and rotor tip clearance loss.

Profile loss is defined here as a combination of frictional effects resulting from the flow of a viscous fluid over a solid surface and the subsequent downstream mixing of the suction surface and the pressure surface boundary layers. Both losses are accounted for through use of the Stewart mixing loss theory[4], which defines them in terms of overall displacement and momentum thicknesses. Secondary flow losses are due to the annulus wall boundary layers and their interaction with blade rows. Dunham's review paper[5] presents an excellent analysis of the phenomenon. Dunham states that two separate effects must be accounted for if losses are to be properly estimated:

(1) a vortex core loss, arising from fluid, originally in the upstream wall boundary layer, being subsequently shed from the trailing edge of the cascade;

(2) a downstream wall boundary layer loss, wherein fluid originally in the mainstream is entrapped in a boundary layer developing on the annulus walls within the cascade.

Rotor clearance, or tip leakage, losses effect turbine performance in two ways:

(1) leäkage diminishes overall work extraction from the flowing gas, since some fluid at the tip is not turned, and

(2) leakage produces an underturning of the flow felt in regions other than the tip region, which further diminishes work extraction.

Profile Loss

When calculating profile boundary layer losses it is possible to utilize models of almost any complexity imaginable. Of primary importance, and of least certainty, is the location along a given blade surface of the point of transition of the boundary layer from laminar to turbulent flow, as well as the point of separation of the boundary layer from the wall. Since the present analysis is of a preliminary design (pitch-line) nature, exceedingly complex loss models are not appropriate.

In its simplest sense, the location of the boundary layer transition point is a cascade Reynolds number effect. As Reynolds number (based on cascade exit velocity and blade mean camberline length) is increased, the transition point tends to move upstream towards the leading edge of the blading. For the laminar portion of the boundary layer, the present analysis calculates loss parameters using the Truckenbrodt approximation for boundary layer growth on a wall with pressure gradient, as described, for instance, in Reference 6. For the turbulent portion, loss parameters are calculated using a simple formulation described in Reference 7. A rough estimate of transition is made using a "critical

Reynolds number" parameter, based on boundary layer displacement thickness, again described in Reference 6. Even though this procedure might be considered "too simple," it provides a way to account for Reynolds number effects on overall cascade loss, and is consistent with the fact that velocity loadings are already assumed to be known. As with any set of assumptions, the final justification lies with how well the model predicts reality. Pertinent relationships are described in Appendix B.

Secondary Flow Loss

The correlation for secondary flow loss as suggested in the conclusion of Dunham's paper[5] requires a knowledge of the boundary layer displacement thickness on the endwalls upstream of the cascade, a parameter which is not readily available, at least with any degree of confidence (especially for the rotor). Actually, the upstream boundary layer, or vortex core, loss adds to a second loss component, called the downstream loss. The present analysis assumes that the sum of these two loss components can be represented as a constant value. The specific expression used for secondary flow loss then becomes

$$Y_{sf} = 0.0138 \, \frac{M}{h} \, \frac{\cos \alpha_e}{\cos \alpha_i} \left(\frac{C_L}{s/M} \right)^2 \frac{\cos^2 \alpha_e}{\cos^3 \alpha_m} \tag{27}$$

where Y_{sf} is a pressure loss coefficient, C_L is a cascade lift coefficient (defined only in terms of inlet and outlet relative flow angles), and the value 0.0138 represents the sum of the two loss components discussed above (see Figure 9 of Reference 5). The remaining parameters are described in the Nomenclature.

Tip Leakage Loss

Though recent work such as that of Lakshminarayana[8] provides insight into the physics of the tip leakage loss mechanism, quantitative predictions of performance loss still require some correlation with experimental data. In this regard, the correlation reported in Reference 7, taken from data originally reported in Reference 9, shows promise. This correlation indicates that, for given blade reaction, the tip-clearance loss varies (approximately) linearly with clearance gap: furthermore, the loss increases for increasing blade reaction. The latter is intuitively correct, since high reactions (large pressure differences) cause more high-kinetic-energy flow to leak through the clearance gap.

The various curves given in Reference 7 can all be approximated by the single expression

$$\frac{\eta_{cg}}{\eta} = 1 - (2.755\,\mathcal{R}^2 + 0.108\,\mathcal{R} + 1.72)\,\frac{\Delta h}{h} \qquad (28)$$

where η_{cg} = efficiency with clearance

η = efficiency without clearance

h = blade height

Δh = clearance gap

and $\mathcal{R}$ is blade reaction at the tip, defined by

$$\mathcal{R} = \frac{W_e^2 - W_i^2}{W_e^2 - W_i^2 + V_i^2} \qquad (29)$$

where W, V represent relative and absolute velocities, respectively.

AERODYNAMIC OPTIMIZATION OF BLADE CHORD

Both blade profile (friction) losses and cascade secondary flow losses are dependent on blade chord. Normally, blade chord is determined from manufacturing trade-offs or prior design experience. For instance, chords below a certain minimum length cannot be made economically; chords which are too large increase overall engine length (weight), etc. While chord lengths can be input to the present model, a theoretically optimum chord can be calculated simply from a consideration of the profile and secondary flow loss mechanisms.

From the Stewert analysis[4] a cascade absolute total pressure loss P_e'/P_i' can be determined. A "profile loss coefficient," $Y_{p\ell}$, can be defined as

$$Y_{p\ell} = \frac{1 - P_e'/P_i'}{P_e'/P_i'(1 - p_e/P_e')} \tag{30}$$

where p_e is the static pressure at the cascade exit. A "total loss coefficient" Y_{tot} can be formed by

$$Y_{tot} = Y_{p\ell} + Y_{sf} \tag{31}$$

where Y_{sf} is defined by Eq. (27). Normally, profile losses are reported as a function of cascade Reynolds number, defined on the basis of cascade exit velocity and blade chord length. In the present model, cascade Reynolds number is varied systematically by varying blade chord while holding all other parameters constant. This is possible since the velocity loading is defined with respect to a dimensionless length parameter (ℳ). Figure 3 illustrates how the different loss coefficients vary with changing rotor chord (mean camberline length). Note that, generally speaking, $Y_{p\ell}$ decreases with increasing chord while Y_{sf} increases (blade height is held constant during the procedure). According to this simplified model there is an optimum Reynolds number, or optimum chord, which minimizes total aerodynamic loss (excluding tip leakage). The optimum value will, of course, change as cascade inlet and outlet conditions change.

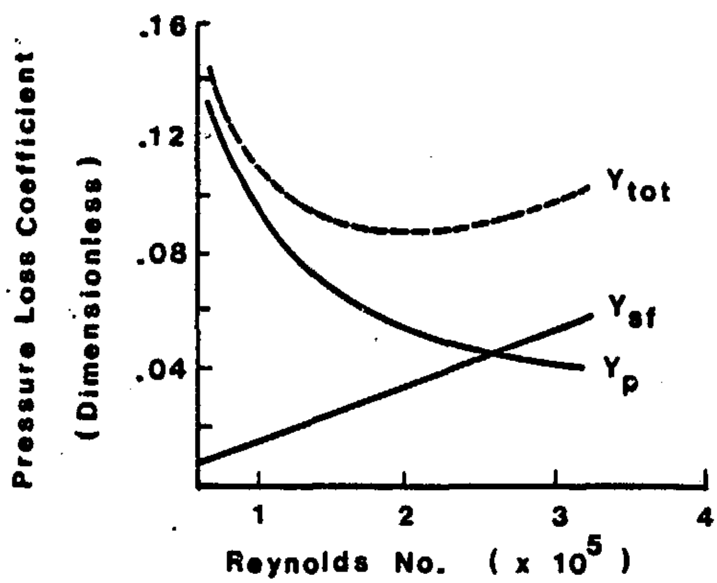

Figure 3: Typical Variation of Cascade Loss Coefficients with Reynolds Number

OPTIMIZATION OF ANNULAR FLOWPATH GEOMETRY

The model considers a range of annular (hub/tip) flowpath geometries, based on calculated mean flow properties along a pitchline radius. The minimum value for pitchline radius is defined by the condition of zero acceleration of the channel centerline velocity in the rotor.

The maximum value for pitchline radius may be set by limitations on blade tip speed or by aerodynamic considerations such as rotor limit loading. In any event, the loss model described previously is applied to a range of configurations within these limits in order to determine the one configuration having optimum aerodynamic performance, as characterized by adiabatic total-total or total-static efficiency. Hub and tip radii at the rotor exit section are obtained from user-specified axial Mach number and swirl conditions. A schematic flowchart of the entire calculation procedure is shown as Figure 4.

ESTIMATION OF MECHANICAL STRESS

Since the present analysis considers such a wide range of possible designs for a single set of cycle constraints, it is desirable to calculate preliminary estimates of mechanical stress conditions for each design. Rough estimates of both average tangential disk stress and blade root stress are made utilizing expressions found in textbooks on turbomachinery design (such as References 10 and 11). Blade root stresses are calculated using a taper correction factor of 2/3, which corresponds to a linearly tapered blade with a ratio of blade tip area to blade hub area of about 0.35. The disk half-area is considered to be a trapezoidal section; the disk rim load is considered to be the sum of 1) the load due to the blades themselves, and 2) the load due to a blade attachment region, also taken to be a trapezoid. It should be noted that these stresses are directly dependent on both blade chord and blade solidity, both of which are optimized in the present analysis. It is impossible, therefore, to completely separate considerations of

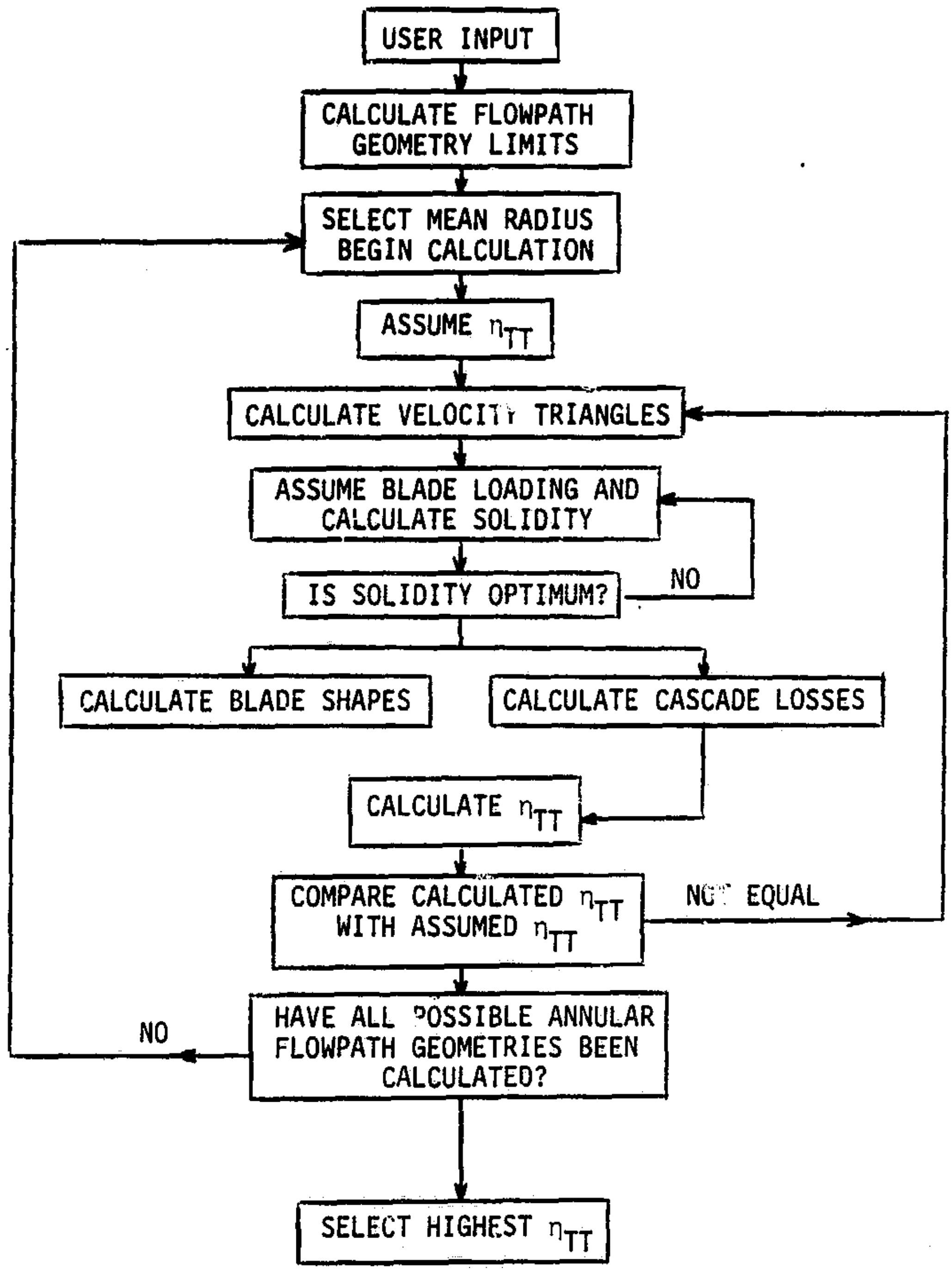

Figure 4: Axial Turbine Design Optimization Procedure

aerothermodynamic optimization from considerations of mechanical integrity. It should also be noted that, while mechanical stress is calculated by the model, no design decisions are made on the basis of such calculations.

VERIFICATION OF THE PERFORMANCE LOSS MODEL

Verification of the performance loss model is accomplished by a process wherein test data, including test rig geometries normally calculated internally, are input to determine whether actual measured test-rig performance can be predicted. Thermodynamic cycle requirements input represent air-equivalent (cold) conditions rather than design (hot) conditions. Quantities such as measured mass flow, rotor torque (specific work), and rotor exit swirl angle are utilized.

Seven (7) NASA turbines have been selected to provide a means of comparison between aerodynamic performance (adiabatic efficiency) as predicted by the model and aerodynamic performance as measued during cold-air testing. These turbines are designated as

Case 1: Low-cost civilian turbojet engine (Reference 12)

Case 2: Research turbine for high temperature core engine application (Reference 13)

Case 3: 12.766 centimeter tip diameter (solid blade configuration) turbine (Reference 14)

Case 4: First stage of a 4½ stage fan-drive turbine (Reference 15)

Case 5: Compressor drive turbine for a 75 KW automotive engine (Reference 16)

Case 6: Uncooled core turbine with high work output (Reference 17)

Case 7: Low-cost turbofan engine (first stage of a two-stage turbine) (Reference 18)

These turbines range in size from 0.6 to 63.8 kg/s (1.3 to 140 lb/s) mass flow and in specific work output from 153 to 558 J/g (65 to 240 Btu/lb), all at design (hot) conditions; stage loading factor ranges from 1.15 to 4.66. For comparison, relevant design parameters for each turbine configuration are given in Table 1.

TABLE 1: COMPARISON OF RELEVANT TURBINE PARAMETERS (DESIGN CONDITIONS) FOR NASA TEST CASES

CASE	INLET TEMP ^oK	INLET PRESSURE N/cm^2	MASS FLOW RATE KG/S	SPECIFIC WORK OUTPUT J/G	WORK FACTOR
1	1089	26.3	3.28	159.3	1.15
2	2200	386.1	63.82	287.3	1.70
3	1478	91.2	0.95	307.3	1.67
4[A]	378	24.3	5.84	25.7	4.66
5	1325	39.8	0.60	198.1	2.10
6	2200	386.1	49.41	557.7	1.94
7	978	28.5	2.99	152.8	1.72

[A]EQUIVALENT DESIGN REQUIREMENTS--ACTUAL CONDITIONS NOT GIVEN.

For each case, the following calculations are made:

(1) With no geometry input, determine the optimum rotor exit mean radius by maximizing the turbine adiabatic total-total

efficiency. This calculation is performed with design (hot) conditions of thermodynamic parameters of flow, work, etc., as well as geometric design values such as rotor tip clearance, and is done merely to demonstrate the flexibility of the model. Thus, total-total efficiency as predicted by, say, Figure 5, need not compare on a one-to-one basis with that of Figures 8 and 9. Further, η values shown in the geometric optimization portion of the present work differ slightly from those values given in Reference 19 due primarily to changes in the blade loading portion of the model.

(2) With detailed test-rig geometry and flow conditions input, determine the predicted total-total efficiency as a function of

(i) rotor solidity, σ_R

(ii) rotor exit swirl angle

In addition, for Case 1 only, a survey of optimum predicted flowpath geometry is made as a function of rotor Zweifel loading coefficient, ψ, and rotor exit swirl angle.

<u>Case 1</u>[12]

Case 1 represents a turbine designed for a low-cost civilian turbojet engine application. The turbine configuration is single-stage, axial flow with a free-vortex whirl distribution. The aerodynamic design is conservative (low work factor) with moderate gas temperatures. Table 2 presents the relevant design parameters and measures test-rig values input to the performance model.

TABLE 2: CASE 1 PERFORMANCE MODEL INPUT

PARAMETER	DESIGN EQUIVALENT CONDITION	TEST-RIG CONDITION
ROTATIVE SPEED, RPM	18075	100% OF DESIGN
INLET TEMPERATURE, ^{o}K	288.2	310
INLET PRESSURE, N/CM^2	10.14	10.8
SPECIFIC WORK, J/G	43.23	1.7% MORE
MASS FLOW, KG/S	2.51	9.5% LESS
ROTOR EXIT MEAN RADIUS, CM	10.06	SAME
ROTOR EXIT ANNULUS AREA, CM^2	269.6	SAME
ROTOR CLEARANCE, CM	0.028	SAME
STATOR SOLIDITY	1.038	SAME
ROTOR SOLIDITY	1.640	SAME
STATOR AXIAL CHORD, CM	1.90	SAME
ROTOR AXIAL CHORD, CM	1.76	SAME
STATOR TE THICKNESS, CM	0.101	SAME
ROTOR TE THICKNESS, CM	0.101	SAME
ROTOR EXIT SWIRL, DEG	-3.8	+14.0

Figure 5 represents a preliminary optimization of annular flow-path geometry, wherein no geometrical constraints are input to the model. An optimum size for the turbine is chosen based on maximum total-total efficiency. The predicted size (rotor exit mean radius) compares well with the actual (design) size for the Case 1 configuration.

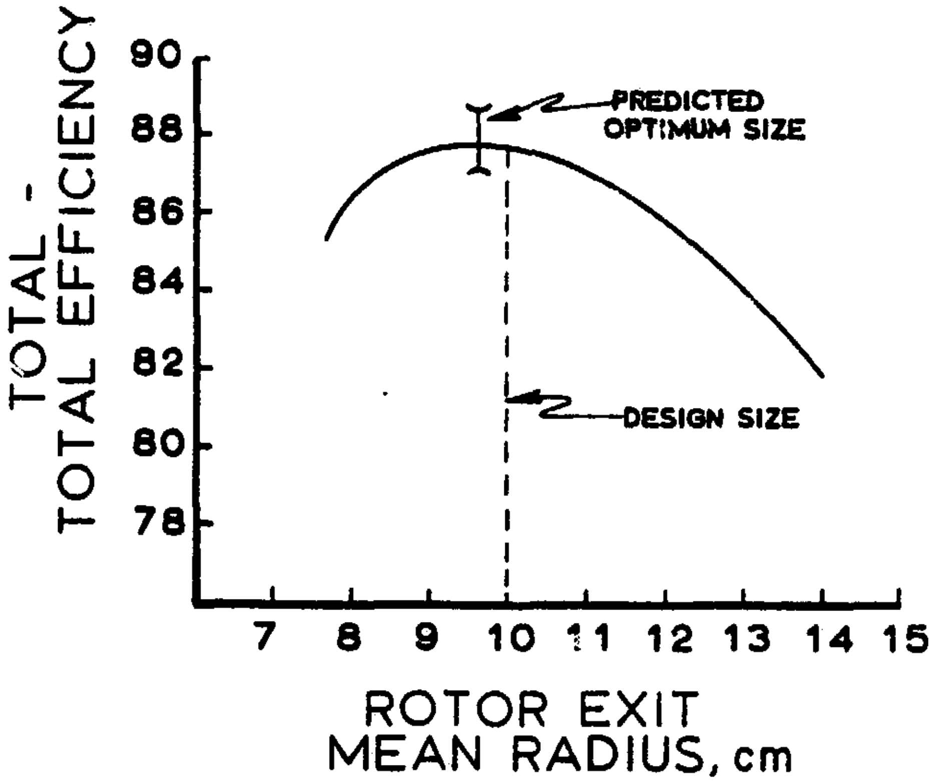

Figure 5: Case 1 Preliminary Geometry Optimization Study

Figures 6 and 7 demonstrate the predicted variation of optimum turbine size with rotor Zweifel coefficient (Figure 6) and rotor exit swirl (Figure 7), all other factors being constant. Figures 8 and 9 are calculations wherein geometry is input to the model. Figure 8 is a parametric study of stage efficiency vs. rotor solidity (blade number); note that exit swirl is constrained to +14°, as opposed to the design value of -3.8°. At the design solidity, the model predicts an efficiency of 91.4, which compares well with the rig measured value of 91.0. Original design (target) efficiency was 88.0. Figure 9 represents a parametric study of predicted efficiency vs. rotor exit swirl, all other factors being constant.

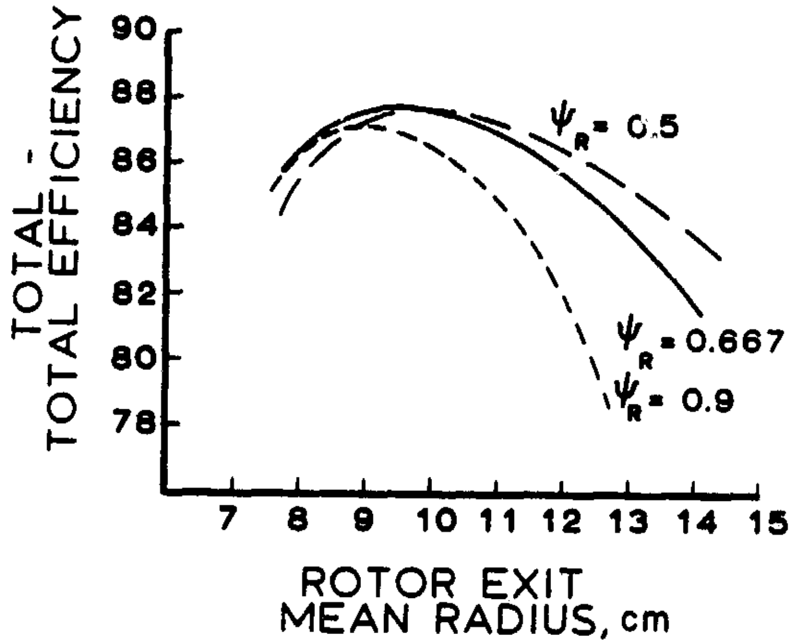

Figure 6: Case 1 Geometry Optimization Study; Rotor Zweifel Coefficient Variation

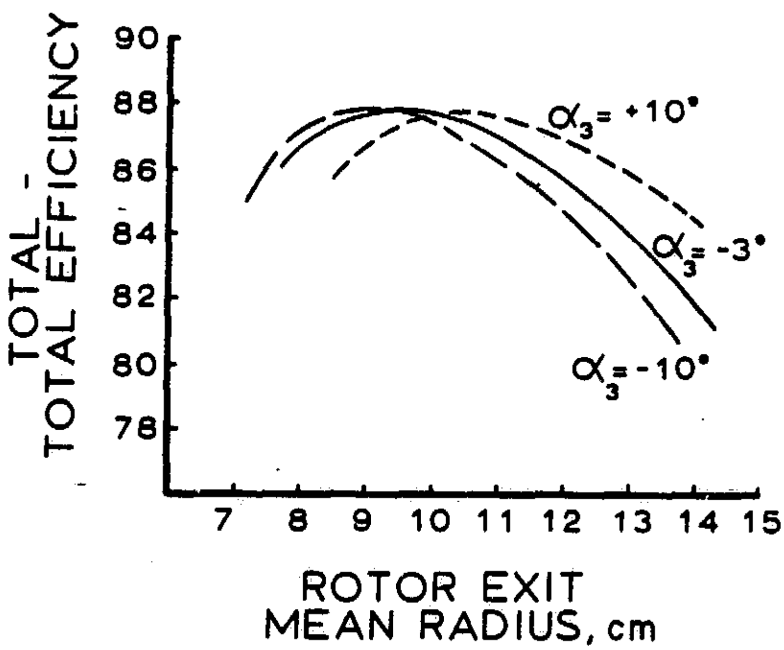

Figure 7: Case 1 Geometry Optimization Study; Rotor Exit Swirl Variation

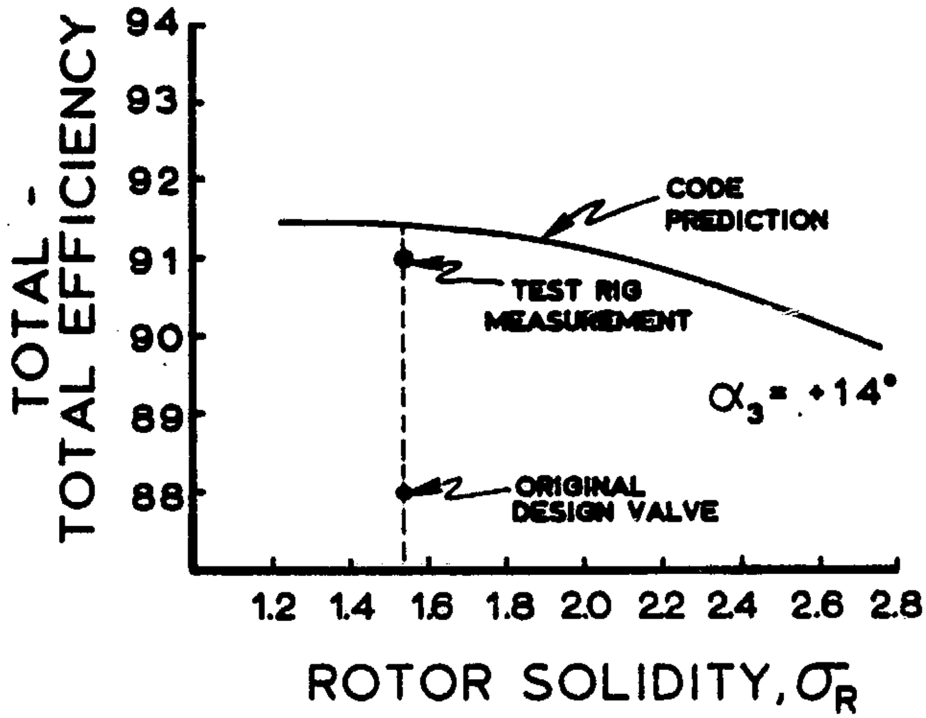

Figure 8: Case 1 Efficiency vs. Rotor Solidity; Comparison of Code Prediction, Original Design Value, and Test-Rig Measurement (Geometry Input)

Case 2[13]

Case 2 is a half-scale model of a 50.8 cm (20 inch) turbine characterized by low aspect ratio, thick trailing edges, low solidity, and relatively large rotor tip clearance. Originally, the rotor blades had a constant section profile from hub to tip with no twist, resulting in relative ease of manufacture but a possible performance penalty. Subsequently, a free-vortex twist rotor was fabricated and tested. Due to the pitchline nature of the model used in the present code, these two conditions cannot be differentiated. Though the measured performance of both designs is reported (see Figures 11 and 12), only the untwisted rotor test-rig conditions are shown in Table 3.

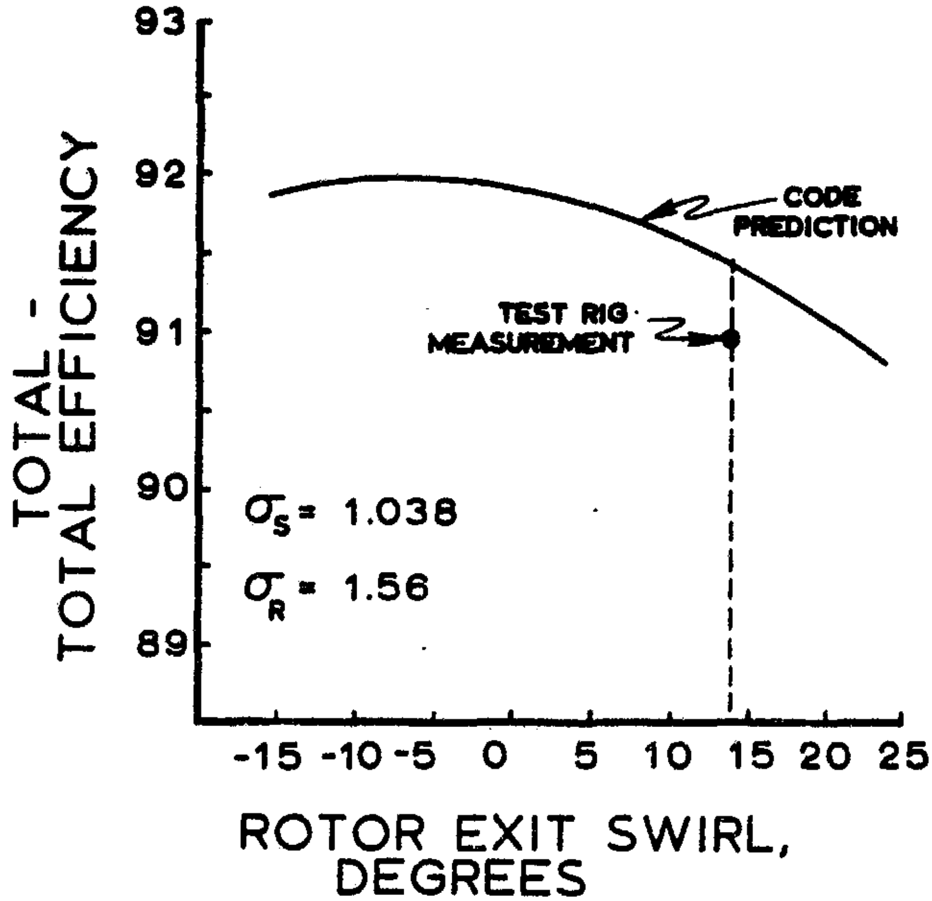

Figure 9: Case 1 Efficiency vs. Rotor Exit Swirl for Fixed Stator and Rotor Solidities (Geometry Input)

TABLE 3: CASE 2 PERFORMANCE MODEL INPUT

PARAMETER	DESIGN EQUIVALENT CONDITION	TEST-RIG CONDITION
ROTATIVE SPEED, RPM	12388	100% OF DESIGN
INLET TEMPERATURE, °K	288.2	306
INLET PRESSURE, N/CM^2	10.14	17.24
SPECIFIC WORK, J/G	39.57	0.5% LESS
MASS FLOW, KG/S	1.207	1.5% LESS
ROTOR EXIT MEAN		SAME
RADIUS, CM	11.75	SAME
ROTOR EXIT ANNULUS		SAME
AREA, CM^2	140.6	SAME
ROTOR CLEARANCE, CM	0.043	SAME
STATOR SOLIDITY	0.929	SAME
ROTOR SOLIDITY	1.487	SAME
STATOR AXIAL CHORD, CM	1.905	SAME
ROTOR AXIAL CHORD, CM	1.715	SAME
STATOR TE THICKNESS, CM	0.089	SAME
ROTOR TE THICKNESS, CM	0.089	SAME
ROTOR EXIT SWIRL, DEG	-17.8	-11.5

Figure 10 represents the preliminary optimization of annular flowpath geometry. As before, the predicted turbine size compares well with the actual size.

Figure 11 is a fixed geometry parametric study of efficiency vs. rotor solidity, with all other factors held constant. Rotor exit swirl is fixed at the test-rig measured value of -11.5°. The measured

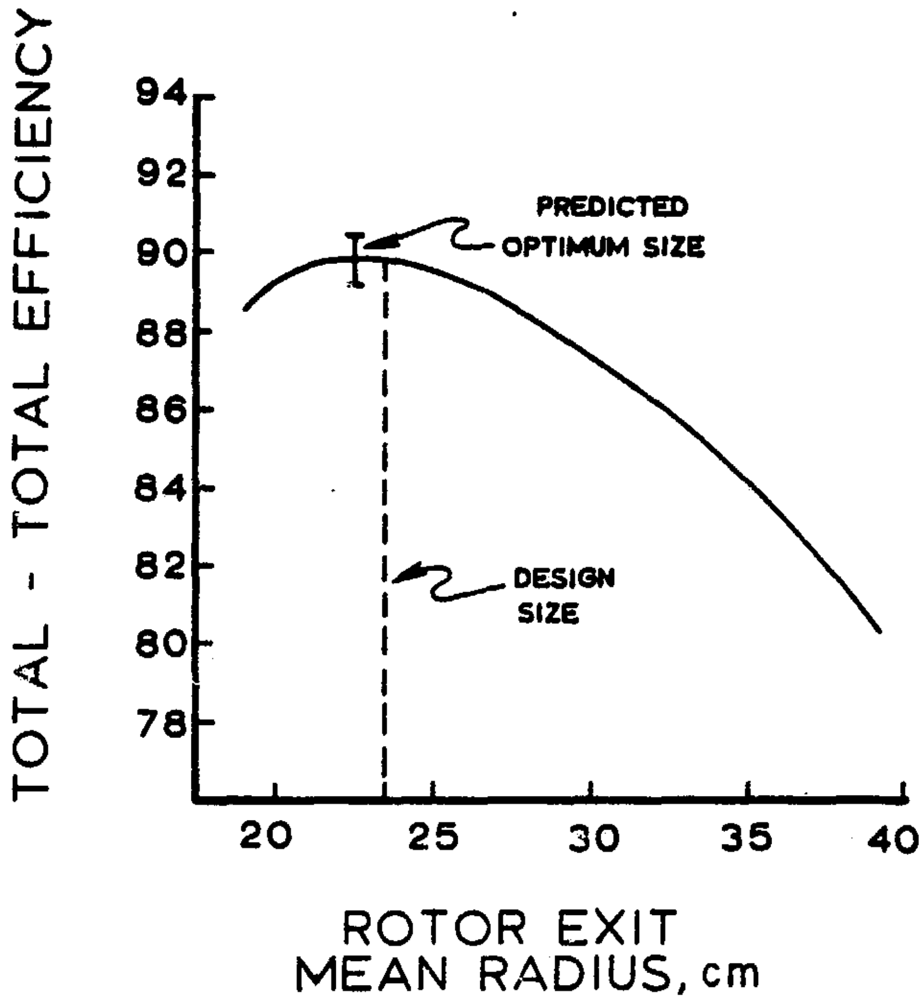

Figure 10: Case 2 Preliminary Geometry Optimization Study

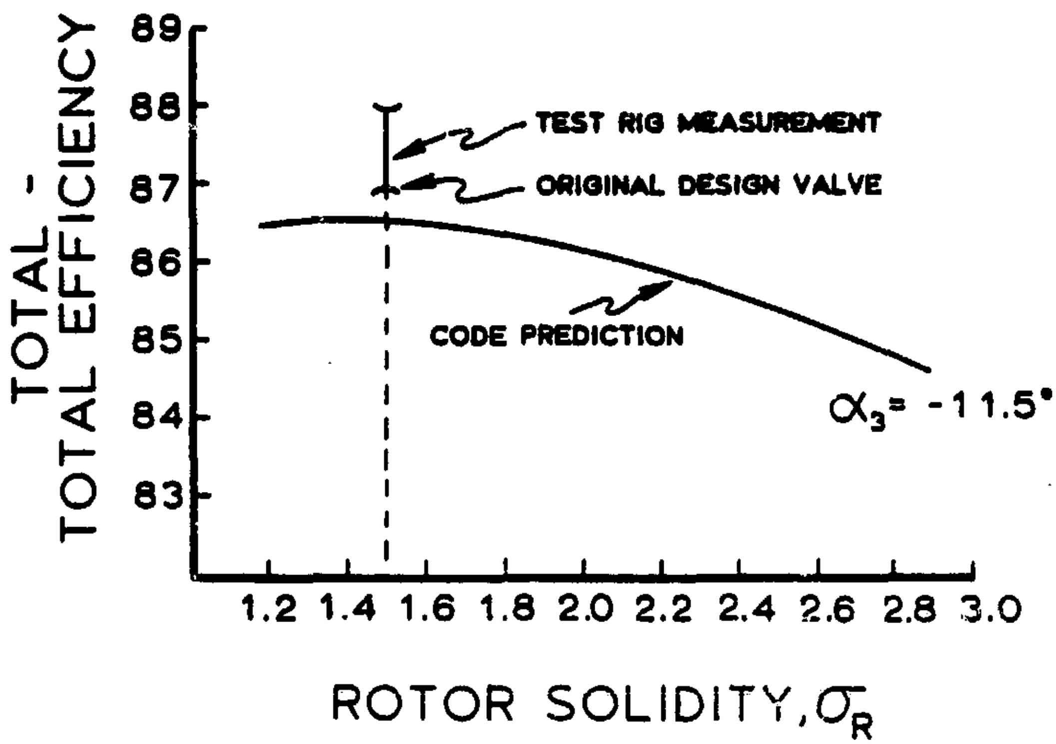

Figure 11: Case 2 Efficiency vs. Rotor Solidity; Comparison of Code Prediction, Original Design Value, and Test-Rig Measurement (Geometry Input)

efficiency is shown as a band between 87.0 (untwisted rotor configuration) and 88.0 (twisted rotor configuration). Predicted performance is 86.6, compared to an original design value of 87.0. Recall that the present model cannot differentiate between the two rotor configurations. Figure 12 presents a parametric study of efficiency vs. rotor exit swirl angle, with all other factors held constant.

Case 3[14]

Case 3 represents an uncooled solid-blade version of a cooled turbine design in the 1 kg per second, 225-375 KW size class. Work factor and solidity are considered to be near optimum by conventional design standards. Both the stator and the rotor blading are untwisted and

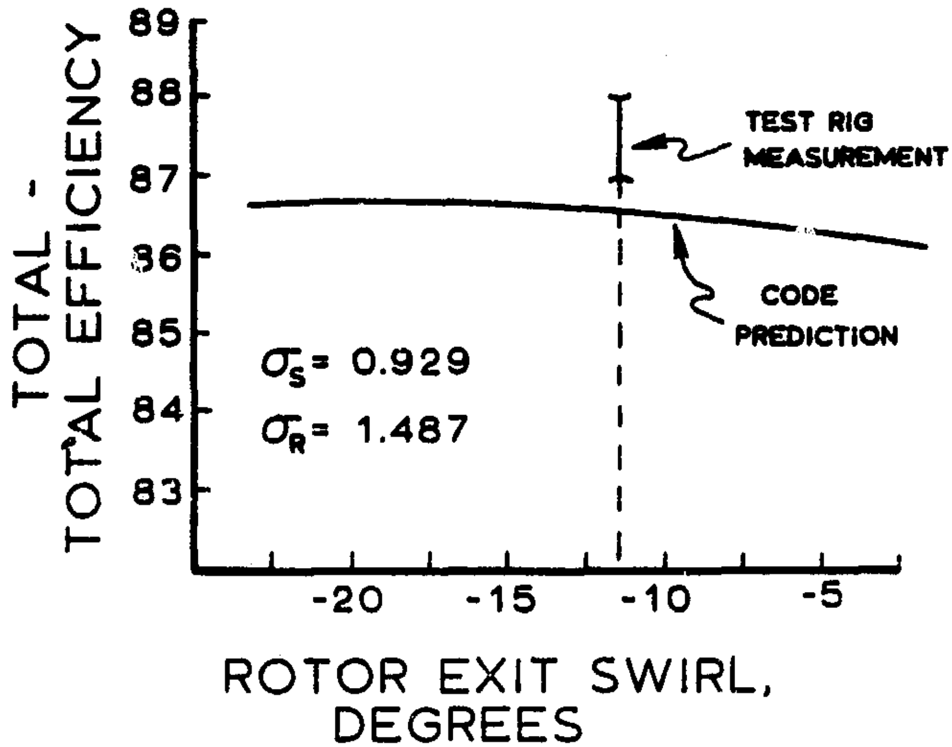

Figure 12. Case 2 Efficiency vs. Rotor Exit Swirl for Fixed Stator and Rotor Solidities (Geometry Input)

untapered. Typical of such small turbines, this design suffers from relatively large rotor tip clearance and secondary flow losses. Relevant test-rig conditions are given in Table 4.

Figure 13 demonstrates that the predicted annular flowpath geometry agrees well with the actual geometry. Figure 14 represents a fixed geometry parametric study of efficiency vs. rotor solidity and indicates that the rotor solidity is indeed near optimum for the thermodynamic cycle requirements of case 3. The model predicts an efficiency of 84.1 for the design solidity compared to a measured efficiency of 83.2. The original design efficiency was 85.0. Figure 15 presents a study of predicted efficiency vs. rotor exit swirl distribution. In the

TABLE 4: CASE 3 PERFORMANCE MODEL INPUT

PARAMETER	DESIGN EQUIVALENT CONDITION	TEST-RIG CONDITION
ROTATIVE SPEED, RPM	31460	100% OF DESIGN
INLET TEMPERATURE, ^{o}K	288.2	300
INLET PRESSURE, N/cm^2	10.13	8.27
SPECIFIC WORK, J/G	62.1	1.4% LESS
MASS FLOW, KG/S	0.246	6.1% LESS
ROTOR EXIT MEAN RADIUS, CM	5.86	SAME
ROTOR EXIT ANNULUS AREA, cm^2	38.72	SAME
ROTOR CLEARANCE, CM	0.025	SAME
STATOR SOLIDITY	1.098	SAME
ROTOR SOLIDITY	1.551	SAME
STATOR AXIAL CHORD, CM	0.721	SAME
ROTOR AXIAL CHORD, CM	0.968	SAME
STATOR TE THICKNESS, CM	0.038	SAME
ROTOR TE THICKNESS, CM	0.050	SAME
ROTOR EXIT SWIRL, DEG	-17.5	-11.0

range of swirl angles shown the total-total efficiency appears to be almost independent of swirl. The region denoted "model limit" represents choked flow conditions at the stator exit.

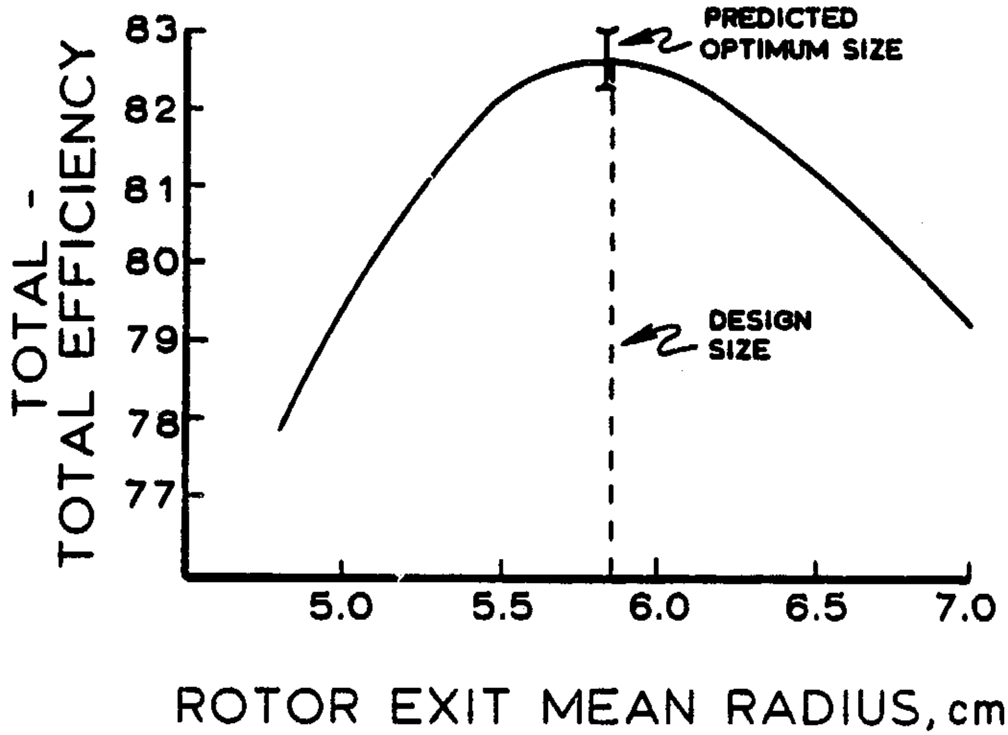

Figure 13: Case 3 Preliminary Geometry Optimization Study

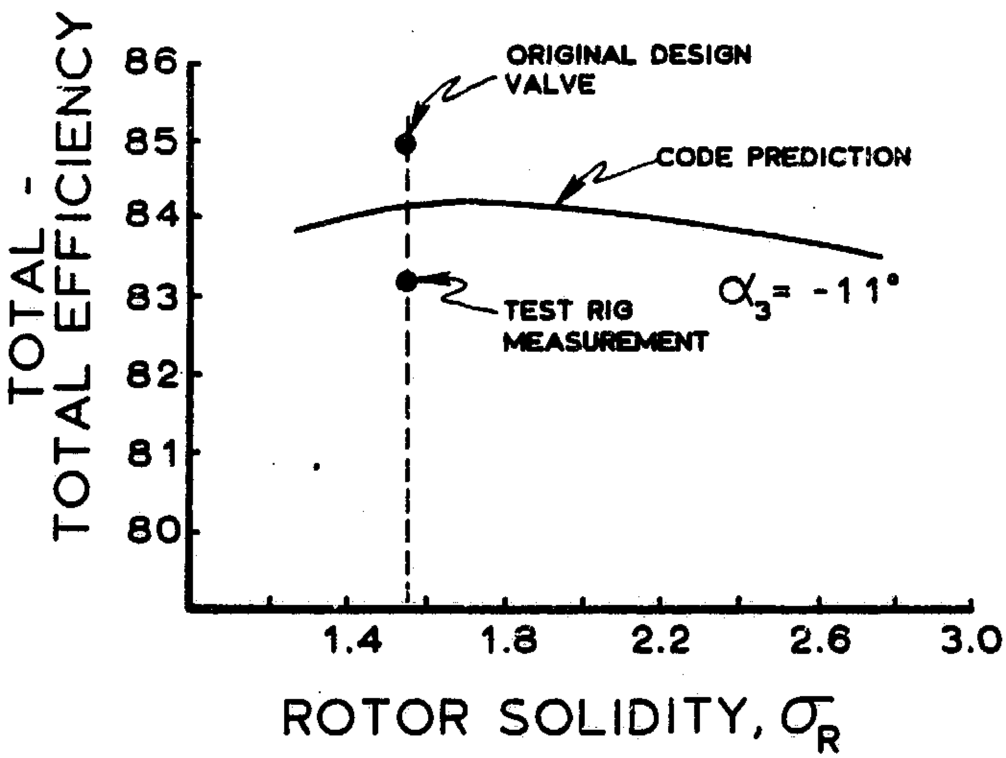

Figure 14: Case 3 Efficiency vs. Rotor Solidity; Comparison of Code Prediction, Original Design Value, and Test-Rig Measurement (Fixed Geometry)

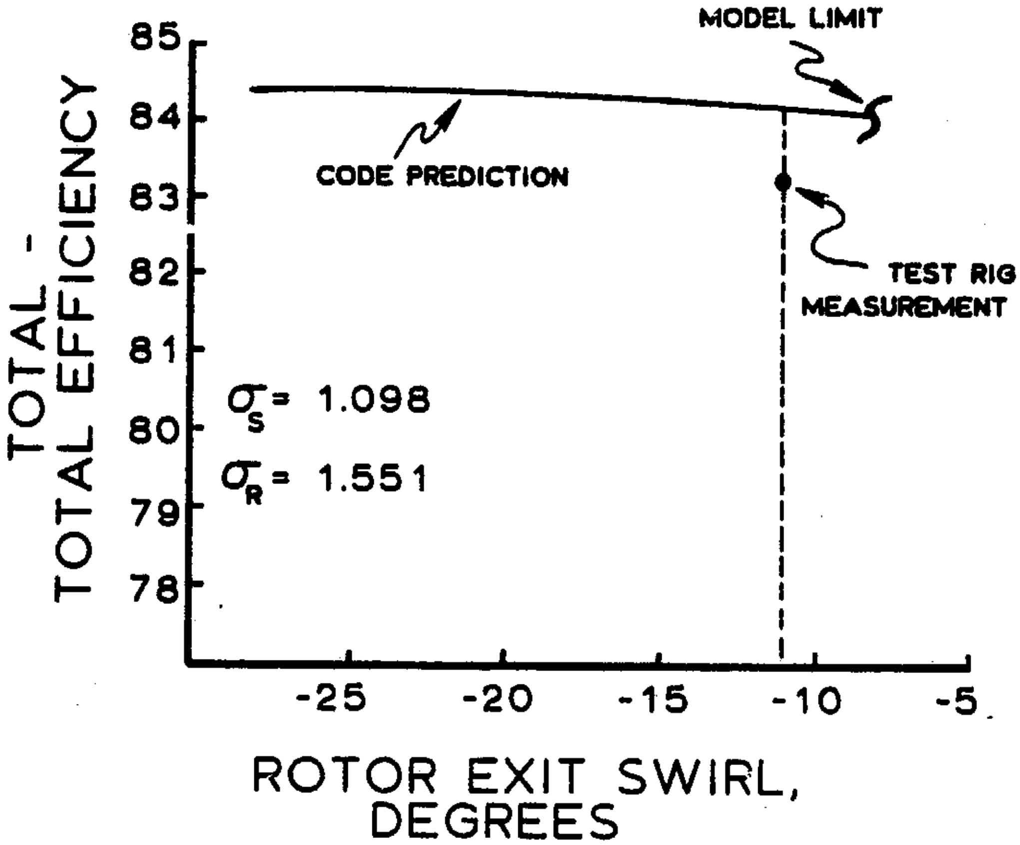

Figure 15: Case 3 Efficiency vs. Rotor Exit Swirl for Fixed Stator and Rotor Solidities (Fixed Geometry)

<u>Case 4</u>[15]

Case 4 represents the first stage of a 4½ stage turbine designed for high stage work factor. This turbine is characterized by shrouded rotors, high turning in both stator and rotor blade rows, and nearly symmetrical mean-radius velocity diagrams. As part of a development program, the first stage alone was fabricated and its performance determined in cold air. Pertinent parameters are given in Table 5.

Figure 16 presents the geometry optimization portion of the parametric study for Case 4. In this instance the predicted and actual sizes are not in good agreement; it should be noted, however, that this

TABLE 5: CASE 4 PERFORMANCE MODEL INPUT

PARAMETER	DESIGN EQUIVALENT CONDITION	TEST-RIG CONDITION
ROTATIVE SPEED, RPM	3098.7	100% OF DESIGN
INLET TEMPERATURE, ^{o}K	288.2	378
INLET PRESSURE, N/CM^2	10.13	24.3
SPECIFIC WORK, J/G	25.65	100% OF DESIGN
MASS FLOW, KG/S	5.84	2.4% MORE
ROTOR EXIT MEAN RADIUS, CM	22.86	SAME
ROTOR EXIT ANNULUS AREA, CM^2	656.7	SAME
ROTOR CLEARANCE, CM	0.0	SAME
STATOR SOLIDITY	0.955	SAME
ROTOR SOLIDITY	1.517	SAME
STATOR AXIAL CHORD, CM	2.29	SAME
ROTOR AXIAL CHORD, CM	2.79	SAME
STATOR TE THICKNESS, CM	0.050	SAME
ROTOR TE THICKNESS, CM	0.060	SAME
ROTOR EXIT SWIRL, DEG	-52	SAME

case represents only the first stage of a multi-stage turbine, so that this result need not be surprising.

Figures 17 and 18 portray the fixed geometry parametric study for rotor solidity and exit swirl, respectively. Unlike the previous case, predicted efficiency is strongly dependent on these parameters. In this instance, the original design efficiency and the measured test-rig efficiency were identical (86.0) as compared to 85.0 for the model prediction.

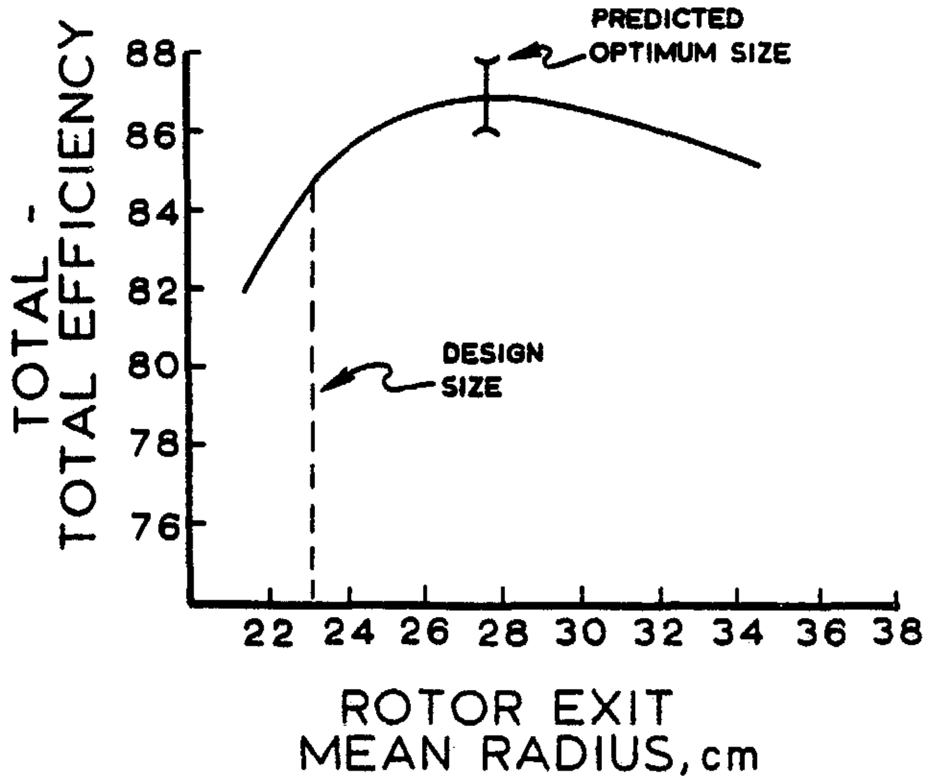

Figure 16: Case 4 Preliminary Geometry Optimization Study

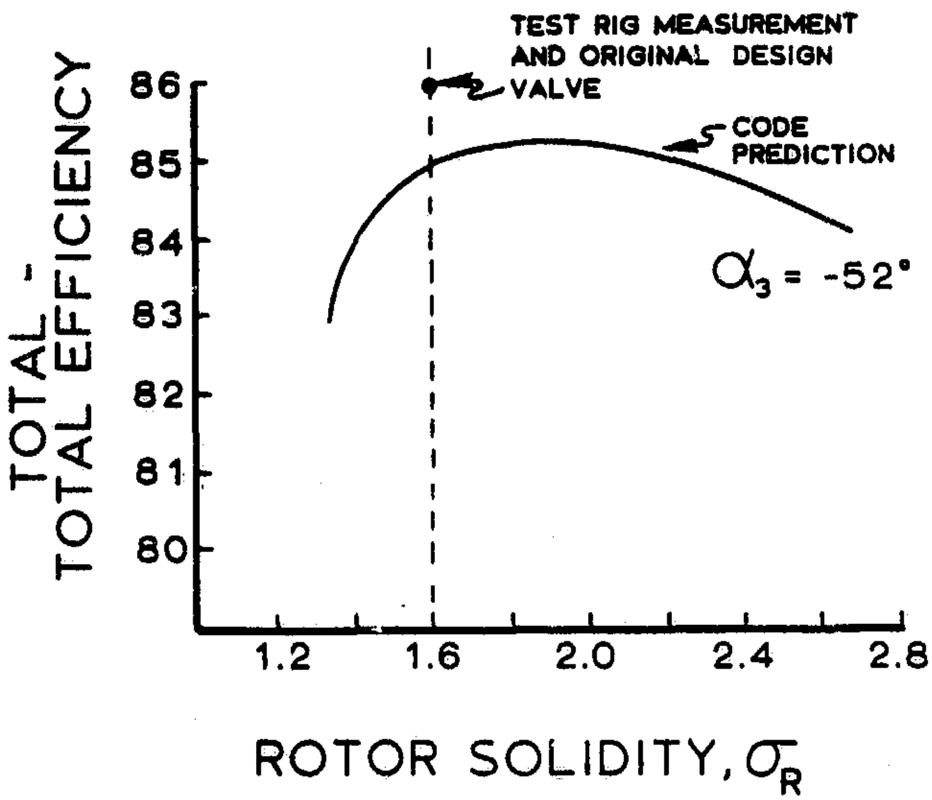

Figure 17: Case 4 Efficiency vs. Rotor Solidity; Comparison of Code Prediction, Original Design Value, and Test-Rig Measurement (Fixed Geometry)

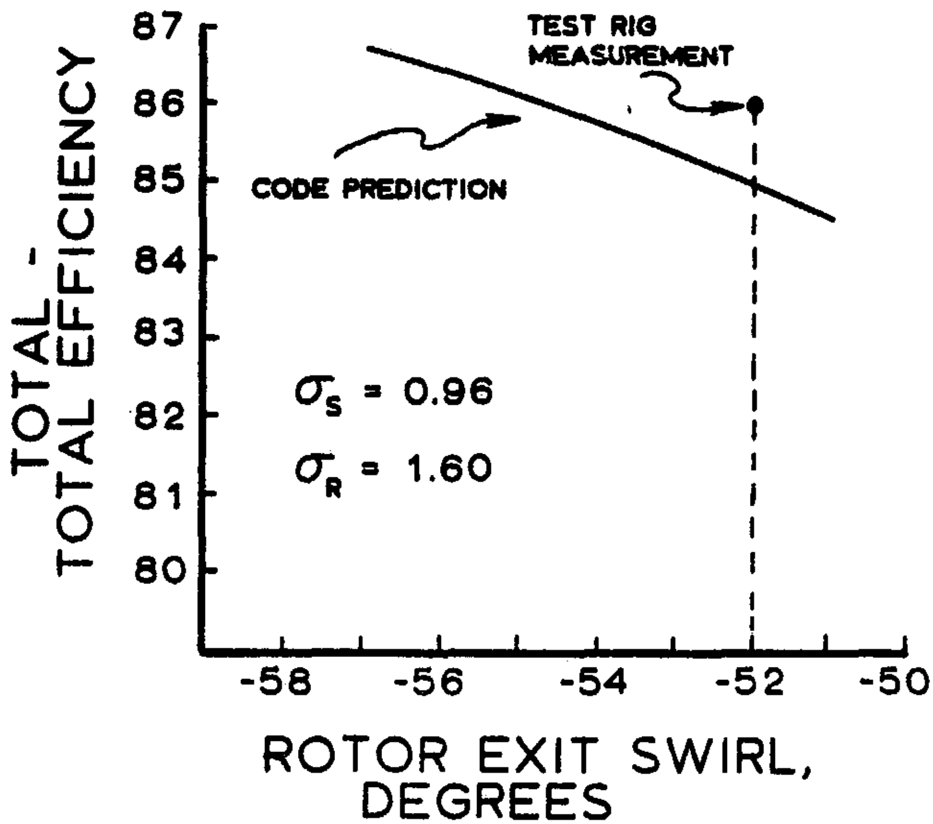

Figure 18: Case 4 Efficiency vs. Rotor Exit Swirl for Fixed Stator and Rotor Solidities (Fixed Geometry)

Case 5[16]

Case 5 represents a compressor drive turbine originally intended for use in a compact automobile. The design is characterized by a large (49°) stator inlet flow angle, required to match the swirl distribution in the tangential entry inlet manifold. Pertinent model input parameters are given in Table 6. It should be noted that the model input corresponds to the so-called "smoothed and thinned profile" test (i.e., smoothed and thinned blades) of Reference 16.

TABLE 6: CASE 5 PERFORMANCE MODEL INPUT

PARAMETER	DESIGN EQUIVALENT CONDITION	TEST-RIG CONDITION
ROTATIVE SPEED, RPM	27673	100% OF DESIGN
INLET TEMPERATURE, °K	288.2	320
INLET PRESSURE, N/cm^2	10.13	8.0
SPECIFIC WORK, J/G	44.4	~5% LESS
MASS FLOW, KG/S	0.325	5% LESS
ROTOR EXIT MEAN RADIUS, CM	5.00	SAME
ROTOR EXIT ANNULUS AREA, cm^2	36.47	SAME
ROTOR CLEARANCE, CM	0.025	SAME
STATOR SOLIDITY	0.557	SAME
ROTOR SOLIDITY	1.803	SAME
STATOR AXIAL CHORD, CM	1.17	SAME
ROTOR AXIAL CHORD, CM	0.91	SAME
STATOR TE THICKNESS, CM	0.038	SAME
ROTOR TE THICKNESS, CM	0.038	SAME
ROTOR EXIT SWIRL, DEG	-21.1	SAME

Figure 19 shows the geometry optimization portion of the parametric study for Case 5. Predicted and actual turbine size are in good, but not excellent agreement. Figures 20 and 21 present the remainder of the parametric study. As with the previous case, efficiency appears to be sensitive to rotor exit swirl. Predicted efficiency at the test-rig conditions is 83.5, which compares to a measured value of 82.5 and a design value of 85.0.

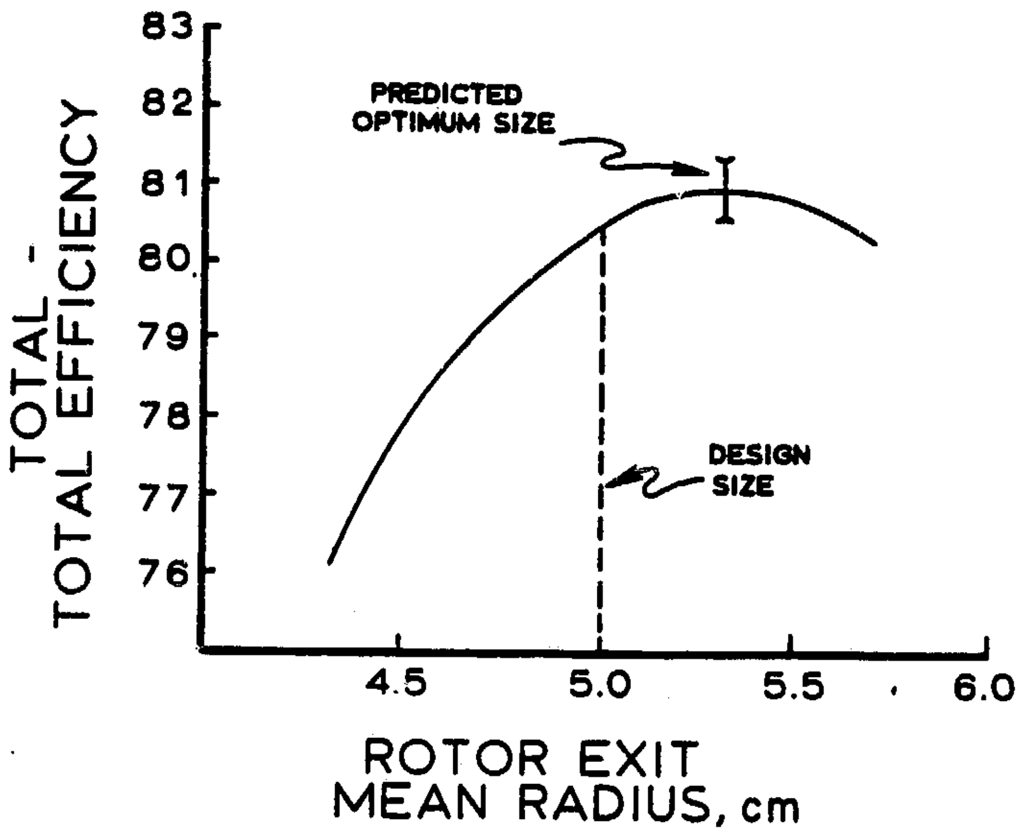

Figure 19: Case 5 Preliminary Geometry Optimization Study

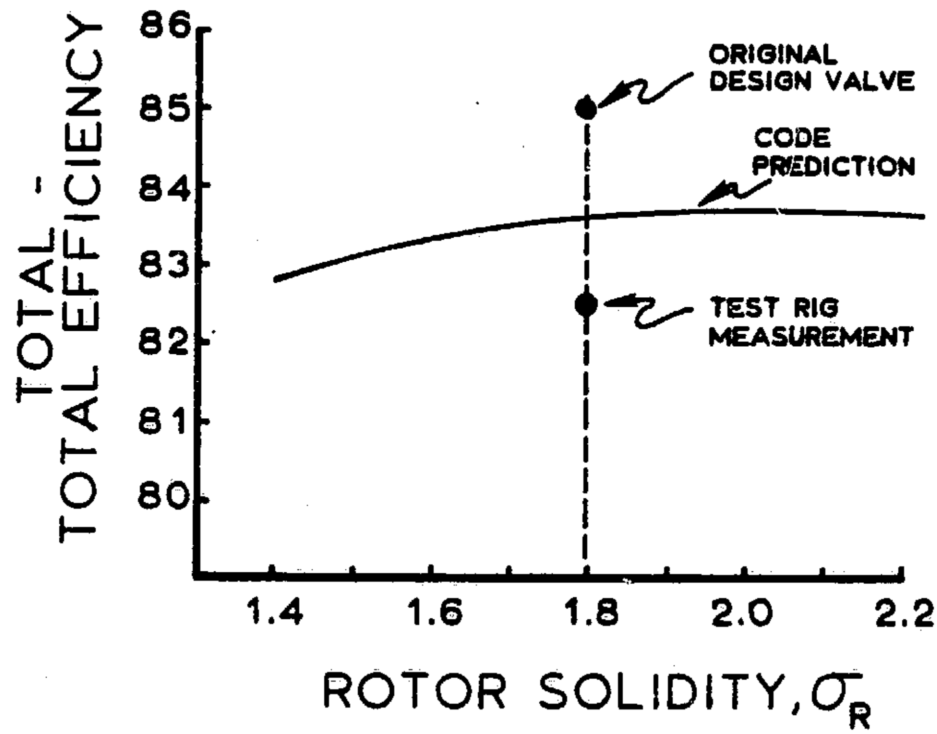

Figure 20: Case 5 Efficiency vs. Rotor Solidity; Comparison of Code Prediction, Original Design Value, and Test-Rig Measurement (Fixed Geometry)

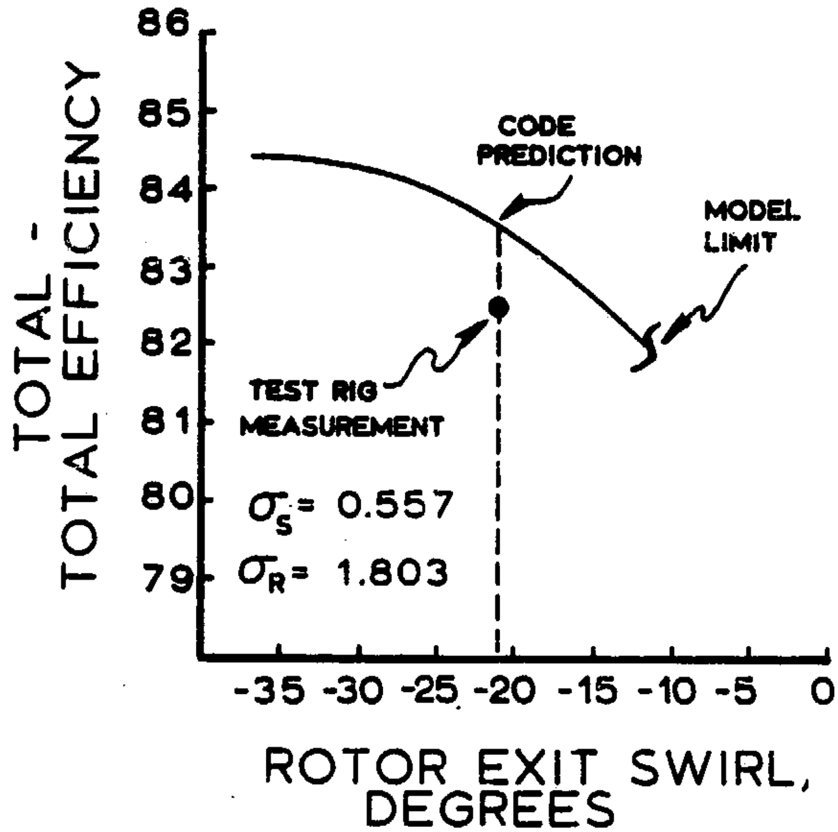

Figure 21: Case 5 Efficiency vs. Rotor Exit Swirl for Fixed Stator and Rotor Solidities (Fixed Geometry)

<u>Case 6</u>[17]

Case 6 represents a single-stage "core" turbine for a turbofan engine and is characterized by relatively high hub-to-tip radius ratio and low aspect ratio. Due to relatively high requirements for work extraction, Mach number levels are also high. The vane exit flow angle is flat, about 73° from axial; the vanes are untwisted and have a constant section profile. Pertinent model input parameters are given in Table 7.

Figure 22 illustrates the geometry optimization calculation for Case 6. Predicted and actual turbine size are in excellent agreement. Figure 23 presents the rotor exit swirl parametric study for this case.

TABLE 7: CASE 6 PERFORMANCE MODEL INPUT

PARAMETER	DESIGN EQUIVALENT CONDITION	TEST-RIG CONDITION
ROTATIVE SPEED, RPM	8081	100% OF DESIGN
INLET TEMPERATURE, ^{o}K	288.2	378
INLET PRESSURE, N/CM^2	10.13	24.13
SPECIFIC WORK, J/G	76.84	0.5% LESS
MASS FLOW, KG/S	3.708	4% MORE
ROTOR EXIT MEAN RADIUS, CM	23.5	SAME
ROTOR EXIT ANNULUS AREA, CM^2	562.5	SAME
ROTOR CLEARANCE, CM	0.030	SAME
STATOR SOLIDITY	0.929	SAME
ROTOR SOLIDITY	1.487	SAME
STATOR AXIAL CHORD, CM	3.81	SAME
ROTOR AXIAL CHORD, CM	3.43	SAME
STATOR TE THICKNESS, CM	0.127	SAME
ROTOR TE THICKNESS, CM	0.127	SAME
ROTOR EXIT SWIRL, DEG	-23.7	-22.6

Note that for the test-rig geometry the calculation model reaches the stator choke condition at a rotor exit swirl of approximately -27°. The measured swirl, on the other hand, is -22.6°, indicating that the flow is supersonic at the stator exit, a condition confirmed by the original design velocity diagrams. Strictly speaking, the model cannot be applied to this situation since it is constrained to stator exit Mach numbers less than unity. If one extrapolates the code prediction curve,

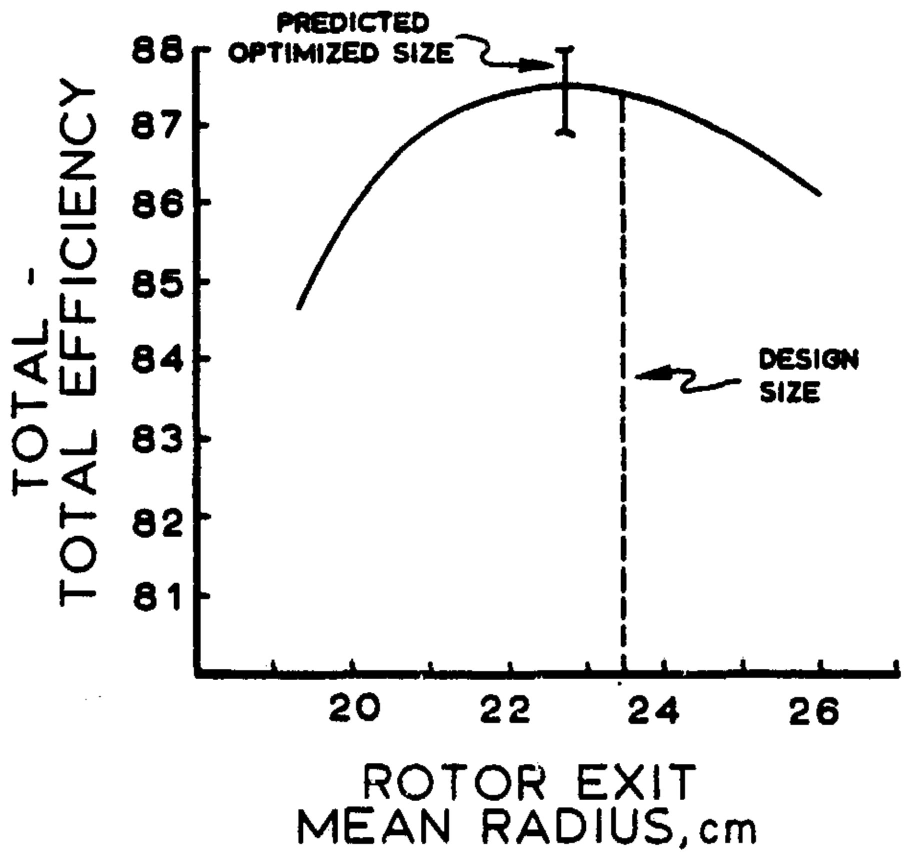

Figure 22: Case 6 Preliminary Geometry Optimization Study

however, the model predicts an efficiency level very near the 88.6 value actually measured. No solidity study was run for this case.

<u>Case 7</u>[18]

Case 7 represents the first stage of a two-stage turbine designed to drive the compressor and fan of a low-cost turbofan engine suitable for light aircraft application. The aerodynamic design is rather conservative, with low Mach number levels and low stator turning. The turbine was tested as both a two-stage and a single-stage unit. Data for the single-stage test are given in Table 8.

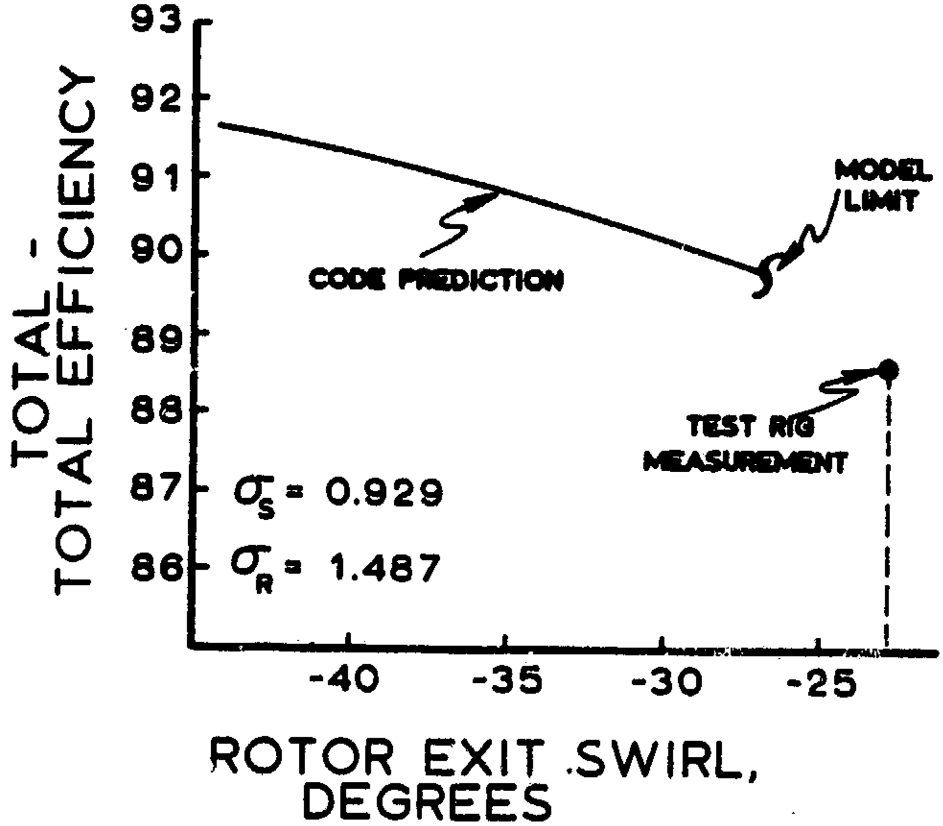

Figure 23: Case 6 Efficiency vs. Rotor Exit Swirl for Fixed Stator and Rotor Solidities (Fixed Geometry)

Figure 24 indicates excellent agreement between predicted and actual turbine size, even though Case 7 is, like Case 4, the first stage of a multi-stage turbine. For fixed geometry input, Figure 25 indicates a predicted efficiency of 91.1, compared to a test efficiency of 93.0. The original design value for this turbine was 87.0. Figure 26 indicates that, within the exit swirl range studied, the predicted efficiency curve is virtually flat.

TABLE 8: CASE 7 PERFORMANCE MODEL INPUT

PARAMETER	DESIGN EQUIVALENT CONDITION	TEST-RIG CONDITION
ROTATIVE SPEED, RPM	15336	100% OF DESIGN
INLET TEMPERATURE, ^{o}K	288.2	300
INLET PRESSURE, N/CM^2	10.13	13.79
SPECIFIC WORK, J/G	45.83	6.5% MORE
MASS FLOW, KG/S	1.989	0.8% MORE
ROTOR EXIT MEAN RADIUS, CM	10.16	SAME
ROTOR EXIT ANNULUS AREA, CM^2	233.5	SAME
ROTOR CLEARANCE, CM	0.030	SAME
STATOR SOLIDITY	1.049	SAME
ROTOR SOLIDITY	1.469	SAME
STATOR AXIAL CHORD, CM	1.91	SAME
ROTOR AXIAL CHORD, CM	2.23	SAME
STATOR TE THICKNESS, CM	0.050	SAME
ROTOR TE THICKNESS, CM	0.050	SAME
ROTOR EXIT SWIRL, DEG	-26.1	-26.5

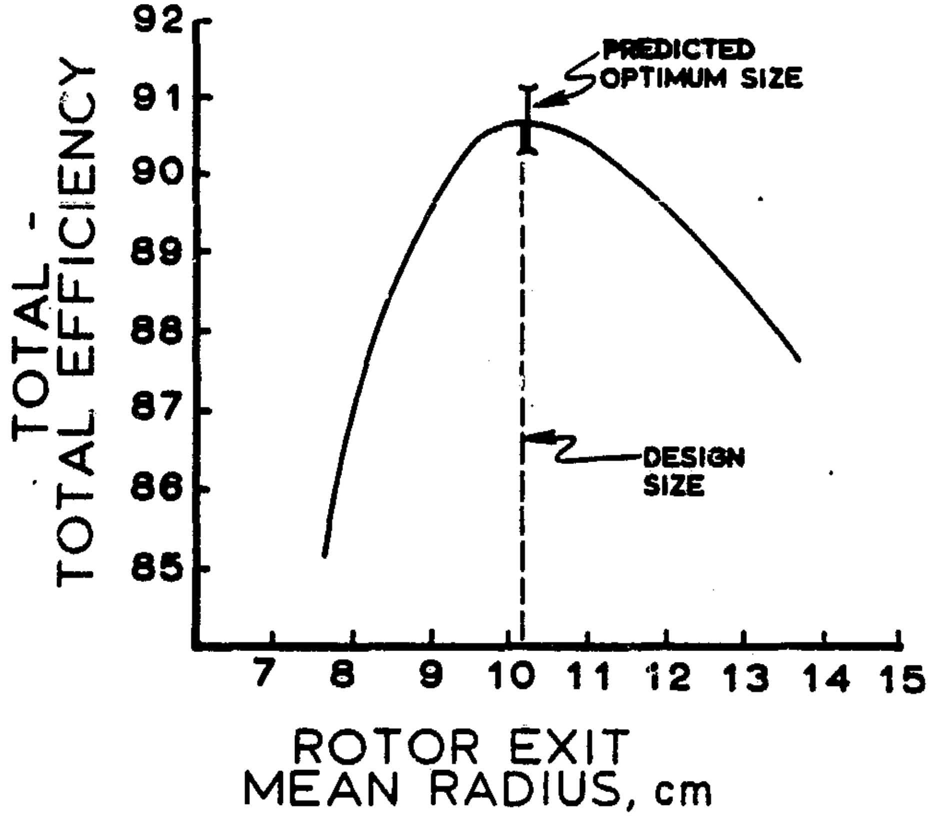

Figure 24: Case 7 Preliminary Geometry Optimization Study

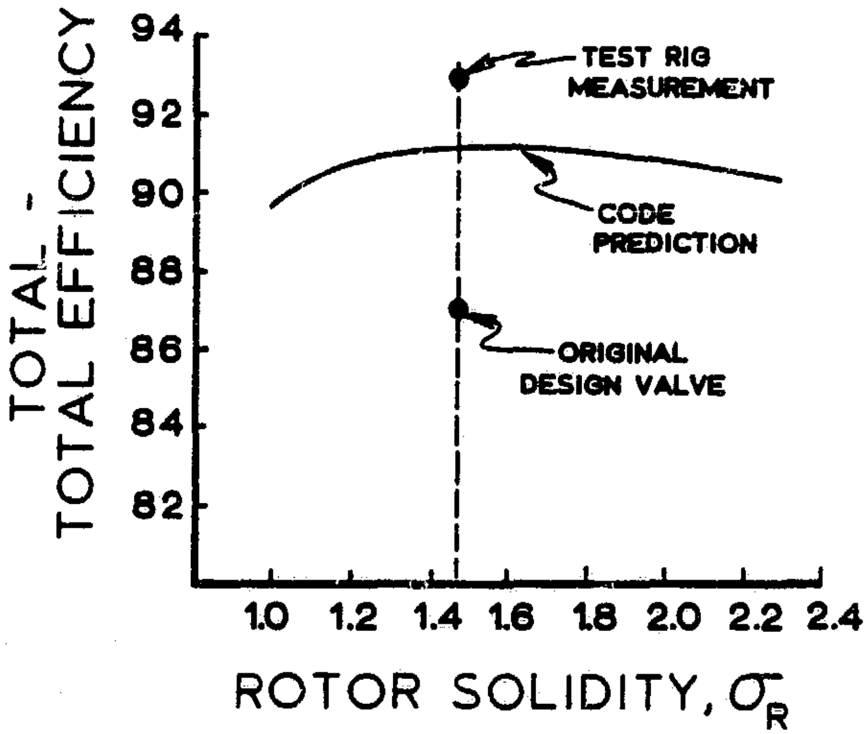

Figure 25: Case 7 Efficiency vs. Rotor Solidity; Comparison of Code Prediction, Original Design Value, and Test-Rig Measurement (Fixed Geometry)

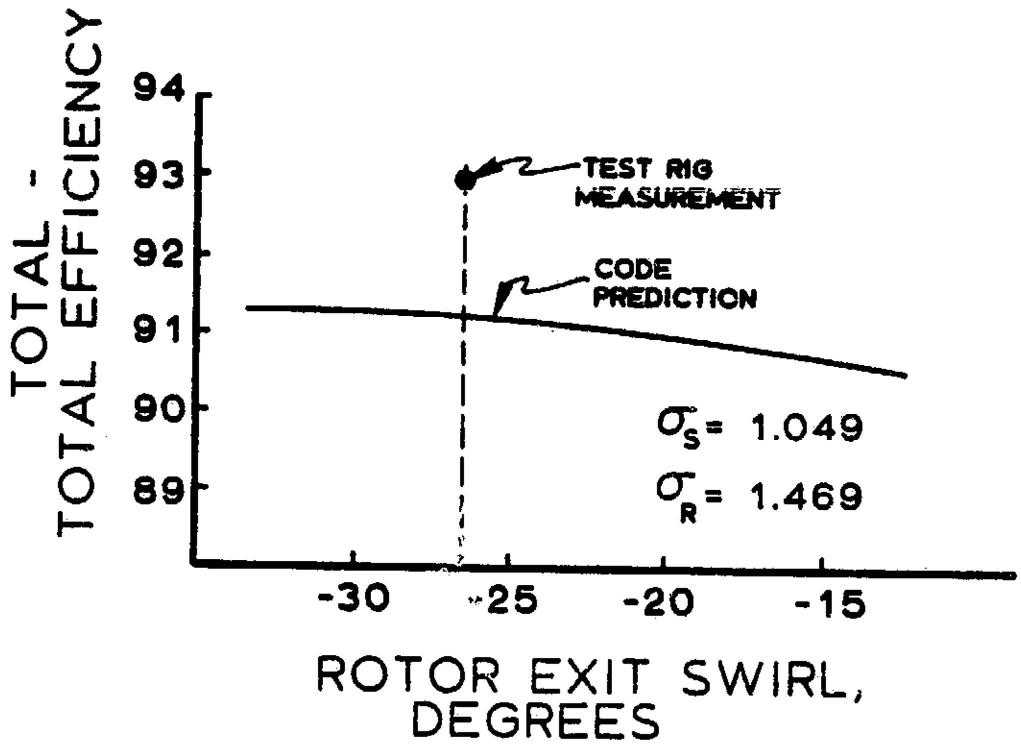

Figure 26: Case 7 Efficiency vs. Rotor Exit Swirl for Fixed Stator and Rotor Solidities (Fixed Geometry)

Summary of Results

Results for each of the seven cases considered in this study are summarized in Figure 27 and Table 9.

Despite obvious limitations of the model such as the pitchline nature of the analysis, simplicity of the boundary layer assumptions, etc., the results for the seven cases detailed above indicate that the model is capable of providing preliminary aerodynamic performance data with an acceptable degree of confidence. Experience with the model has shown that it is important to set up the correct stator inlet flow conditions (Mach number and pre-swirl) in order to achieve optimum results.

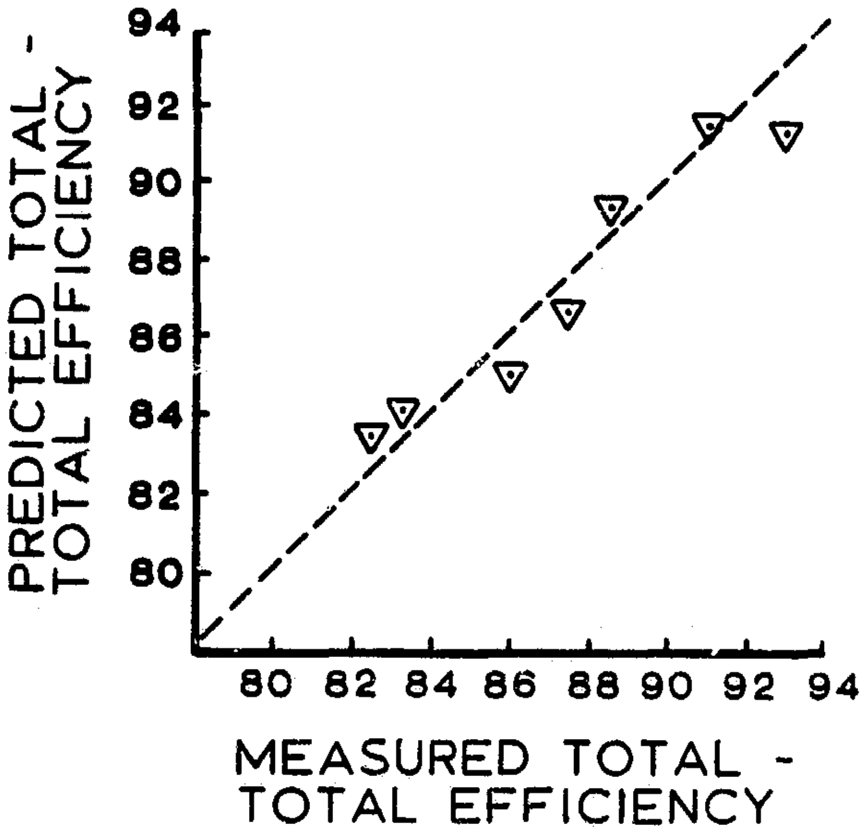

Figure 27: Predicted vs. Measured Efficiency; All Cases

Finally, a description of the model and code verification results have been presented at the 18th and 19th AIAA/SAE/ASME Joint Propulsion Conferences held in Cleveland, Ohio (1982) and Seattle, Washington (1983), respectively[19-20].

Appendices A-E contain supporting equations and analyses for the model. Appendix F describes the required model input; Appendix G contains a sample output; and Appendix H is a listing of the FORTRAN program.

TABLE 9: SUMMARY OF PREDICTED VS. MEASURED TOTAL-TOTAL EFFICIENCY; ALL TEST CASES

CASE	PREDICTED[A] EFFICIENCY	MEASURED EFFICIENCY
1	91.4	91.0
2	86.6	87-88[B]
3	84.1	83.2
4	85.0	86.0
5	83.5	82.5
6	89.3[C]	88.6
7	91.2	93.0

[A]AT MEASURED ROTOR SOLIDITY AND EXIT SWIRL.
[B]DEPENDING ON TWISTED VS. UNTWISTED ROTOR CONFIGURATION.
[C]EXTRAPOLATED FROM FIGURE 23 DATA.

References

1. Stanitz, J. D., "An Approximate Design Method for High-Solidity Blade Elements in Compressors and Turbines," NACA TN 2408 (1951).

2. Stewart, W. L., Glassman, A. J., and Vanco, M. R., "Examination of Axial-Flow Turbine Blade-Loading Characteristics Using Diffusion Parameters," ASME paper No. 67-WA/GT-8.

3. Zweifel, O., "The Spacing of Turbo-Machine Blading, Expecially with Large Angular Deflection," Brown Boveri Review, Vol. 32, No. 12 (Dec. 1945).

4. Stewart, W. L., "Analysis of Two-Dimensional Compressible Flow Loss Characteristics Downstream of Turbomachine Blade Rows in Terms of Basic Boundary Layer Characteristics," NACA TN 3515 (1955).

5. Dunham, J., "A Review of Cascade Data on Secondary Losses in Turbines," Jour. Mech. Eng. Science, Vol. 12 (1970).

6. Schlichting, H., Boundary Layer Theory, 4th edition.

7. Glassman, A. J., ed., Turbine Design and Application, Vol. 2, NASA SP-290 (1973).

8. Lakshminarayana, B., "Methods of Predicting the Tip Clearance Effects in Axial Flow Turbomachinery," Jour. Basic Eng. (Sept. 1970).

9. Hong, Y. S., and Groh, F. G., "Axial Turbine Loss Analysis and Efficiency Prediction Method," Ref. D4-3220, Boeing Co. (March 1966).

10. Shepherd, D. G., Principles of Turbomachinery, MacMillan Co. (1969).

11. Horlock, J. H., Axial Flow Turbines, Butterworths (1966).

12. Kofskey, M., Roelke, R., and Haas, J., "Turbine for a Low-Cost Turbojet Engine," NASA TN D-7625 (1974).

13. Szanca, E., Schum, H., and Hotz, G., "Research Turbine for High-Temperature Core Engine Application," NASA TN-7557 (1974).

14. Haas, J., and Kofskey, M., "Cold-Air Performance of a 12.766-Centimeter-Tip-Diameter Axial-Flow Cooled Turbine," NASA TN D-7881 (1975).

15. Whitney, W., Moffitt, T., and Behning, F., "Cold-Air Investigation of First Stage of 4½-Stage, Fan-Drive Turbine with Average Stage-Loading Factor of 4.66," NASA Technical Paper 1780 (1981).

16. Roelke, R., and Haas, J., "Cold-Air Performance of Compressor Drive Turbine of Department of Energy Upgraded Automobile Gas Turbine Engine," NASA TM 82818 (1982).

17. Moffitt, T., Szanca, E., Whitney, W., and Behning, F., "Design and Cold-Air Test of Single-Stage Uncooled Core Turbine with High Work Output," NASA Technical Paper 1680 (1980).

18. Kofskey, M., and Nusbaum, W., "Design and Cold-Air Investigation of a Turbine for a Small Low-Cost Turbofan Engine," NASA TN D-6967 (1972).

19. Jenkins, R. M., "A Comprehensive Method for Preliminary Design Optimization of Axial Gas Turbine Stages," presented at AIAA/SAE/ASME 18th Joint Propulsion Conference, AIAA-82-1264, June 1982.

20. Jenkins, R. M., "A Comprehensive Method for Preliminary Design Optimization of Axial Gas Turbine Stages, Part II: Code Verification," presented at AIAA/SAE/ASME 19th Joint Propulsion Conference, AIAA-83-1403, June 1983.

APPENDIX A

STANITZ METHOD SUPPORTING EQUATIONS

The Stanitz method explicitly requires the following thermodynamic flow properties:

$$\frac{T''_M}{T'_M}\ ,\quad \frac{T'_M}{T'_i}\ ,\quad \frac{T''_M}{T''_i}\ ,\quad \frac{P_M}{P'_i}\ ,\quad \frac{P''_M}{P''_i}$$

Energy Equation:

$$c_p T_M + \frac{V_M^2}{2gJ} = c_p T_i + \frac{V_i^2}{2gJ} + W_{shaft} \qquad (1)$$

Moment of Momentum:

$$W_{shaft} = \frac{1}{gJ}\left[(UV_u)_M - (UV_u)_i\right] \qquad (2)$$

Upon substitution of Eq. (2) into Eq. (1), we have

$$\frac{T'_M}{T'_i} = 1 - \frac{(UV_u)_i - (UV_u)_M}{gJc_pT'_i} \qquad (3)$$

which can be written, after some manipulation, as

$$\frac{T'_M}{T'_i} = 1 - 2\left(\frac{\gamma - 1}{\gamma + 1}\right)\left(\frac{U}{a'_{cr}}\right)_i\left[\left(\frac{V_u}{a'_{cr}}\right)_i - R^*_M\left(\frac{V_u}{a'_{cr}}\right)_M\sqrt{\frac{T'_M}{T'_i}}\right] \qquad (4)$$

Eq. (4) can be combined with Eq. (5) of the main text to yield

$$\boxed{\frac{T'_M}{T'_i} = 1 + \frac{\left(\frac{\gamma - 1}{\gamma}\right)\left(\frac{U}{a'_{cr}}\right)_i}{\left(\frac{\rho V}{\rho' a'_{cr}}\right)_i \cos \alpha_i} \sigma \int_0^M h^* R^* \frac{\Delta P}{P'_i}\, dM} \tag{5}$$

Eqs. (1), (2), and the law of cosines relationship between absolute velocity, V, and relative velocity, W, can be combined to yield

$$\boxed{\frac{T''_M}{T''_i} = 1 - \frac{\gamma-1}{\gamma+1} \left(\frac{U}{a'_{cr}}\right)_i^2 \left(\frac{T'_i}{T''_i}\right) (1 - R^{*2}_M)} \tag{6}$$

From the definitions of absolute and relative total temperature we can write

$$T''_M - T'_M = \frac{U_M^2}{2gJc_p}\left[1 - 2\left(\frac{V_u}{U}\right)_M\right] \tag{7}$$

with

$$\left(\frac{V_u}{U}\right)_M = \frac{\left(\frac{V_u}{a'_{cr}}\right)_M \sqrt{\frac{T'_M}{T'_i}}}{\left(\frac{U}{a'_{cr}}\right)_i R^*_M} \tag{8}$$

Eqs. (7) and (8) may be combined to give

$$\boxed{\frac{T''_M}{T'_M} = 1 - \frac{\gamma-1}{\gamma+1}\left(\frac{U}{a'_{cr}}\right)_i^2\left(\frac{T'_i}{T'_M}\right) R^{*2}_M \left[\frac{2\left(\frac{V_u}{a'_{cr}}\right)_M \sqrt{\frac{T'_M}{T'_i}}}{\left(\frac{U}{a'_{cr}}\right)_i R^*_M} - 1\right]} \tag{9}$$

Now if no flow losses existed,

$$\frac{P''_M}{P''_i} = \left(\frac{P''_M}{P''_i}\right)_{isen} = \left(\frac{T''_M}{T''_i}\right)^{\frac{\gamma}{\gamma-1}} \tag{10}$$

so that

$$P''_{M_{isen}} = P''_i\left(\frac{T''_M}{T''_i}\right)^{\frac{\gamma}{\gamma-1}} \tag{11}$$

Since blade losses do exist, the actual relative total pressure, $P''_{M_{act}}$, will differ from $P''_{M_{isen}}$ for all values of M. It will be assumed that the difference between isentropic and actual total pressure conditions varies linearly with axial distance along the mean camberline. Thus

$$\frac{P''_{M_{act}} - P''_{M_{isen}}}{P''_{e_{act}} - P''_{e_{isen}}} = M \tag{12}$$

or

$$\left(\frac{P''_M}{P''_i}\right)_{act} = \left(\frac{P''_M}{P''_i}\right)_{isen} + \left\{\left(\frac{P''_e}{P''_i}\right)_{act} - \left(\frac{P''_e}{P''_i}\right)_{isen}\right\} M \tag{13}$$

Substituting Eq. (10) into Eq. (13), we have

$$\boxed{\left(\frac{P''_M}{P''_i}\right)_{act} = \left(\frac{T''_M}{T''_i}\right)^{\frac{\gamma}{\gamma-1}} + \left\{\left(\frac{P''_e}{P''_i}\right)_{act} - \left(\frac{T''_e}{T''_i}\right)^{\frac{\gamma}{\gamma-1}}\right\} M} \tag{14}$$

Equation (14) is usable in both rotating and non-rotating reference frames. For stators, Eq. (14) reduces to the familiar assumption of linear total pressure loss, i.e.,

$$\frac{P'_M}{P'_i} = 1 + \left(\frac{P'_e}{P'_i} - 1\right) M \tag{15}$$

The quantity $(P''_e/P''_i)_{act}$ is determined from the Stewart mixing hypothesis (Appendix B).

Finally, since

$$\frac{P_M}{P'_i} = \frac{P_M}{P''_M}\,\frac{P''_M}{P''_i}\,\frac{P''_i}{P'_i}$$

we have

$$\boxed{\frac{P_M}{P'_i} = \left\{\frac{T_M}{T''_M}\,\frac{T''_i}{T'_i}\right\}^{\frac{\gamma}{\gamma-1}} \left(\frac{P''_M}{P''_i}\right)} \tag{16}$$

where

$$\frac{T_M}{T''_M} = 1 - \frac{\gamma-1}{\gamma+1}\left(\frac{W}{a''_{cr}}\right)^2_M$$

must be evaluated for both the suction surface and the pressure surface of each blade.

APPENDIX B

PROFILE LOSS

Profile loss is defined here as a combination of frictional effects arising from the flow of a viscous fluid over a solid surface and the subsequent downstream mixing of the suction-surface and the pressure-surface boundary layers. Pressure drag, which results from the flow of fluid past a finite-thickness trailing edge, is implicitly contained in the Stewart analyses (Appendix C).

Laminar Regime

Laminar boundary layer properties are calculated as follows:[6]

1. The freestream velocity function V(x) and its derivative dV/dx are known.

2. The momentum thickness, $\theta(x)$ is calculated by

$$\frac{\theta(x)}{\ell} = \frac{V}{V_\ell}^{-3} \cdot \left[\frac{1}{2} C_f \left\{\int_0^{x_t/\ell} \left(\frac{V}{V_\ell}\right)^5 d\left(\frac{x}{\ell}\right)\right\}^{1/2}\right] \tag{1}$$

where V_ℓ = free stream velocity at the cascade exit, i.e., at $x = \ell$

$C_f = 1.328\ (Re_\ell)^{-1/2}$; Re_ℓ = Reynolds No.

x_t = location where boundary layer transition occurs

3. The parameter Z, given by

$$Z = \frac{\theta^2}{\nu} \tag{2}$$

where ν = dynamic viscosity, is defined.

4. The parameter K, given by

$$K = Z \frac{dV}{dx} \tag{3}$$

is defined.

5. The shape factor Λ, given by

$$K = \left(\frac{37}{315} - \frac{1}{945}\Lambda - \frac{1}{9072}\Lambda^2\right)^2 \Lambda \tag{4}$$

is obtained by iteration.

6. The displacement thickness, δ^*, is then calculated from

$$\frac{\delta^*}{\theta} = \frac{\frac{3}{10} - \frac{1}{120}\Lambda}{\frac{37}{315} - \frac{1}{945}\Lambda - \frac{1}{9072}\Lambda^2} \tag{5}$$

Transition

Reference 6 indicates that the point of instability for boundary layers in a pressure gradient (that is, the point at which disturbances begin to amplify) can be determined through consideration of a "critical" Reynolds number, Re_{cr}, based on boundary layer displacement thickness. Further, this critical Reynolds number is a function of the shape factor Λ. For the present model, two assumptions are made:

(1) $Re_{cr}(\Lambda)$ is obtained from a curve fit of data given in [6].

(2) The point of instability is assumed to coincide with the point of transition.

Turbulent Regime

Boundary layer momentum thickness is computed from an equation appearing in References (3) and (4):

$$\theta(x) =$$

$$\frac{0.231}{\left(\frac{\rho}{\rho'}\frac{V}{a'_{cr}}\right)\left(\frac{V}{a'_{cr}}\right)^{(1+H_b)}}\left\{\int_0^x \frac{\left[\left(\frac{\rho}{\rho'}\frac{V}{a'_{cr}}\right)\left(\frac{V}{a'_{cr}}\right)^{(1+H)}\right]^{1.268}\left(\frac{\mu}{\rho V}\right)^{0.268}(1-A)^{0.467}dx}{10^{0.678(2n+1)}}\right\}^{0.7886} \tag{6}$$

where θ = boundary layer momentum thickness at the blade trailing edge

μ = viscosity

n = exponent in the boundary layer power-law velocity profile, taken as 1/7

x = distance along blade surface

The quantity "A" is defined as

$$A = \frac{\gamma-1}{\gamma+1}\left(\frac{V}{a'_{cr}}\right)^2 \tag{7}$$

and "H" is the boundary layer form factor, defined as

$$H = \frac{\sum_{m=0}^{\infty}\frac{(2m+1)A^m}{(2m+1)n+1}}{\sum_{m=0}^{\infty}\frac{A^m}{[(2m+1)n+1][2(m+1)n+1]}} \tag{8}$$

from Reference (7). All other parameters used in Equation (6) are defined elsewhere.

Since the form factor is also defined as

$$H = \frac{\delta^*}{\theta} \tag{9}$$

where δ^* is boundary layer displacement thickness, Equations (6), (7), (8) and (9) adequately describe all the pertinent turbulent boundary layer parameters required to calculate profile loss. Profile loss itself is calculated from the Stewart Mixing Hypothesis of Reference (4), which is detailed in Appendix C.

APPENDIX C

STEWART MIXING HYPOTHESIS[4]

Following Stewart, we define stations at the cascade inlet, cascade exit, and (somewhere) downstream of the cascade exit, as shown in Figure C-1.

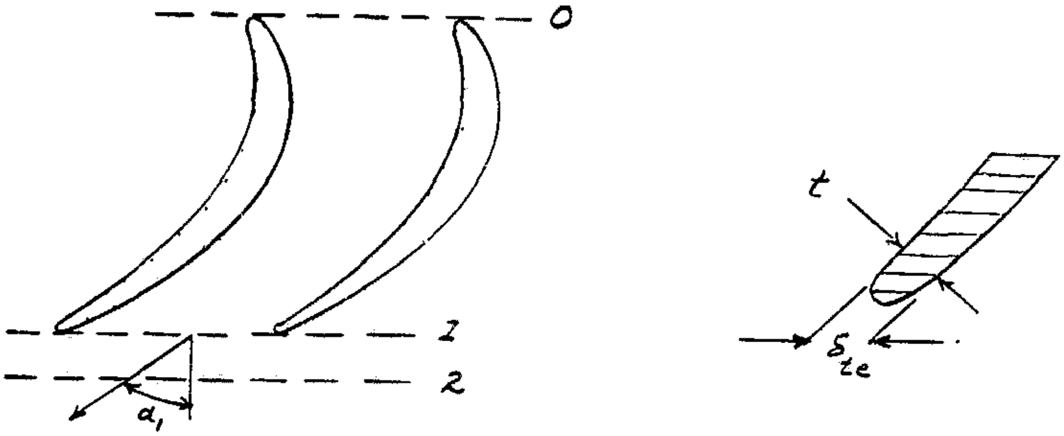

Figure C-1

Continuity:

$$\cos\,\alpha_1 \int_0^1 (\rho V)_1 d(\tfrac{u}{s}) = (\rho V)_2 \cos\,\alpha_2 \tag{1}$$

Axial Momentum:

$$gP_1 + \cos^2\,\alpha_1 \int_0^1 (\rho V^2)_1 d(\tfrac{u}{s}) = gP_2 + \cos^2\,\alpha_2 (\rho V^2)_2 \tag{2}$$

Tangential Momentum:

$$\sin\,\alpha_1\,\cos\,\alpha_1 \int_0^1 (\rho V^2)_1 d(\tfrac{u}{s}) = \sin\,\alpha_2\,\cos\,\alpha_2 (\rho V^2)_2 \tag{3}$$

Define

$$1 - \delta^* - \delta_{te} = \int_0^1 \left(\frac{\rho V}{\rho_{fs} V_{fs}}\right)_1 d(\frac{u}{s}) \tag{4-a}$$

$$\theta^* = \int_0^1 \left[1 - \left(\frac{V}{V_{fs}}\right)_1\right] \left(\frac{\rho V}{\rho_{fs} V_{fs}}\right)_1 d(\frac{u}{s}) \tag{4-b}$$

where the subscript "fs" refers to freestream conditions (assumed isentropic).

We shall define a set of reference (total) conditions at station 1 and assume adiabatic flow throughout. Eqs. (1) and (4-a) can then be written as

$$(1 - \delta^* - \delta_{te})\left(\frac{\rho V_x}{\rho' a'_{cr}}\right)_{fs,1} = \left(\frac{\rho V_x}{\rho' a'_{cr}}\right)_2 \frac{P'_2}{P'_{fs,1}} \tag{5}$$

where the subscript "x" refers to the axial direction.

Eq. (4-b) can be combined with (4-a) to become

$$\theta^* = (1 - \delta^* - \delta_{te}) - \int_0^1 \left(\frac{\rho}{\rho_{fs}}\right)_1 \left(\frac{V}{V_{fs}}\right)_1^2 d(\frac{u}{s}) \tag{6}$$

Eq. (2) can then be written, after algebraic manipulation, as

$$\left(\frac{\gamma+1}{2\gamma}\right)\left(\frac{P_1}{P'_{fs,1}}\right) + (1 - \delta^* - \delta_{te} - \theta^*)\left(\frac{\rho V_x^2}{\rho' a'^2_{cr}}\right)_{fs,1} = \left(\frac{\gamma+1}{2\gamma}\right)\left(\frac{P_2}{P'_2}\right)\left(\frac{P'_2}{P'_{fs,1}}\right) + \left(\frac{\rho V_x^2}{\rho' a'^2_{cr}}\right)_2 \left(\frac{P'_2}{P'_{fs,1}}\right) \tag{7}$$

while Eq. (3) can be written as

$$(1 - \delta^* - \delta_{te} - \theta^*)\left(\frac{\rho}{\rho'} \frac{V_x}{a'_{cr}} \frac{V_u}{a'_{cr}}\right)_{fs,1} = \left(\frac{\rho}{\rho'} \frac{V_x}{a'_{cr}} \frac{V_u}{a'_{cr}}\right)_2 \left(\frac{P'_2}{P'_{fs,1}}\right) \tag{8}$$

where the subscript "u" refers to the tangential direction. We shall define

$$A_{fs,1} = \frac{\gamma-1}{\gamma+1}\left(\frac{V}{a'_{cr}}\right)^2_{fs,1} \tag{9}$$

and set

$$\frac{P_1}{P'_{fs,1}} = \frac{\rho_1}{\rho'_{fs,1}} \frac{T_1}{T'_{fs,1}} = \left(\frac{\rho}{\rho'}\right)_{fs,1} (1 - A_{fs,1}) \tag{10}$$

Now solve Eq. (5) for $\dfrac{P'_2}{P'_{fs,1}}$:

$$\frac{P'_2}{P'_{fs,1}} = (1 - \delta^* - \delta_{te}) \frac{\left(\dfrac{\rho V_x}{\rho' a'_{cr}}\right)_{fs,1}}{\left(\dfrac{\rho V_x}{\rho' a'_{cr}}\right)_2} \tag{11}$$

Substitute Eqs. (11) and (10) into Eq. (7) and solve for $\left(\dfrac{V_x}{a'_{cr}}\right)_2$:

$$\left(\frac{V_x}{a'_{cr}}\right)^2_2 - C\left(\frac{V_x}{a'_{cr}}\right)_2 + \left(\frac{\gamma+1}{2\gamma}\right) \left\{1 - \frac{\gamma-1}{\gamma+1}\left[\left(\frac{V_x}{a'_{cr}}\right)^2_2 + \left(\frac{V_u}{a'_{cr}}\right)^2_2\right]\right\} = 0 \tag{12}$$

where

$$C = \frac{(1 - A_{fs,1}) \left(\frac{\gamma+1}{2\gamma}\right) + (1 - \delta^* - \delta_{te} - \theta^*) \left(\frac{V_x}{a'_{cr}}\right)^2_{fs,1}}{(1 - \delta^* - \delta_{te}) \left(\frac{V_x}{a'_{cr}}\right)_{fs,1}} \tag{13}$$

Substitute Eq. (11) into Eq. (8) and solve for $\left(\frac{V_u}{a'_{cr}}\right)_2$:

$$\left(\frac{V_u}{a'_{cr}}\right)_2 = \frac{(1 - \delta^* - \delta_{te} - \theta^*) \left(\frac{V_u}{a'_{cr}}\right)_{fs,1}}{(1 - \delta^* - \delta_{te})} = D \tag{14}$$

Eq. (12) can then be written as

$$\left(\frac{V_x}{a'_{cr}}\right)^2_2 - \frac{2\gamma}{\gamma+1} C \left(\frac{V_x}{a'_{cr}}\right)_2 + \left(1 - \frac{\gamma-1}{\gamma+1} D^2\right) = 0 \tag{15}$$

which has the solution

$$\left(\frac{V_x}{a'_{cr}}\right)_2 = \frac{\gamma C}{\gamma+1} - \sqrt{\left(\frac{\gamma C}{\gamma+1}\right)^2 - 1 + \frac{\gamma-1}{\gamma+1} D^2} \tag{16}$$

Then

$$\left(\frac{\rho}{\rho'}\right)_2 = \left\{1 - \frac{\gamma-1}{\gamma+1} \left[\left(\frac{V_x}{a'_{cr}}\right)^2_2 + D^2\right]\right\}^{\frac{1}{\gamma-1}} \tag{17}$$

and

$$\frac{P'_2}{P'_{fs,1}} = (1 - \delta^* - \delta_{te}) \frac{\left(\frac{\rho V_x}{\rho' a'_{cr}}\right)_{fs,1}}{\left(\frac{\rho V_x}{\rho' a'_{cr}}\right)_2} \tag{18}$$

For stators, $P'_{fs,1} = P'_0$ so that

$$\frac{P'_2}{P'_0} = (1 - \delta^* - \delta_{te}) \frac{\left(\frac{\rho V_x}{\rho' a'_{cr}}\right)_{fs,1}}{\left(\frac{\rho V_x}{\rho' a'_{cr}}\right)_2} \tag{19}$$

For rotors, we will assume no radius change between the cascade exit (station 1) and the mixed plane (station 2); there may, however, be a change in radius between the cascade inlet (station 0) and the cascade exit. We have

$$\frac{P''_2}{P''_{fs,1}} = (1 - \delta^* - \delta_{te}) \frac{\left(\frac{\rho W_x}{\rho'' a''_{cr}}\right)_{fs,1}}{\left(\frac{\rho W_x}{\rho'' a''_{cr}}\right)_2}$$

Now

$$\frac{P''_2}{P''_{fs,1}} = \frac{P''_2}{P''_0} \frac{P''_0}{P''_{fs,1}}$$

where $\frac{P''_0}{P''_{fs,1}}$ is an isentropic change given by

$$\frac{P''_0}{P''_{fs,1}} = \left(\frac{T''_0}{T''_{fs,1}}\right)^{\frac{\gamma}{\gamma-1}}$$

Thus, we have

$$\left(\frac{P_2''}{P_0''}\right)\left(\frac{T_0''}{T_1''}\right)^{\frac{\gamma}{\gamma-1}} = (1 - \delta^* - \delta_{te})\,\frac{\left(\dfrac{\rho W_x}{\rho'' a_{cr}''}\right)_1}{\left(\dfrac{\rho W_x}{\rho'' a_{cr}''}\right)_{mix}} \tag{20}$$

where the subscript "mix" refers to station 2 conditions. Note that the LHS of Eq. (20) appears in the efficiency equation, Eq. (11) of Appendix E. Pressure loss terms are thus functions of δ^*, and θ^*; no isentropic terms appear.

APPENDIX D

BLOCKAGE CALCULATIONS

The effect of leading edge and trailing edge blockage is determined from the continuity equation and the assumption that moving from blocked to unblocked flow (and vice versa) leaves the tangential momentum (velocity) unchanged. Thus, one can easily show that, for the trailing edge,

$$\cos \beta_{TE} = \frac{\dfrac{t_{TE}}{s}}{1 - \dfrac{\left[1 - \left(\dfrac{\gamma-1}{\gamma+1}\right)\left(\dfrac{V}{a'_{cr}}\right)^2_{MIX}\right]^{\frac{1}{\gamma-1}} \tan \beta_{TE}}{\left[1 - \left(\dfrac{\gamma-1}{\gamma+1}\right)\left(\dfrac{V}{a'_{cr}}\right)^2_{MIX} \dfrac{\sin^2 \beta_{MIX}}{\sin^2 \beta_{TE}}\right]^{\frac{1}{\gamma-1}} \tan \beta_{MIX}}} \quad (1)$$

and for the leading edge

$$\cos \beta_{LE} = \frac{\dfrac{t_{LE}}{s}}{1 - \dfrac{\left[1 - \left(\dfrac{\gamma-1}{\gamma+1}\right)\left(\dfrac{V}{a'_{cr}}\right)^2_{MIX}\right]^{\frac{1}{\gamma-1}} \tan \beta_{LE}}{\left[1 - \left(\dfrac{\gamma-1}{\gamma+1}\right)\left(\dfrac{V}{a'_{cr}}\right)^2_{MIX} \dfrac{\sin^2 \beta_{MIX}}{\sin^2 \beta_{LE}}\right]^{\frac{1}{\gamma-1}} \tan \beta_{MIX}}} \quad (2)$$

where β_{TE}, β_{LE}, β_{MIX} = trailing edge blade angle, leading edge blade angle, and appropriate downstream and upstream flow angles, respectively

t_{TE}, t_{LE} = trailing edge and leading edge blade thickness, respectively

s = blade spacing

The critical velocity ratio, $\frac{V}{a'_{cr}}$, is always defined relative to the blade, whether for stators or for rotors.

It should be noted that the present model uses Equations (1) and (2) to modify (assumed) blade loadings to account for finite leading and trailing edge blade thickness.

APPENDIX E

STAGE EFFICIENCY

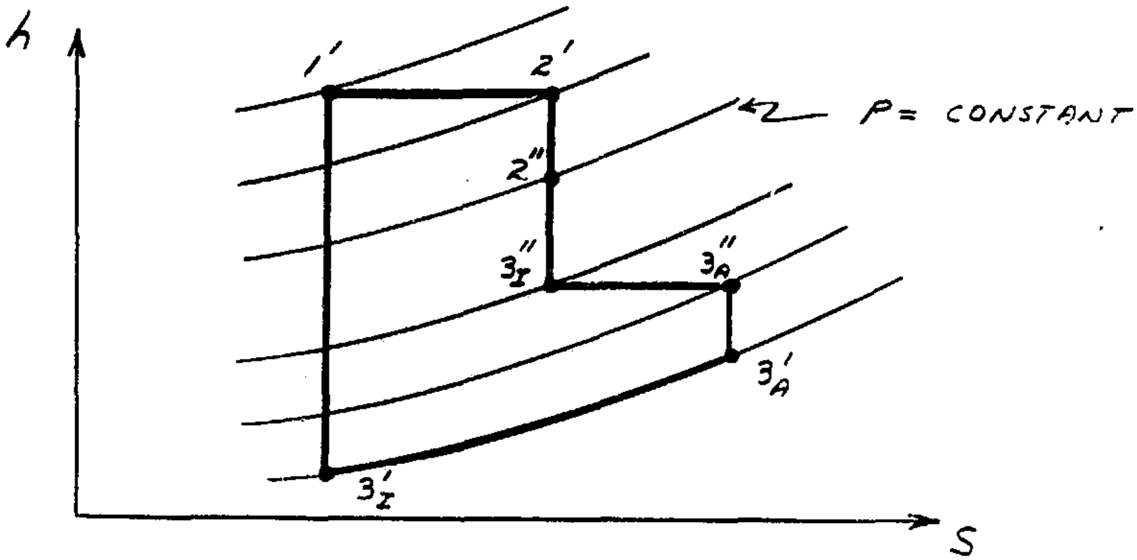

Figure E-1

By definition, the adiabatic efficiency of the turbine (stage) expansion process shown schematically in Figure E-1 is

$$\eta_{T-T} = \frac{T_1' - T_{3A}'}{T_1' - T_{3I}'} \tag{1}$$

which can be written as

$$\eta_{T-T} = \frac{1}{1 + \frac{T_{3A}'}{T_1' - T_{3A}'}\left(1 - \frac{T_{3I}'}{T_{3A}'}\right)} \tag{2}$$

Denoting entropy changes by Δs, we have

$$\Delta s_{total} = \Delta s_{stator} + \Delta s_{rotor} \tag{3}$$

where

$$\Delta s \equiv c_p \ell n \frac{T_y}{T_x} - R\ \ell n \frac{P_y}{P_x} = c_p \ell n \frac{\frac{T_y}{T_x}}{\left(\frac{P_y}{P_x}\right)^{\frac{\gamma-1}{\gamma}}} \tag{4}$$

Now

$$\Delta s_{total} = \Delta s_{1'\to 3_I'\to 3_A'} = c_p \ell n \frac{T_{3A}'}{T_{3I}'} \tag{5}$$

$$\Delta s_{stator} = \Delta s_{1'\to 2'} = c_p \ell n \left(\frac{P_2'}{P_1'}\right)^{-\frac{\gamma-1}{\gamma}} \tag{6}$$

$$\Delta s_{rotor} = \Delta s_{2''\to 3_I''\to 3_A''} = c_p \ell n \left(\frac{P_{3A}''}{P_{3I}''}\right)^{-\frac{\gamma-1}{\gamma}} \tag{7}$$

From Eq. (7) we can write

$$\frac{P_{3A}''}{P_{3I}''} = \frac{P_{3A}''}{P_2''}\left(\frac{P_2''}{P_3''}\right)_I = \frac{P_{3A}''}{P_2''}\left(\frac{T_2''}{T_3''}\right)^{\frac{\gamma}{\gamma-1}} \tag{8}$$

so that

$$\Delta s_{rotor} = c_p \ell n \left[\left(\frac{P_{3A}''}{P_2''}\right)\left(\frac{T_2''}{T_3''}\right)^{\frac{\gamma}{\gamma-1}}\right]^{-\frac{\gamma-1}{\gamma}} = c_p \ell n \left[\left(\frac{P_{3A}''}{P_2''}\right)^{-\frac{\gamma-1}{\gamma}}\left(\frac{T_3''}{T_2''}\right)\right] \tag{9}$$

Thus, combining Eqs. (3), (5), (6), and (9) we have

$$c_p \ln \frac{T'_{3A}}{T'_{3I}} = c_p \ln \left(\frac{P'_2}{P'_1}\right)^{-\frac{\gamma-1}{\gamma}} + c_p \ln \left[\left(\frac{P''_{3A}}{P''_2}\right)^{-\frac{\gamma-1}{\gamma}}\left(\frac{T''_3}{T''_2}\right)\right]$$

or

$$\frac{T'_{3I}}{T'_{3A}} = \left[\left(\frac{P'_2}{P'_1}\right)\left(\frac{P''_{3A}}{P''_2}\right)\right]^{\frac{\gamma-1}{\gamma}} \left(\frac{T''_2}{T''_3}\right) \tag{10}$$

Substituting Eq. (10) into Eq. (2) yields the stage efficiency:

$$\eta_{T-T} = \frac{1}{1 + \frac{T'_{3A}}{T'_1 - T'_{3A}}\left\{1 - \left[\left(\frac{P'_2}{P'_1}\right)\left(\frac{P''_{3A}}{P''_2}\right)\right]^{\frac{\gamma-1}{\gamma}}\left(\frac{T''_2}{T''_3}\right)\right\}} \tag{11}$$

APPENDIX F

MODEL INPUT

The calculation model is set up to use the English system of units (ft, sec, lb_m). Required program input is as follows:

1. GAMMA: ratio of gas specific heats, assumed constant throughout the calculation
2. RGAS: gas constant, ft·lbs/lb_m/°R
3. SPEED: rotor rotational speed, RPM
4. P1P: turbine inlet total pressure, psia
5. T1P: turbine inlet total temperature, °R
6. RWORK: turbine work output required, BTU/lb_m
7. WFLOW: mass flow rate, lb_m/sec
8. RM1, RM2, RM3: pitch line radius at stator inlet, rotor inlet, and rotor exit, respectively (inches). If DSTRES = 0, input RM as zero also.
9. AREA1, AREA2, AREA3: annular flowpath area at stator inlet, rotor inlet, and rotor exit, respectively (sq. inches). If DSTRES = 0, input AREA as zero also.
10. CLEAR: rotor tip clearance, inches
11. TETS: stator trailing edge thickness, inches
12. TETR: rotor trailing edge thickness, inches
13. ALP2: stator exit flow angle, degrees. IF ALP2 = 0, angle will be calculated assuming zero rotor exit swirl. See note on ALP3.
14. ZWFS: stator Zweifel coefficient. Assumed 0.8 if none is input.
15. ZWFR: rotor Zweifel coefficient. Assumed 0.8 if none is input.

16. ALP1: stator inlet flow angle, degrees

17. CHORDS, CHORDR: stator and rotor axial chord, respectively (inches). If input as zero, chords will be calculated by aerodynamic optimization.

18. TELS, TELR: stator and rotor leading edge thickness, respectively (inches)

19. DSTRES: maximum allowable disk stress, psi. If DSTRES ≠ 0, program will calculate a range of possible turbine sizes and performances. If DSTRES = 0, program will perform an aerodynamic optimization for a single case only; RM and AREA must be input in this case.

20. VEXIT: rotor exit axial critical velocity ratio, V_x/a'_{cr}

21. ALP3: rotor exit swirl angle, degrees. ALP3 and ALP2 cannot both be input; if both are, only ALP3 is used. If neither ALP3 or ALP2 is input, program will calculate ALP2 assuming ALP3 = 0.

22. IPLOT: key for blade plot generation. Set IPLOT = 0 for no plot. Note: user will have to tailor program for local plot subroutines.

23. RHODI: disk material density, lb_m/ft^3

24. RHOBL: blade material density, lb_m/ft^3

25. RHOAT: blade-disk attachment region material density, lb_m/ft^3

75KW AUTOMOTIVE TURBINE

APPENDIX G

PROGRAM INPUT PARAMETERS

GAMMA	RGAS	ROTOR SPEED (RPM)	MASS FLOW RATE (LB-SEC)	TURBINE INLET PRESSURE (PSI)	TURBINE INLET TEMPERATURE, R	WORK REQUIRED (BTU/LB)
1.300	53.370	58500.0	1.318	57.652	2385.0	85.261

STATOR INLET MEAN RADIUS (INCHES)	ROTOR INLET MEAN RADIUS (INCHES)	ROTOR EXIT MEAN RADIUS (INCHES)	STATOR INLET AREA (SQ INCHES)	ROTOR INLET AREA (SQ INCHES)	ROTOR EXIT AREA (SQ INCHES)	STATOR T.E. THICKNESS (INCHES)	ROTOR T.E. THICKNESS (INCHES)	ROTOR CLEARANCE (INCHES)
0.000	0.000	0.000	0.000	0.000	0.000	0.000	0.000	0.010

STATOR INLET FLOW ANGLE	STATOR EXIT FLOW ANGLE	STATOR ZWEIFEL COEFFICIENT	ROTOR ZWEIFEL COEFFICIENT	STATOR CHORD (INCHES)	ROTOR CHORD (INCHES)
48.70	0.00	0.664	0.889	0.000	0.000

STATOR L.E. THICKNESS (INCHES)	ROTOR L.E. THICKNESS (INCHES)	ALLOWABLE DISK STRESS (PSI)	ROTOR EXIT AXIAL MACH NUMBER	BLADE PLOT OPTION 0 = NO PLOT 1 = PLOT	ROTOR EXIT SWIRL ANGLE
0.000	0.000	50000.	0.486	0	-21.12

DISK MATERIAL DENSITY (LBS/FT3)	BLADE MATERIAL DENSITY (LBS/FT3)	DISK RIM MATERIAL DENSITY (LBS/FT3)
500.0	500.0	500.0

PROGRAM DEFAULT VALUES

STATOR EXIT FLOW ANGLE	CALCULATED FROM WORK AND FLOW CONDITIONS
STATOR ZWEIFEL COEFFICIENT	0.8
ROTOR ZWEIFEL COEFFICIENT	0.8
STATOR CHORD	OPTIMIZED ON MINIMUM CASCADE LOSS COEFFICIENT
ROTOR CHORD	OPTIMIZED ON MINIMUM CASCADE LOSS COEFFICIENT

THE FOLLOWING IS A LIST OF POSSIBLE CONFIGURATIONS FOR THE INPUT CONDITIONS SPECIFIED

EACH CONFIGURATION IS CONSTRAINED BY THE FOLLOWING (CONSTANT) PARAMETERS

RPM
MASS FLOW
TURBINE INLET TOTAL TEMPERATURE AND PRESSURE
WORK REQUIREMENT
ROTOR CLEARANCE
ROTOR EXIT AXIAL MACH NO.
ROTOR EXIT SWIRL
STATOR AND ROTOR ZWEIFEL COEFFICIENTS

PASS	ETA T-T	ETA T-S	U HUB (FPS)	U TIP (FPS)	ROTOR EXIT HUB RADIUS (INCHES)	ROTOR EXIT TIP RADIUS (INCHES)	BLADE STRESS (PSI)	DISK STRESS (PSI)	ROTOR LIFE (HOURS)
1	0.7010	0.5919	717.	1025.	1.404	2.008	23171.	19024.	0.2404E 03
	NOTE ..... PROGRAM PREDICTS STATOR (MEANLINE) CHOKING FOR THE CONDITIONS OF PASS 1								
2	0.7538	0.6271	742.	1027.	1.453	2.012	21785.	18705.	0.2944E 03
	NOTE ..... PROGRAM PREDICTS STATOR (MEANLINE) CHOKING FOR THE CONDITIONS OF PASS 2								
3	0.7633	0.6332	759.	1037.	1.486	2.031	21550.	18699.	0.2925E 03
	NOTE ..... PROGRAM PREDICTS STATOR (MEANLINE) CHOKING FOR THE CONDITIONS OF PASS 3								
4	0.7694	0.6368	775.	1047.	1.519	2.052	21401.	18748.	0.2858E 03
	NOTE ..... PROGRAM PREDICTS STATOR (MEANLINE) CHOKING FOR THE CONDITIONS OF PASS 4								
5	0.7743	0.6397	791.	1058.	1.550	2.073	21278.	18841.	0.2777E 03
	NOTE ..... PROGRAM PREDICTS STATOR (MEANLINE) CHOKING FOR THE CONDITIONS OF PASS 5								
6	0.7775	0.6415	807.	1069.	1.581	2.094	21192.	18980.	0.2676E 03
7	0.7805	0.6432	823.	1080.	1.612	2.116	21111.	19131.	0.2574E 03
8	0.7826	0.6442	839.	1091.	1.643	2.138	21047.	19340.	0.2466E 03
9	0.7850	0.6454	856.	1103.	1.673	2.160	20979.	19555.	0.2364E 03
10	0.7853	0.6452	870.	1114.	1.703	2.183	20952.	19782.	0.2245E 03

11	0.7861	0.6454	885.	1126.	1.733	2.205	20915.	20051.	0.2136E 03
12	0.7872	0.6457	900.	1138.	1.763	2.228	20873.	20329.	0.2033E 03
13	0.7877	0.6456	915.	1149.	1.793	2.251	20841.	20640.	0.1930E 03
14	0.7881	0.6455	930.	1161.	1.822	2.274	20811.	20970.	0.1831E 03
15	0.7872	0.6445	945.	1173.	1.852	2.298	20808.	21299.	0.1727E 03
16	0.7883	0.6448	960.	1185.	1.881	2.321	20763.	21664.	0.1642E 03
17	0.7877	0.6440	975.	1197.	1.910	2.344	20751.	22029.	0.1549E 03
18	0.7870	0.6430	990.	1209.	1.939	2.368	20742.	22424.	0.1461E 03
19	0.7854	0.6416	1005.	1221.	1.968	2.392	20748.	22822.	0.1372E 03
20	0.7845	0.6406	1020.	1233.	1.997	2.415	20743.	23245.	0.1292E 03
21	0.7826	0.6389	1034.	1245.	2.026	2.439	20756.	23671.	0.1211E 03
...									

NOTE ... OF 21 SOLUTIONS OBTAINED 21 ARE (IS) WITHIN THE RANGE OF THE SPECIFIED DISK STRESS

THE FOLLOWING IS AN AERODYNAMICALLY OPTIMIZED STAGE CHOSEN FROM THE POSSIBLE FLOWPATH CONFIGURATIONS ABOVE

COMPUTED FLOW PARAMETERS AND VELOCITY DIAGRAMS

STATOR

STATOR INLET CRITICAL VELOCITY RATIO, V/VCR	0.509
STATOR INLET SWIRL VELOCITY RATIO, VU/VCR	0.383
STATOR EXIT CRITICAL VELOCITY RATIO, V/VCR	0.877
STATOR EXIT AXIAL VELOCITY RATIO, VX/VCR	0.456
STATOR EXIT SWIRL VELOCITY RATIO, VU/VCR	0.749
STATOR EXIT ABSOLUTE TOTAL PRESSURE	54.513
STATOR ABSOLUTE TOTAL PRESSURE LOSS RATIO, ...	0.946

ROTOR

ROTOR EXIT AXIAL CRITICAL VELOCITY RATIO, VX/VCR .	0.486
ROTOR EXIT SWIRL VELOCITY RATIO, VU/VCR	-0.188
ROTOR EXIT CRITICAL VELOCITY RATIO, V/VCR	0.521
ROTOR INLET RELATIVE VELOCITY RATIO, W/WCR	0.538
ROTOR EXIT RELATIVE VELOCITY RATIO, W/WCR	0.842
ROTOR INLET BLADE SPEED RATIO, U/VCR	0.498
ROTOR EXIT BLADE SPEED RATIO, U/VCR	0.531
ROTOR RELATIVE TOTAL PRESSURE LOSS RATIO	0.946
ROTOR EXIT ABSOLUTE TOTAL PRESSURE	29.590
ROTOR EXIT ABSOLUTE TOTAL TEMPERATURE	2098.1
ROTOR TIP SPEED (FT PER SEC)	1183.5

STAGE

ROTOR EXIT HUB RADIUS (INCHES)	1.884
ROTOR EXIT TIP RADIUS (INCHES)	2.318
ROTOR INLET HUB RADIUS (INCHES)	1.884
ROTOR INLET TIP RADIUS (INCHES)	2.233
STATOR INLET HUB RADIUS (INCHES)	1.884
STATOR INLET TIP RADIUS (INCHES)	2.233

ROTOR EXIT ANNULUS AREA (SQ INCHES)	5.736
ROTOR INLET ANNULUS AREA (SQ INCHES)	4.514
STAGE REACTION	0.425
STAGE WORK COEFFICIENT BASED ON MEAN RADIUS .	1.856
STAGE WORK COEFFICIENT BASED ON HUB RADIUS ..	2.308
TURBINE TOTAL-TOTAL PRESSURE RATIO	1.948

FLOW ANGLES

STATOR INLET ANGLE	48.699
STATOR EXIT ANGLE	58.678
ROTOR INLET ANGLE	28.797
ROTOR EXIT ANGLE	-55.951
ROTOR EXIT SWIRL ANGLE ...	-21.119

CALCULATIONS FOR GENERATION OF STATOR BLADE GEOMETRY

*** COMPUTED AERODYNAMIC LOADING ***

PERCENT MERIDIONAL DISTANCE	SUCTION SURFACE RELATIVE CRITICAL VELOCITY RATIO	PRESSURE SURFACE RELATIVE CRITICAL VELOCITY RATIO
0.000	0.509	0.509
0.100	0.517	0.520
0.200	0.563	0.526
0.300	0.643	0.528
0.400	0.726	0.547
0.500	0.790	0.597
0.600	0.835	0.665
0.700	0.862	0.740
0.800	0.875	0.808
0.900	0.878	0.858
1.000	0.877	0.877

OVERALL BLADE REACTION (R=1-VIN/VOUT) = 0.419
PRESSURE SURFACE DIFFUSION (DP=1-VMIN/VIN) = -0.036
SUCTION SURFACE DIFFUSION (DS=1-VOUT/VMAX) = -0.017

*** (ITERATED) STANITZ METHOD BLADE EXIT PARAMETERS ***

	ITERATED VALUE	ACTUAL VALUE
EXIT (ABSOLUTE) TEMPERATURE	2385.0000	2385.0000
EXIT (ABSOLUTE) TANGENTIAL VELOCITY	0.7490	0.7490
EXIT BLADE ANGLE	58.6776	58.6775
SOLIDITY	2.2719	2.2641
TRAILING EDGE THICKNESS	0.000	0.000

*** FINAL STATOR BLADE PROFILE ***
*** COORDINATES NORMALIZED WITH RESPECT TO BLADE CHORD ***

PERCENT MERIDIONAL DISTANCE	PITCHLINE RADIUS	MEAN CAMBERLINE COORDINATE	BLADE SURFACE COORDINATE	BLADE SURFACE COORDINATE
0.000	2.101	0.0000	0.0000	0.0000
0.100	2.101	0.1123	0.1196	0.1050
0.200	2.101	0.2174	0.2389	0.1959
0.300	2.101	0.3167	0.3478	0.2857
0.400	2.101	0.4197	0.4501	0.3894
0.500	2.101	0.5367	0.5581	0.5153
0.600	2.101	0.6736	0.6815	0.6657
0.700	2.101	0.8303	0.8266	0.8341
0.800	2.101	0.9997	0.9926	1.0068
0.900	2.101	1.1707	1.1677	1.1737
1.000	2.101	1.3370	1.3370	1.3370

BLADE CHORD (INCHES)	BLADE SOLIDITY	BLADE CAMBERLINE LENGTH (INCHES)	BLADE STAGGER ANGLE	BLADE NUMBER
0.2473	2.2719	0.4160	53.21	121

CALCULATIONS FOR GENERATION OF STATOR BLADE ROW AERODYNAMIC PERFORMANCE LOSSES

*** STEWART MIXING LOSS PARAMETERS ***

TOTAL MOMENTUM THICKNESS (DIMENSIONLESS)	0.0356
TOTAL DISPLACEMENT THICKNESS (DIMENSIONLESS)	0.0756
CASCADE EXIT (MIXED) CRITICAL MACH NUMBER	0.8348
PROFILE (FRICTION) TOTAL PRESSURE LOSS	0.9642

*** CASCADE LOSS COEFFICIENTS ***

PROFILE LOSS COEFFICIENT	0.1011
SECONDARY FLOW LOSS COEFFICIENT	0.0556
TOTAL CASCADE LOSS COEFFICIENT	0.1567

NOTE ..... CASCADE GEOMETRY OPTIMIZED AT REYNOLDS NUMBER = 0.87E 05

NOTE ..... PREDICTED SUCTION SURFACE BOUNDARY LAYER TRANSITION AT100.0 PERCENT OF CAMBER LENGTH
PREDICTED PRESSURE SURFACE BOUNDARY LAYER TRANSITION AT**** PERCENT OF CAMBER LENGTH

CALCULATIONS FOR GENERATION OF ROTOR BLADE GEOMETRY

*** COMPUTED AERODYNAMIC LOADING ***

PERCENT MERIDIONAL DISTANCE	SUCTION SURFACE RELATIVE CRITICAL VELOCITY RATIO	PRESSURE SURFACE RELATIVE CRITICAL VELOCITY RATIO
0.000	0.538	0.538
0.100	0.708	0.383
0.200	0.849	0.285
0.300	0.958	0.244
0.400	1.027	0.258
0.500	1.059	0.321
0.600	1.058	0.416
0.700	1.029	0.530
0.800	0.978	0.648
0.900	0.912	0.757
1.000	0.842	0.842

OVERALL BLADE REACTION (R=1-VIN/VOUT) = 0.361
PRESSURE SURFACE DIFFUSION (DP=1-VMIN/VIN) = 0.550
SUCTION SURFACE DIFFUSION (DS=1-VOUT/VMAX) = 0.189

*** (ITERATED) STANITZ METHOD BLADE EXIT PARAMETERS ***

	ITERATED VALUE	ACTUAL VALUE
EXIT (ABSOLUTE) TEMPERATURE	2098.0845	2098.0840
EXIT (ABSOLUTE) TANGENTIAL VELOCITY	-0.1877	-0.1877
EXIT BLADE ANGLE	-55.9507	-55.9508
SOLIDITY	1.4372	1.4314
TRAILING EDGE THICKNESS	0.000	0.000

*** FINAL ROTOR BLADE PROFILE ***
*** COORDINATES NORMALIZED WITH RESPECT TO BLADE CHORD ***

PERCENT MERIDIONAL DISTANCE	PITCHLINE RADIUS	MEAN CAMBERLINE COORDINATE	BLADE SURFACE COORDINATE	BLADE SURFACE COORDINATE
0.000	2.101	0.0000	0.0000	0.0000
0.100	2.101	0.0529	0.0751	0.0307
0.200	2.101	0.0927	0.1489	0.0365
0.300	2.101	0.1124	0.1956	0.0293
0.400	2.101	0.1142	0.2116	0.0169
0.500	2.101	0.1142	0.2128	0.0157
0.600	2.101	0.1142	0.2014	0.0271
0.700	2.101	0.1142	0.1782	0.0503
0.800	2.101	0.1142	0.1474	0.0811
0.900	2.101	0.1142	0.1208	0.1077
1.000	2.101	0.1142	0.1142	0.1142

BLADE CHORD (INCHES)	BLADE SOLIDITY	BLADE CAMBERLINE LENGTH (INCHES)	BLADE STAGGER ANGLE	BLADE NUMBER
0.3979	1.4372	0.4965	6.52	47

CALCULATIONS FOR GENERATION OF ROTOR BLADE ROW AERODYNAMIC PERFORMANCE LOSSES

*** STEWART MIXING LOSS PARAMETERS ***

TOTAL MOMENTUM THICKNESS (DIMENSIONLESS)	0.0425
TOTAL DISPLACEMENT THICKNESS (DIMENSIONLESS)	0.0644
CASCADE EXIT (MIXED) CRITICAL MACH NUMBER	0.8003
PROFILE (FRICTION) TOTAL PRESSURE LOSS	0.9617

*** CASCADE LOSS COEFFICIENTS ***

PROFILE LOSS COEFFICIENT	0.1161
SECONDARY FLOW LOSS COEFFICIENT	0.0504
TOTAL CASCADE LOSS COEFFICIENT	0.1665

NOTE ..... CASCADE GEOMETRY OPTIMIZED AT REYNOLDS NUMBER = 0.78E 05

NOTE ..... PREDICTED SUCTION SURFACE BOUNDARY LAYER TRANSITION AT 53.0 PERCENT OF CAMBER LENGTH
PREDICTED PRESSURE SURFACE BOUNDARY LAYER TRANSITION AT 3.7 PERCENT OF CAMBER LENGTH

FINAL CALCULATIONS FOR STAGE EFFICIENCY

STAGE ADIABATIC EFFICIENCY CALCULATED FROM BLADE
BOUNDARY LAYER AND SECONDARY FLOW LOSSES 0.8433

STAGE EFFICIENCY DECREMENT FOR ROTOR CLEARANCE ... -0.043

FINAL STAGE TOTAL-TOTAL EFFICIENCY 0.8002

FINAL STAGE TOTAL-STATIC EFFICIENCY 0.6523

FINAL STAGE RATING EFFICIENCY 0.7769

STRESS DATA

ALLOWABLE AVERAGE DISK STRESS (INPUT) .... 50000. PSI

COMPUTED AVERAGE DISK STRESS .... 28224. PSI

COMPUTED ROOT BLADE STRESS .... 20531. PSI

EFFICIENCY ITERATION CONVERGED AFTER 4 PASSES

```
C
C      PROGRAM TO COMPUTE ADIABATIC EFFICIENCY FOR
C      SINGLE STAGE AXIAL GAS TURBINES
C
C      WORK PERFORMED UNDER NASA GRANT NO. NSG 3295
C      NASA LEWIS RESEARCH CENTER
C      CLEVELAND, OHIO
C
       DIMENSION VRELS(51),VRELP(51),AM(51),RMSTR(51),HMSTR(51),TMT2P(51)
       DIMENSION PMPIP(51),GRAN(51),SIG(2),CORD(2),TMT2(51),VUCRM(51)
       DIMENSION WUCRM(51),WCRM(51),BETAM(51),EPSM(51),TPTPM(51),THIK(51)
       DIMENSION THIKR(51),THIKL(51),THETA(51),RTHET(51),R(51),DIFF1(2)
       DIMENSION HMS(51),HMP(51),WS(51),WP(51),DTE(2),PLOSS(2),DIFF2(2)
       DIMENSION YPRO(2),YSF(2),YTOT(2),CHRD(200),YTOTL(200),REYNO(200)
       DIMENSION FSL(51),FPL(51),BNUS(51),BNUP(51),DUDXS(51),DUDXP(51)
       DIMENSION FS(51),FP(51),GS(51),GP(51),SEFFY(11),ROS(51),ROP(51)
       DIMENSION CXLEN(51),RADEX(21),EADIAB(21),FADIAB(200),DPSI(21)
       DIMENSION RADEXX(21),TITLE(20),VDP(200)
 4000  READ(45,*,END=999)GAMMA,RGAS,SPEED,P1P,T1P,RWORK,WFLOW
       READ(45,*)RM1,RM2,RM3,AREA1,AREA2,AREA3,CLEAR
       READ(45,*)TETS,TETR,ALP2,ZWFS,ZWFR,ALP1,CHORDS
       READ(45,*)CHORDR,TELS,TELR,DSTRES,VEXIT,ALP3,IPLOT
       READ(45,*)RHODI,RHOBL,RHOAT
       WRITE(6,2101)
       WRITE(6,2102)
       WRITE(6,2103)GAMMA,RGAS,SPEED,WFLOW,P1P,T1P,RWORK
       WRITE(6,2104)
       WRITE(6,2105)RM1,RM2,RM3,AREA1,AREA2,AREA3,TETS,TETR,CLEAR
       WRITE(6,2201)
       WRITE(6,2202) ALP1,ALP2,ZWFS,ZWFR,CHORDS,CHORDR
       WRITE(6,2204) TELS,TELR,DSTRES,VEXIT,IPLOT,ALP3
       WRITE(6,2245)RHODI,RHOBL,RHOAT
       WRITE(6,2203)
       IF(DSTRES.EQ.0.0) WRITE(6,2242)
       IF(DSTRES.EQ.0.0) WRITE(6,2243)
       GAMM1=(GAMMA-1.)/(GAMMA+1.)
       GAMM2=(GAMMA-1.)/GAMMA
       GAMM3=1./(GAMMA-1.)
       SETAL3=ALP3*3.14159/180.
       IF(DSTRES.NE.0.0) RM1=0.0
       IF(DSTRES.NE.0.0) RM2=0.0
       IF(DSTRES.NE.0.0) RM3=0.0
       IF(DSTRES.NE.0.0) AREA1=0.0
       IF(DSTRES.NE.0.0) AREA2=0.0
       IF(DSTRES.NE.0.0) AREA3=0.0
       IF(DSTRES.NE.0.0) ALP1=ALP1*3.14159/180.
       ALP3=ALP3*3.14159/180.
       KPASS=0
       RBEST=0.0
 190   DO 19 I=1,200
       CHRD(I)=0.
       YTOTL(I)=0.
       REYNO(I)=0.
 19    CONTINUE
       IPRINT=0
       NPASS=1
       IF(DSTRES.EQ.0.0) GO TO 175
 180   CALL FDISK(GAMMA,VEXIT,GAMM1,GAMM2,GAMM3,NPASS,KPASS,RGAS,SPEED,
      1P1P,T1P,RWORK,WFLOW,ALP1,RM1,RM2,RM3,H1,H2,H3,T2P,U2,UACR2,U3,
      2V1,VU1,ETA,P2P,T3P,P3P,PRTURB,ALP2,V2,VU2,VWRK2,VWRK3,UACR3,VU3,
      3TPTP2,T2PP,PDPP2,T32PP,T3PP,WU2,WUPP2,BETA2,WPP2,WU3,WUPP3,V3,
      4ALP3,VX3,WXPP3,WPP3,BETA3,P32PP,PLOS1,PLOS2,RH3,RT3,RTS,ACR1,ADP3,
      5H1A,H2A,H3A,VX2,WFACTM,WFACTH,UT3,STGACC,RBEST,T2PPH,ACR3)
       GO TO 11
```

```
175   BLP2=ALP2
      RM1=RM1/12.
      RM2=RM2/12.
      RM3=RM3/12.
      H1=(AREA1/144.)/(2.*3.14159*RM1)
      H2=(AREA2/144.)/(2.*3.14159*RM2)
      H3=(AREA3/144.)/(2.*3.14159*RM3)
      H1A=H1
      H2A=H2
      H3A=H3
      T2P=T1P
      TSTD=518.7
      ASTD=ACRIT(GAMMA,RGAS,TSTD)
      RHSTD=2116.22/(RGAS*TSTD)
      CP=(1./GAMM2)*RGAS/778.26
      U2=3.14159*SPEED*RM2/30.
      ACR1=ACRIT(GAMMA,RGAS,T1P)
      UACR2=U2/ACR1
      U3=U2*RM3/RM2
      UT3=U3*(RM3+H3/2.)/RM3
      ALP1=ALP1*3.14159/180.
      BLP1=ABS(ALP1)
      V1=VELIT(WFLOW,T1P,GAMM1,GAMM3,BLP1,AREA1   ,P1P,RHSTD,ASTD)
      VU1=V1*SIN(ALP1)
      SWPM=(U2**2)/(25036.62*RWORK)
      WORKC=1./SWPM
      ETA=(0.92*SWPM)/(S     0.0227)
      P2P=0.98*P1P
      T3P=T1P-RWORK/CP
10    P3P=P1P*((1.-(1.-T3P/T1P)/ETA)**(1./GAMM2))
      PRTURB=P1P/P3P
      KALP=0
      IF(BLP2.EQ.0.0) GO TO 210
      ALP2=BLP2
      BNGCHK=WFLOW*SQRT(T1P/TSTD)/(((1.-GAMM1)**GAMM3)*AREA2/144.*P2P/
     114.696*RHSTD*ASTD)
      ANGCHK=ACOS(BNGCHK)
      ANGCHK=ANGCHK*180./3.14159
      IF(IPRINT.EQ.1) WRITE(6,2210) ANGCHK
      IF(ALP2.GT.ANGCHK.AND.IPRINT.EQ.1) WRITE(6,2200) ANGCHK
      ALP2=ALP2*3.14159/180.
      ANGCHK=ANGCHK*3.14159/180.
      IF(ALP2.GT.ANGCHK) ALP2=ANGCHK
      V2=VELIT(WFLOW,T1P,GAMM1,GAMM3,ALP2,AREA2,P2P,RHSTD,ASTD)
      VU2=V2*SIN(ALP2)
      VWRK2=VU2*ACR1
      VWRK3=RM2/RM3*VWRK2-32.174*778.26*CP*T1P/U3*(1.-T3P/T1P)
      IF(VWRK3.NE.0.0) KALF=1
      GO TO 220
210   IF(SETAL3.EQ.0.0) GO TO 211
      AL3=ABS(SETAL3)
      V3=VELIT(WFLOW,T3P,GAMM1,GAMM3,AL3,AREA3,P3P,RHSTD,ASTD)
      VU3=V3*SIN(SETAL3)
      VX3=V3*COS(SETAL3)
      ALP3=SETAL3
      ACR3=ACRIT(GAMMA,RGAS,T3P)
      VWRK3=VU3*ACR3
      VWRK2=32.174*778.26*CP*T1P/U2*(1.-T3P/T1P)+RM3/RM2*VWRK3
      VU2=VWRK2/ACR1
      IF(VU2.GT.1.0) GO TO 212
      ALP2=ANGIT(WFLOW,T1P,GAMM1,GAMM3,VU2,AREA2,P2P,RHSTD,ASTD,0)
      CHEK=VU2/SIN(ALP2)
      IF(CHEK.LT.1.0) GO TO 213
212   WRITE(6,2239)
      GO TO 4000
213   V2=CHEK
```

```
      VX2=V2*COS(ALP2)
      UACR3=U3/ACR3
      GO TO 214
211   VWRK3=0.0
13    VWRK2=32.174*778.26*CP*T1P/U2*(1.-T3P/T1P)+RM3/RM2*VWRK3
      VU2=VWRK2/ACR1
      IF(VU2.GE.1.0) GO TO 15
      ALP2=ANGIT(WFLOW,T1P,GAMM1,GAMM3,VU2,AREA2   ,P2P,RHSTD,ASTD,0)
      CHEK=VU2/SIN(ALP2)
      IF(CHEK.LT.1.0) GO TO 12
15    VWRK3=VWRK3-10.
      KALP=1
      GO TO 13
12    V2=CHEK
220   ACR3=ACRIT(GAMMA,RGAS,T3P)
      VX2=V2*COS(ALP2)
      UACR3=U3/ACR3
      VU3=VWRK3/ACR3
214   TPTP2=1.-GAMM1*(UACR2**2.)*(2.*VU2/UACR2-1.)
      T2PP=TPTP2*T2P
      PDPP2=TPTP2**(1./GAMM2)
      T32PP=1.-GAMM1*(UACR2**2.)*(1./TPTP2)*(1.-((RM3/RM2)**2.))
      T3PP=T32PP*T2PP
      ADP2=ACRIT(GAMMA,RGAS,T2PP)
      ADP3=ADP2*SQRT(T32PP)
      WU2=VWRK2-U2
      WUPP2=WU2/ADP2
      BETA2=ASIN((VU2-UACR2)/(SQRT(V2**2+UACR2**2-2.*VU2*UACR2)))
      WPP2=WUPP2/SIN(BETA2)
      WU3=VWRK3-U3
      WUPP3=WU3/ADP3
      IF(SETAL3.NE.0.0) GO TO 216
      IF(KALP.EQ.1) GO TO 14
      V3=VELIT(WFLOW,T3P,GAMM1,GAMM3,0.0,AREA3   ,P3P,RHSTD,ASTD)
      ALP3=0.0
      GO TO 17
14    VUM=VU3
      VUM=ABS(VUM)
      ALP3=ANGIT(WFLOW,T3P,GAMM1,GAMM3,VUM,AREA3   ,P3P,RHSTD,ASTD,1)
      IF(VU3.LT.0.0) ALP3=-ALP3
      V3=VU3/SIN(ALP3)
17    VX3=V3*COS(ALP3)
216   WXPP3=VX3*ACR3/ADP3
      WPP3=SQRT(WXPP3**2+WUPP3**2)
      WFACTM=25036.62*RWORK/(U3**2)
      WFACTH=WFACTM*((RM3/(RM3-H3/2.))**2)
      BETA3=ASIN(WUPP3/WPP3)
      IF(NPASS.NE.1) GO TO 11
      P32PP=T32PP**(1./GAMM2)
      PLOS1=0.98
      PLOS2=P32PP
11    CONTINUE
      IF(IPRINT.EQ.1) WRITE(6,2100)
      IF(RBEST.GT.0.0.AND.IPRINT.EQ.1) WRITE(6,2233)
      IF(IPRINT.EQ.1) WRITE(6,2106)
      IF(IPRINT.EQ.1)WRITE(6,2107)V1,VX3,VU1,VU3,V2,V3,VX2,WPP2
      IF(IPRINT.EQ.1)WRITE(6,2108)VU2,WPP3,P2P,UACR2,PLOS1,UACR3,PLOS2,
     1P3P,T3P,UT3
      IF(DSTRES.EQ.0.0.AND.IPRINT.EQ.1)WRITE(6,2097)
      IF(DSTRES.EQ.0.0.AND.IPRINT.EQ.1)WRITE(6,2240)WFACTM,WFACTH,PRTURB
      IF(DSTRES.EQ.0.0) GO TO 215
      IF(RBEST.EQ.0.0)RADEX(KPASS+1)=RM3
      RH3=RH3*12.
      RH2=RH3
      RH1=RH3
      RT3=RT3*12.
```

```
      ANGZ2=BETA3
      ANGGAM=ABS(BETA2+BETA3)/2.
      ZWEIFL=0.80
      IF(ZWFR.NE.0.0) ZWEIFL=ZWFR
      HEIGHT=(H2A+H3A)*6.
      CHORDB=CHORDR
      R3STR=RM3/RM2
      H3STR=H3/H2
      VUCRI=VU2
      VUCRO=VU3
      AIN=ALP2
      VCRI=V2
      RIN=RM2*12.
      TIPDP=1./TPTP2
      POPI=PLOS2
      TOTIA=T3P/T1P
      TOTIR=T32PP
      PIPDP=1./PDPP2
      TPTPM(1)=TPTP2
      WCRM(1)=WPP2
      TIVIS=T2PP
      RHO2=144.*PDPP2*PLOS1*P1P/(RGAS*T2PP)
      CALL VISCO(T3PP,VISRE)
      RHORP=RHO2*P32PP
      RHORE=RHOV(GAMMA,WPP3)/WPP3*RHORP
      VELRE=WPP3*ADP3
      VELBL=WPP3
      UELBL=WUPP3
      TLE=TELR
      VELBLO=WPP2
      BETALE=BETA2
      TTE=TETR
      BETATE=BETA3
 60   CONTINUE
      IF(DSTRES.EQ.0.0)GO TO 251
      IF(CHORDB.EQ.0.0.AND.RBEST.GT.0.0) GO TO 250
      IF(CHORDB.NE.0.0.AND.RBEST.GT.0.0) GO TO 252
      SOLEST=2.*COS(ANGZ2)*SIN(ABS(ANGZ1-ANGZ2))/(ZWEIFL*COS(ANGZ1))
      CHORD=0.26807*HEIGHT*SOLEST/COS(ANGGAM)
      ITRIG=1
      ICHORD=1
      GO TO 500
 251  IF(CHORDB.EQ.0.0) GO TO 250
 252  CHORD=CHORDB
      ITRIG=1
      ICHORD=1
      GO TO 500
 250  ICHORD=1
      ITRIG=0
      CHORD=HEIGHT/4.
      CHMAX=HEIGHT*3.0
 500  KZWFL=0
  119 SOLID=2.*COS(ANGZ2)*SIN(ABS(ANGZ1-ANGZ2))/(ZWEIFL*COS(ANGZ1))
      SPAC=CHORD/SOLID
      CALL BLOCK(GAMMA,TTE,SPAC,BETATE,UELBL,BETTE,VTE)
      BETLE=BETALE
      VLE=VELBLO
      EXTRM=0.3
      CALL DRANGE(GAMMA,VLE,VTE,EXTRM,DSTART,DCHNGE)
      DPBLD=DSTART
      ABLD=DCHNGE
      DELBD=DCHNGE
      K=1
      KK=0
  117 CONTINUE
 118  IF(IBLD.EQ.2) GO TO 115
```

```
      RT2=RTS*12.
      RT1=RT2
      AREAR=3.14159*(RT3**2-RH3**2)
      AREAS=3.14159*(RT2**2-RH2**2)
      IF(IPRINT.EQ.1)WRITE(6,2109)RH3,RT3,RH2,RT2,RH1,RT1,AREAR,AREAS,
     1STGACC
      IF(IPRINT.EQ.1)WRITE(6,2146)WFACTM,WFACTH,PRTURB
 215  ALP1=ALP1*180./3.14159
      ALP2=ALP2*180./3.14159
      BETA2=BETA2*180./3.14159
      BETA3=BETA3*180./3.14159
      ALP3=ALP3*180./3.14159
      IF(IPRINT.EQ.1) WRITE(6,2098)
      IF(IPRINT.EQ.1) WRITE(6,2141) ALP1,ALP2,BETA2,BETA3,ALP3
      ALP1=ALP1*3.14159/180.
      ALP2=ALP2*3.14159/180.
      BETA2=BETA2*3.14159/180.
      BETA3=BETA3*3.14159/180.
      ALP3=ALP3*3.14159/180.
      IF(IPRINT.EQ.1) WRITE(6,2100)
C
C     COMPUTATION OF TRIAL VELOCITY DIAGRAMS IS COMPLETE
C
      IBLD=1
 20   IF(IBLD.EQ.2) GO TO 50
      IF(IPRINT.EQ.1) WRITE(6,2110)
      RPM=0.0
      ANGZ1=ALP1
      ANGZ2=ALP2
      ANGGAM=ABS(ALP1+ALP2)/2.
      ZWEIFL=0.8
      IF(ZWFS.NE.0.0) ZWEIFL=ZWFS
      HEIGHT=(H1A+H2A)*6.
      CHORDB=CHORDS
      R3STR=RM2/RM1
      H3STR=H2/H1
      VUCRI=VU1
      VUCRO=VU2
      AIN=ALP1
      VCRI=V1
      RIN=RM1*12.
      TIPDP=1.0
      POPI=PLOS1
      TOTIA=1.0
      TOTIR=1.0
      PIPDP=1.0
      TPTPM(1)=1.0
      WCRM(1)=V1
      TIVIS=T1P
      RHO2=144.*P1P/(RGAS*T1P)
      CALL VISCO(T1P,VISRE)
      RHORP=RHO2*P2P/P1P
      RHORE=RHOV(GAMMA,V2)/V2*RHORP
      VELRE=V2*ACR1
      VELBL=V2
      UELBL=VUCRO
      TLE=TELS
      VELBLO=V1
      BETALE=ALP1
      IF(ALP1.EQ.0.0) BETALE=0.00001
      TTE=TETS
      BETATE=ALP2
      GO TO 60
 50   RPM=UACR2
      IF(IPRINT.EQ.1) WRITE(6,2111)
      ANGZ1=BETA2
```

```
      CALL VNEG(VLE,VTE,EXTRM,DPBLD,VRATIO)
      DO 21 I=1,51
      AI=(I-1)/50.
21    CALL DIST(VLE,VTE,DPBLD,AI,VRELS(I),VRELP(I),DUDXS(I),DUDXP(I),
     1EXTRM,VRATIO)
      GO TO 116
  115 CALL VNEG(VLE,VTE,EXTRM,DPBLD,VRATIO)
      DO 22 J=1,51
      AJ=(J-1)/50.
      CALL DIST(VLE,VTE,DPBLD,AJ,VRELS(J),VRELP(J),DUDXS(J),DUDXP(J),
     1EXTRM,VRATIO)
22    CONTINUE
116   DO 30 J=1,51
      AJ=J-1
      AM(J)=AJ/50.
      RMSTR(J)=(R3STR-1.0)*AM(J)+1.0
      HMSTR(J)=(H3STR-1.0)*AM(J)+1.0
      TMT2P(J)=1.0-GAMM1*(RPM**2)*TIPDP*(1.-(RMSTR(J)**2))
      PMPIP(J)=TMT2P(J)**(1./GAMM2)+(POPI-TOTIR**(1./GAMM2))*AM(J)
      PMP2S    =PMPIP(J)*((1./TIPDP*(1.0-GAMM1*(VRELS(J)**2)))
     1**(1./GAMM2))
      PMP2P    =PMPIP(J)*((1./TIPDP*(1.0-GAMM1*(VRELP(J)**2)))
     1**(1./GAMM2))
      IF(IBLD.EQ.2) GO TO 31
      DELP=PMP2P-PMP2S
      GO TO 32
31    DELP=PMP2S-PMP2P
32    GRAN(J)=HMSTR(J)*RMSTR(J)*DELP
30    CONTINUE
      SUM=SIMP2(GRAN,0.0,0.02,50)
      SIGM =(2.*GAMMA/(GAMMA+1.0))*RHOV(GAMMA,VCRI)*COS(AIN)*(R3STR*
     1VUCRO*SQRT(TOTIA)-VUCRI)/SUM
      SIG(K)=SIGM
  160 DPBLD=DPBLD+DELBD
      K=K+1
      IF(K.EQ.2) GO TO 117
      DPBLD=DPBLD-2.*DELBD
      K=1
      KK=KK+1
      IF(KK.GT.20) GO TO 125
      DIFF1(1)=ABS(SOLID-SIG(1))
      DIFF1(2)=ABS(SOLID-SIG(2))
      DIFF2(1)=SOLID-SIG(1)
      DIFF2(2)=SOLID-SIG(2)
      IF(DIFF1(1).LE.0.01) GO TO 120
      IF(DIFF1(2).LE.0.01) GO TO 121
      GBLD=DIFF2(1)*DIFF2(2)
      IF(GBLD.LT.0.0) GO TO 122
      IF(DIFF1(2).GT.DIFF1(1)) GO TO 123
      DPBLD=DPBLD+ABLD*1.0
      GO TO 117
122   DELBD=DELBD/2.
      ABLD=ABLD/2.
      GO TO 117
123   DELBD=-DELBD
      ABLD=-ABLD
      GO TO 117
120   SIGMA=SIG(1)
      IF(IBLD.EQ.2) GO TO 126
      CALL VNEG(VLE,VTE,EXTRM,DPBLD,VRATIO)
      DO 127 I=1,51
      AI=(I-1)/50.
127   CALL DIST(VLE,VTE,DPBLD,AI,VRELS(I),VRELP(I),DUDXS(I),DUDXP(I),
     1EXTRM,VRATIO)
      GO TO 305
  126 CALL VNEG(VLE,VTE,EXTRM,DPBLD,VRATIO)
```

```
      DO 128 I=1,51
      AI=(I-1)/50.
128   CALL DIST(VLE,VTE,DPBLD,AI,VRELS(I),VRELP(I),DUDXS(I),DUDXP(I),
     1EXTRM,VRATIO)
305   DO 306 I=1,51
      PMP2S   =PMPIP(I)*((1./TIPDP*(1.0-GAMM1*(VRELS(I)**2)))
     1**(1./GAMM2))
      PMP2P   =PMPIP(I)*((1./TIPDP*(1.0-GAMM1*(VRELP(I)**2)))
     1**(1./GAMM2))
      IF(IBLD.EQ.2) GO TO 310
      DELP=PMP2P-PMP2S
      GO TO 320
310   DELP=PMP2S-PMP2P
320   GRAN(I)=HMSTR(I)*RMSTR(I)*DELP
306   CONTINUE
      GO TO 130
121   SIGMA=SIG(2)
      DPBLD=DPBLD+DELBD
      GO TO 130
125   SIGMA=SIG(2)
      WRITE(6,2129)
130   CONTINUE
      IF(DSTRES.NE.0.0.AND.IBLD.EQ.2)CALL SDISK(RH3,RT3,CHORD,RHODI,
     1RHOBL,RHOAT,SPEED,SIGMA,AREAR,STRESD,STRESB)
C     ASSUME THE ROTOR SEES THE ROTOR INLET RELATIVE TOTAL TEMPERATURE
      IF(DSTRES.NE.0.0.AND.IBLD.EQ.2) CALL ALIFE(STRESB,T2PPH,BLIFE)
      IF(IPRINT.EQ.1                  ) WRITE(6,2112)
      IF(IPRINT.EQ.1                  ) WRITE(6,2113)
      IF(IPRINT.EQ.0)GO TO 502
      DO 2000 J=1,51,5
      WRITE(6,2114) AM(J),VRELS(J),VRELP(J)
2000  CONTINUE
  502 REDIS=1.-(VRELS(1)/VRELS(51))**2
      DSDIS=DPBLD
      DO 131 I=1,51
  131 VDP(I)=VRELP(I)
      CALL SMALST(VDP,51,MDP)
      DPDIS=1.-VDP(MDP)/VDP(1)
      IF(IPRINT.EQ.1                  ) WRITE(6,2140) REDIS,DPDIS,DSDIS
      IF(DSTRES.NE.0.0.AND.RBEST.EQ.0.0) GO TO 501
      IF(ITRIG.EQ.0) GO TO 501
      IF(KZWFL.EQ.1.AND.IPRINT.EQ.1) WRITE(6,2143)XWEIFL
501   TMT2(1)=1.0
      VUCRM(1)=VUCRI
      WUCRM(1)=(VUCRI-RPM)*SQRT(TIPDP)
      BETAM(1)=BETLE
      EPSM(1)=1.0-TLE/(SPAC*COS(BETLE))
      THIK(1)=RMSTR(1)*(1.0-EPSM(1))/SIGMA
      ANGCK=TAN(BETTE)
      BNGCK=TAN(BETLE)
      WXCRI=VRELS(1)*COS(ANGZ1)
      WXCRO=VRELS(51)*COS(ANGZ2)
      DO 40 K=2,51
      KNT=K-1
      AKNT=KNT
      IF(KNT.NE.1)GO TO 43
      SUMM=0.5*(GRAN(1)+GRAN(2))*0.02
      GO TO 41
43    SUMM=SIMP2(GRAN,0.0,0.02,KNT)
41    IF(IBLD.EQ.2) GO TO 44
      TMT2(K)=1.0
      GO TO 42
44    TMT2(K)=1.0+GAMM2*RPM*SIGMA*SUMM/(RHOV(GAMMA,VCRI)*COS(AIN))
42    VUCRM(K)=(VUCRI+(GAMMA+1.0)*SIGMA*SUMM/(2.*GAMMA*RHOV(GAMMA,VCRI)
     1*COS(AIN)))/(RMSTR(K)*SQRT(TMT2(K)))
      IF(IBLD.EQ.2) GO TO 45
```

```
      TPTPM(K)=1.0
      GO TO 46
45    TPTPM(K)=1.0-GAMM1*(RPM**2)/TMT2(K)*(RMSTR(K)**2)*(2.*VUCRM(K)*
     1SQRT(TMT2(K))/(RPM*RMSTR(K))-1.0)
46    WUCRM(K)=(VUCRM(K)-RPM*RMSTR(K)*SQRT(1./TMT2(K)))/SQRT(TPTPM(K))
      WXCRM=WXCRI+(WXCRO-WXCRI)*AKNT/50.
      ARGCK=WUCRM(K)/WXCRM
      IF(IBLD.EQ.2) GO TO 51
      IF(ARGCK.LE.ANGCK) GO TO 52
      BETAM(K)=BETTE
      WCRM(K)=WUCRM(K)/SIN(BETTE)
      GO TO 53
   51 IF(WUCRM(K).LT.0.0) GO TO 54
      IF(ARGCK.LE.BNGCK) GO TO 52
      BETAM(K)=BETLE
      WCRM(K)=WUCRM(K)/SIN(BETLE)
      GO TO 53
   54 IF(ABS(ARGCK).LT.ABS(ANGCK)) GO TO 52
      BETAM(K)=BETTE
      WCRM(K)=WUCRM(K)/SIN(BETTE)
      GO TO 53
   52 BETAM(K)=ATAN(ARGCK)
      WCRM(K)=SQRT(WXCRM**2+WUC      )**2)
   53 EPSM(K)=RHOV(GAMMA,VCRI)*COS(AIN)*PIPDP*SQRT(1./TIPDP)*(1./
     1PMPIP(K))*SQRT(TMT2P(K))/(RHOV(GAMMA,WCRM(K))*HMSTR(K)*RMSTR(K)*
     2COS(BETAM(K)))
      THIK(K)=RMSTR(K)*(1.0-EPSM(K))/SIGMA
40    CONTINUE
      SUM=0.
      CXLEN(1)=1.E-10
      DO 35 I=2,51
      BETAV=(BETAM(I)+BETAM(I-1))/2.
      SUM=SUM+ABS(0.02/COS(BETAV))
      CXLEN(I)=SUM
35    CONTINUE
      THIKR(1)=THIK(1)/2.
      THIKL(1)=-THIK(1)/2.
      THETA(1)=0.0
      RTHET(1)=0.0
      R(1)=RIN
      AMAVE=GAMM1*(VELBL**2)
      CALL HM(AMAVE,HFAVE)
      ANGMN=ATAN((TAN(ANGZ1)+TAN(ANGZ2))/2.)
      CLSC=2.*(TAN(ANGZ1)-TAN(ANGZ2))*COS(ANGMN)
      SECO=0.0138
      YSEC=(COS(ANGZ2)/COS(ANGZ1))*(0.0075*(CLSC**2)*(COS(ANGZ2)**2)/
     1(COS(ANGMN)**3)+0.035)
      PSPTTE=(1.-AMAVE)**(1./GAMM2)
      DO 90 I=1,51
      AKS=(1.-GAMM1*(VRELS(I)**2))**0.467
      AKP=(1.-GAMM1*(VRELP(I)**2))**0.467
      AMS=GAMM1*(VRELS(I)**2)
      AMP=GAMM1*(VRELP(I)**2)
      CALL HM(AMS,HMS(I))
      CALL HM(AMP,HMP(I))
      TVIS=TMT2P(I)*TIVIS
      CALL VISCO(TVIS,VIS)
      ASON=ACRIT(GAMMA,RGAS,TVIS)
      WS(I)=VRELS(I)*ASON
      WP(I)=VRELP(I)*ASON
      ZS=WS(I)
      ZP=WP(I)
      RHOS=RHOV(GAMMA,VRELS(I))/VRELS(I)*PMPIP(I)/TMT2P(I)*RHO2
      RHOP=RHOV(GAMMA,VRELP(I))/VRELP(I)*PMPIP(I)/TMT2P(I)*RHO2
      ROS(I)=RHOS
      ROP(I)=RHOP
```

```
      CXACT=CHORD*CXLEN(I)
      REOS=RHOS*ZS*CXACT/VIS/12.
      REOP=RHOP*ZP*CXACT/VIS/12.
      EXPOS=1./(2.6*(REOS**(1./14.)))
      EXPOP=1./(2.6*(REOP**(1./14.)))
      IF(REOS.LT.4300.)EXPOS=0.212
      IF(REOP.LT.4300.)EXPOP=0.212
      VEXOS=1./EXPOS
      VEXOP=1./EXPOP
      FS(I)=((((RHOV(GAMMA,VRELS(I))*(VRELS(I)**(1.+HMS(I))))**1.268)
     1*((VIS/(RHOS*ZS))**0.268)*AKS)/(10.**(0.678*(2.*EXPOS+1.))))
     2/COS(BETAM(I))
      FP(I)=((((RHOV(GAMMA,VRELP(I))*(VRELP(I)**(1.+HMP(I))))**1.268)
     1*((VIS/(RHOP*ZP))**0.268)*AKP)/(10.**(0.678*(2.*EXPOP+1.))))
     2/COS(BETAM(I))
      FSL(I)=((VRELS(I)/VELBL)**5)/COS(BETAM(I))
      FPL(I)=((VRELP(I)/VELBL)**5)/COS(BETAM(I))
      BNUS(I)=VIS/RHOS
      BNUP(I)=VIS/RHOP
      DUDXS(I)=12.*DUDXS(I)*ASON*COS(BETAM(I))
      DUDXP(I)=12.*DUDXP(I)*ASON*COS(BETAM(I))
90    CONTINUE
   92 CHRD(ICHORD)=CHORD
      REYN=RHORE*VELRE*SUM*CHORD/(12.*VISRE)
93    RNOSE=TLE/24.
      REZNO=WS(1)*RNOSE/BNUS(1)
      IF(RNOSE.NE.0.0) THESO=0.21*RNOSE*12./SQRT(REZNO)
      IF(RNOSE.EQ.0.0) THESO=0.0
      THEPO=THESO
      CAMLT=CHORD*SUM
      XLEN=0.02
      CFLAM=1.328/SQRT(REYN)
      INGS=1
      INGP=1
      IFLAGS=0
      IFLAGP=0
      DO 95 I=2,51
      J=I-1
      IF(IFLAGS.EQ.1) GO TO 96
      INGS=INGS+1
      THESJ=((VELBL/VRELS(I))**3)*0.5*CFLAM*SQRT(SIMP2(FSL,0.0,XLEN,J))*
     1CAMLT+THESO
      ZTRUKS=((THESJ/12.)**2)/BNUS(I)
      FTRUKS=ZTRUKS*DUDXS(I)/CHORD
      FLAMS=FIT(FTRUKS)
      HLAMS=(0.3-1./120.*FLAMS)/(37./315.-1./945.*FLAMS-1./9072.*
     1(FLAMS**2))
      DELSJ=HLAMS*THESJ
      BLREYS=WS(I)*DELSJ/12./BNUS(I)
      RECRTS=RECRIT(FLAMS)
      IF(BLREYS.GE.RECRTS)IFLAGS=1
96    IF(IFLAGP.EQ.1) GO TO 95
      INGP=INGP+1
      THEPJ=((VELBL/VRELP(I))**3)*0.5*CFLAM*SQRT(SIMP2(FPL,0.0,XLEN,J))*
     1CAMLT+THEPO
      ZTRUKP=((THEPJ/12.)**2)/BNUP(I)
      FTRUKP=ZTRUKP*DUDXP(I)/CHORD
      FLAMP=FIT(FTRUKP)
      HLAMP=(0.3-1./120.*FLAMP)/(37./315.-1./945.*FLAMP-1./9072.*
     1(FLAMP**2))
      DELPJ=HLAMP*THEPJ
      BLREYP=WP(I)*DELPJ/12./BNUP(I)
      RECRTP=RECRIT(FLAMP)
      IF(BLREYP.GE.RECRTP)IFLAGP=1
95    CONTINUE
      YLEN=CHORD/600.
```

```
      SPACE=CHORD/SIGMA*COS(BETAM(51))
      NS=52-INGS
      NP=52-INGP
      IS=NS-1
      IP=NP-1
      DO 97 I=1,NS
      J=INGS+I-1
      GS(I)=FS(J)
97    CONTINUE
      DO 98 I=1,NP
      J=INGP+I-1
      GP(I)=FP(J)
98    CONTINUE
      THES3=((0.156/((RHOV(GAMMA,VRELS(51))*(VRELS(51)**(1.+HMS(51))))
     1**1.268)*SIMP2(GS,0.0,YLEN,IS)+(ROS(INGS)*(WS(INGS)**(2.+HMS(INGS)
     2))/(ROS(51)*(WS(51)**(2.+HMS(51))))*(THESJ/12.))**1.268)**0.7886)
     3*12.
      THEP3=((0.156/((RHOV(GAMMA,VRELP(51))*(VRELP(51)**(1.+HMP(51))))
     1**1.268)*SIMP2(GP,0.0,YLEN,IP)+(ROP(INGP)*(WP(INGP)**(2.+HMP(INGP)
     2))/(ROP(51)*(WP(51)**(2.+HMP(51))))*(THEPJ/12.))**1.268)**0.7886)
     3*12.
      TSTAR=(THES3+THEP3)/SPACE
      DELS3=HFAVE*THES3
      IF(IFLAGS.EQ.0)DELS3=DELSJ
      DELP3=HFAVE*THEP3
      IF(IFLAGP.EQ.0)DELP3=DELPJ
      DSTAR=(DELS3+DELP3)/SPACE
      DTE(1)=TETS/SPACE
      DTE(2)=TETR/SPACE
      AFS1=GAMM1*(WCRM(51)**2)
      BLOK1=1.-DSTAR-DTE(IBLD)-TSTAR
      BLOK2=1.-DSTAR-DTE(IBLD)
      CSTW=((1.-AFS1)*((GAMMA+1.)/(2.*GAMMA))+BLOK1*((WCRM(51)*
     1COS(BETAM(51)))**2))/(BLOK2*WCRM(51)*COS(BETAM(51)))
      DSTW=BLOK1*WCRM(51)*SIN(BETAM(51))/BLOK2
      WXMIX=GAMMA*CSTW/(GAMMA+1.)-SQRT(((GAMMA*CSTW/(GAMMA+1.))**2)-1.0+
     1GAMM1*(DSTW**2))
      RHMIX=(1.-GAMM1*(WXMIX**2+DSTW**2))**GAMM3
      PLOSS(IBLD)=BLOK2*RHOV(GAMMA,WCRM(51))*COS(BETAM(51))/(RHMIX*
     1WXMIX)
      SPLOSS=PLOSS(IBLD)
      YPRO(IBLD)=(1.-PLOSS(IBLD))/(PLOSS(IBLD)*(1.-PSPTTE))
      YSF(IBLD)=YSEC*CHORD/HEIGHT
      YTOT(IBLD)=YPRO(IBLD)+YSF(IBLD)
      PLOSS(IBLD)=1./(1.+YTOT(IBLD)*(1.-PSPTTE))
      IF(ITRIG.EQ.1)GO TO 94
      YTOTL(ICHORD)=YTOT(IBLD)
      IF(ICHORD.LE.2) GO TO 400
      IF(YTOTL(ICHORD).GT.YTOTL(ICHORD-1).AND.YTOTL(ICHORD-1).GT.
     1YTOTL(ICHORD-2)) GO TO 91
400   ICHORD=ICHORD+1
      CHORD=CHORD+0.02
      IF(CHORD.GT.CHMAX) GO TO 91
      IF(TTE.EQ.0.0) GO TO 92
      GO TO 500
91    MINMUM=ICHORD-2
      CHORD=CHRD(MINMUM)
      ITRIG=1
      KNZW=1
      IF(TTE.EQ.0.0) GO TO 92
      GO TO 500
94    CONTINUE
      TRANS=CXLEN(INGS)*CHORD/CAMLT*100.
      TRANP=CXLEN(INGP)*CHORD/CAMLT*100.
      ALPHA=RIN*(R3STR-1.)/CHORD
      DO 70 N=2,51
```

```
      KN=0
      NN=N-1
      TO=THETA(NN)
      R(N)=RIN*RMSTR(N)
      BE=BETAM(NN)
      IF(BE.EQ.0.0) BE=0.000001
76    RHS1=R(NN)*THETA(NN)+(TAN(BE)+TO*ALPHA)*0.02*CHORD
75    TOO=RHS1/R(N)
      RHS2=R(NN)*THETA(NN)+(TAN(BE)+TOO*ALPHA)*0.02*CHORD
      IF(ABS((RHS2-RHS1)/RHS1)-.00002) 71,71,72
72    KN=KN+1
      IF(KN-100) 73,73,74
73    RHS1=RHS2
      GO TO 75
74    IF(IPRINT.EQ.1) WRITE(6,2118)
71    THETA(N)=RHS2/R(N)
      RTHET(N)=R(N)*THETA(N)/CHORD
      THIKR(N)=RTHET(N)+THIK(N)/2.
      THIKL(N)=RTHET(N)-THIK(N)/2.
70    CONTINUE
      PITCH=1./SIGMA
      DISTAN=ABS(RTHET(51))
      STAGR=ATAN(DISTAN)
      STAGR=STAGR*180./3.14159
      CAMLTH=CHORD*SUM
      ZNUM=2.*3.14159*RIN*SIGMA/CHORD
      NUMBER=ZNUM
      IF(IPRINT.EQ.1) WRITE(6,2115)
      IF(IPRINT.EQ.1) WRITE(6,2116)
      TCAL=THIK(51)*COS(BETAM(51))*CHORD
      ANACT=BETTE*180./3.14159
101   T3IT=TMT2(51)*T1P
      ANIT=BETAM(51)*180./3.14159
      IF(IBLD.EQ.2) GO TO 102
      IF(IPRINT.EQ.1) WRITE(6,2117)T3IT,T1P,VUCRM(51),VUCRO,ANIT,ANACT,
     1SIGMA,SOLID,TCAL,TETS
      GO TO 103
102   IF(IPRINT.EQ.1) WRITE(6,2117)T3IT,T3P,VUCRM(51),VUCRO,ANIT,ANACT,
     1SIGMA,SOLID,TCAL,TETR
  103 CONTINUE
      IF(IPRINT.EQ.1) WRITE(6,2100)
      IF(IBLD.EQ.2) GO TO 80
      IF(IPRINT.EQ.1) WRITE(6,2119)
      GO TO 81
80    IF(IPRINT.EQ.1) WRITE(6,2120)
81    IF(IPRINT.EQ.1) WRITE(6,2121)
      DO 82 I=1,51,5
      IF(IPRINT.EQ.1)WRITE(6,2122)AM(I),R(I),RTHET(I),THIKR(I),THIKL(I)
82    CONTINUE
      IF(IPRINT.EQ.1) WRITE(6,2123)
      IF(IPRINT.EQ.1) WRITE(6,2124)CHORD,SIGMA,CAMLTH,STAGR,NUMBER
      IF(IBLD.EQ.2) GO TO 110
      IF(IPRINT.EQ.1) WRITE(6,2125)
      GO TO 111
110   IF(IPRINT.EQ.1) WRITE(6,2126)
111   IF(IPRINT.EQ.1) WRITE(6,2127)
      VMIX=SQRT(WXMIX**2+DSTW**2)
      DSTW=ABS(DSTW)
      IF(IPRINT.EQ.1) WRITE(6,2128)TSTAR,DSTAR,VMIX,SPLOSS
      IF(IPRINT.EQ.1) WRITE(6,2144)YPRO(IBLD),YSF(IBLD),YTOT(IBLD),REYN
      IF(IPRINT.EQ.1) WRITE(6,2221) TRANS,TRANP
      IF(IPRINT.EQ.1) WRITE(6,2100)
      IBLD=IBLD+1
      IF(IBLD.LT.3) GO TO 20
      ETATT=1./(1.0+(T3P/(T1P-T3P)*(1.0-((PLOSS(1)*PLOSS(2))**GAMM2))))
      IF(IPRINT.EQ.1) WRITE(6,2099)
```

```
      IF(IPRINT.EQ.1) WRITE(6,2132)
      IF(IPRINT.EQ.1) WRITE(6,2133) ETATT
      VX3C=VX3*ACR3
      VX2C=V2*ACR1*COS(ALP2)
      VUM3C=VWRK3
      UM3C=U3
      VUM2C=VWRK2
      UM2C=U2
      R3C=1.+H3/(2.*RM3)
      R2C=1.+H2/(2.*RM2)
      R3CI=1./R3C
      R2CI=1./R2C
      REACTC=(VX3C**2+(R3CI*VUM3C-R3C*UM3C)**2-VX2C**2-(R2CI*VUM2C-R2C
     1*UM2C)**2)/(VX3C**2+(R3CI*VUM3C-R3C*UM3C)**2+2.*UM2C*VUM2C-(R2C
     2*UM2C)**2)
      HROTOR=(H2+H3)*6.
      ETATTM= ETATT*(1.-CLEAR/HROTOR*(2.755*(REACTC**2)+0.108*REACTC+
     11.72))
      DELETA=ETATTM-ETATT
      IF(IPRINT.EQ.1) WRITE(6,2145)DELETA,ETATTM
      PTTEX=P1P*((1.-(1.-T3P/T1P)/ETATT)**(1./GAMM2))
      PSTEX=PTTEX*((1.-GAMM1*(V3**2))**(1./GAMM2))
      PXTEX=PSTEX/((1.-GAMM1*(VX3**2))**(1./GAMM2))
      ETATX=(ETA*(1.-(PTTEX/P1P)**GAMM2)/(1.-(PXTEX/P1P)**GAMM2))+DELETA
      ETATST=(ETA*(1.-(PTTEX/P1P)**GAMM2)/(1.-(PSTEX/P1P)**GAMM2))+
     1DELETA
      IF(IPRINT.EQ.1) WRITE(6,2220) ETATST,ETATX
      IF(DSTRES.NE.0.0) GO TO 600
      HUBR=(RM3-H3/2.)*12.
      TIPR=(RM3+H3/2.)*12.
      REARA=3.14159*(TIPR**2-HUBR**2)
      CALL SDISK(HUBR,TIPR,CHORD,RHODI,RHOBL,RHOAT,SPEED,SIGMA,REARA,
     1STRESD,STRESB)
      IF(IPRINT.EQ.1) WRITE(6,2241) STRESD,STRESB
600   SEFFY(NPASS)=ETATST
      PCHEK=ABS(ETATT-ETA)
      IF(PCHEK.LE.0.002.AND.DSTRES.EQ.0.0) IPRINT=1
      IF(PCHEK.LE.0.002.AND.RBEST.GT.0.0) IPRINT=1
      IF(NPASS.EQ.1) GO TO 150
      DETA=ABS(SEFFY(NPASS)-SEFFY(NPASS-1))
      IF(DETA.LE.0.002) GO TO 142
      IF(NPASS.GT.6) GOTO 141
150   NPASS=NPASS+1
      ETA=ETATT
      P2P=PLOSS(1)*P1P
      PLOS1=PLOSS(1)
      PLOS2=PLOSS(2)*(T32PP**(1./GAMM2))
      P32PP=PLOS2
      IF(DSTRES.NE.0.0) GO TO 180
      GO TO 10
141   WRITE(6,2134)
142   CONTINUE
      IF(RBEST.GT.0.0)WRITE(6,2234)DSTRES,STRESD,STRESB
      IF(IPRINT.EQ.1)WRITE(6,2142) NPASS
      IF(DSTRES.EQ.0.0) GO TO 4000
      IF(RBEST.GT.0.0) GO TO 4000
      KPASS=KPASS+1
      EADIAB(KPASS)=1.-ETATTM
      DPSI(KPASS)=STRESD
      UHUBC=UT3*RH3/RT3
      IF(KPASS.EQ.1)WRITE(6,2100)
      IF(KPASS.EQ.1)WRITE(6,2230)
      IF(KPASS.EQ.1)WRITE(6,2244)
      IF(KPASS.EQ.1)WRITE(6,2231)
      WRITE(6,2232)KPASS,ETATTM,ETATST,UHUBC,UT3,RH3,RT3,STRESB,STRESD,
     1BLIFE
```

```
      IF(V2.GE.1.0)WRITE(6,2237) KPASS
      IF(WPP3.GE.1.0)WRITE(6,2238) KPASS
      IF(KPASS.LE.20)GO TO 190
      K=0
      DO 450 I=1,21
      IF(DPSI(I).GT.DSTRES) GO TO 450
      K=K+1
      FADIAB(K)=EADIAB(I)
      RADEXX(K)=RADEX(I)
450   CONTINUE
      IF(K.EQ.0) GO TO 460
      WRITE(6,2236) K
      IF(K.EQ.1) MINETA=K
      IF(K.GT.1)CALL SMALST(FADIAB,K,MINETA)
      RBEST=RADEXX(MINETA)
      KPASS=0
      GO TO 190
460   WRITE(6,2235)
      GO TO 4000
1000  FORMAT(7F10.3)
 1001 FORMAT(6F10.3,I1)
 1002 FORMAT(3F10.3)
 2097 FORMAT(///)
2098  FORMAT(///56X,11HFLOW ANGLES/56X,11H-----------)
2099  FORMAT(////////)
2100  FORMAT(1H1)
2101  FORMAT(50X,24HPROGRAM INPUT PARAMETERS/50X,24H--------------------
     1----///)
2102  FORMAT(8X,5HGAMMA,6X,4HRGAS,6X,11HROTOR SPEED,6X,14HMASS FLOW RATE
     1,6X,13HTURBINE INLET,6X,13HTURBINE INLET,6X,13HWORK REQUIRED/32X,
     25H(RPM),12X,8H(LB-SEC),9X,14HPRESSURE (PSI),5X,14HTEMPERATURE, R,
     38X,8H(BTU/LB)/
 ..03 FORMAT(7X,F6.3,4X,F7.3,7X,F7.1,11X,F7.3,13X,F7.3,12X,F7.1,12X,F7.3
     1)
2104  FORMAT(///////2X,12HSTATOR INLET,2X,11HROTOR INLET,2X,10HROTOR EXI
     1T,2X,12HSTATOR INLET,2X,11HROTOR INLET,2X,10HROTOR EXIT,2X,11HSTAT
     2OR T.E.,2X,10HROTOR T.E.,2X,15HROTOR CLEARANCE/2X,11HMEAN RADIUS,
     33X,11HMEAN RADIUS,2X,11HMEAN RADIUS,5X,4HAREA,10X,4HAREA,8X,4HAREA
     4,6X,9HTHICKNESS,3X,9HTHICKNESS,5X,8H(INCHES)/4X,8H(INCHES),6X,8H(I
     5NCHES),4X,8H(INCHES),3X,11H(SQ INCHES),3X,11H(SQ INCHES),2X,11H(SQ
     6 INCHES),3X,8H(INCHES),4X,8H(INCHES)/)
2105  FORMAT(5X,F6.3,8X,F6.3,6X,F6.3,7X,F7.3,6X,F7.3,6X,F7.3,6X,F6.3,6X,
     1F6.3,9X,F6.3)
2106  FORMAT(////40X,46HCOMPUTED FLOW PARAMETERS AND VELOCITY DIAGRAMS/
     140X,46H----------------------------------------------///)
2107  FORMAT(22X,6HSTATOR,60X,5HROTOR/22X,6H------,60X,5H-----///2X,
     150HSTATOR INLET CRITICAL VELOCITY RATIO, V/VCR .......,F7.3,5X,
     250HROTOR EXIT AXIAL CRITICAL VELOCITY RATIO, VX/VCR .,F7.3//2X,
     350HSTATOR INLET SWIRL VELOCITY RATIO, VU/VCR .........,F7.3,5X,
     450HROTOR EXIT SWIRL VELOCITY RATIO, VU/VCR ...........,F7.3//2X,
     550HSTATOR EXIT CRITICAL VELOCITY RATIO, V/VCR ........,F7.3,5X,
     650HROTOR EXIT CRITICAL VELOCITY RATIO, V/VCR .........,F7.3//2X,
     750HSTATOR EXIT AXIAL VELOCITY RATIO, VX/VCR ..........,F7.3,5X,
     850HROTOR INLET RELATIVE VELOCITY RATIO, W/WCR ........,F7.3/)
2108  FORMAT(2X,50HSTATOR EXIT SWIRL VELOCITY RATIO, VU/VCR ..........,
     1F7.3,5X,50HROTOR EXIT RELATIVE VELOCITY RATIO, W/WCR .........,F7.3
     2//2X,49HSTATOR EXIT ABSOLUTE TOTAL PRESSURE ...............,F8.3,
     35X,50HROTOR INLET BLADE SPEED RATIO, U/VCR ...............,F7.3//2X,
     450HSTATOR ABSOLUTE TOTAL PRESSURE LOSS RATIO, ........,F7.3,5X,
     550HROTOR EXIT BLADE SPEED RATIO, U/VCR ...............,F7.3//64X,
     650HROTOR RELATIVE TOTAL PRESSURE LOSS RATIO ..........,F7.3//64X,
     749HROTOR EXIT ABSOLUTE TOTAL PRESSURE ...............,F8.3//64X,
     849HROTOR EXIT ABSOLUTE TOTAL TEMPERATURE ............,F8.1//64X,
     949HROTOR TIP SPEED (FT PER SEC) .....................,F8.1)
2109  FORMAT(//59X,5HSTAGE/59X,5H-----///37X,45HROTOR EXIT HUB RADIUS (I
     1NCHES) ..............,F7.3//37X,45HROTOR EXIT TIP RADIUS (INCHES)
```

```
     2..............,F7.3//37X,45HROTOR INLET HUB RADIUS (INCHES) ......
     3.......,F7.3//37X,45HROTOR INLET TIP RADIUS (INCHES) ............
     4,F7.3//37X,45HSTATOR INLET HUB RADIUS (INCHES) ............,F7.3//
     537X,45HSTATOR INLET TIP RADIUS (INCHES) ............,F7.3//37X,
     645HROTOR EXIT ANNULUS AREA (SQ INCHES) .........,F7.3//37X,45HROTO
     7R INLET ANNULUS AREA (SQ INCHES) .........,F7.3//37X,45HSTAGE REACT
     8ION ..............................,F7.3/)
2110 FORMAT(////36X,52HCALCULATIONS FOR GENERATION OF STATOR BLADE GEOM
     1ETRY/36X,52H----------------------------------------------------)
2111 FORMAT(////36X,51HCALCULATIONS FOR GENERATION OF ROTOR BLADE GEOME
     1TRY/36X,51H---------------------------------------------------)
2112 FORMAT(//44X,36H*** COMPUTED AERODYNAMIC LOADING ***/)
2113 FORMAT(30X,' PERCENT                        SUCTION SURFACE
     1PRESSURE SURFACE'/29X,' MERIDIONAL                 RELATIVE CRITICAL
     2              RELATIVE CRITICAL'/30X,' DISTANCE                VELOCIT
     3Y RATIO                VELOCITY RATIO'/)
2114 FORMAT(31X,F5.3,21X,F5.3,25X,F5.3)
2115 FORMAT(////35X,55H*** (ITERATED) STANITZ METHOD BLADE EXIT PARAMET
     1ERS ***/)
2116 FORMAT(45X,14HITERATED VALUE,8X,12HACTUAL VALUE/)
2117 FORMAT(11X,27HEXIT (ABSOLUTE) TEMPERATURE,9X,F9.4,12X,F9.4//3X,
     135HEXIT (ABSOLUTE) TANGENTIAL VELOCITY,11X,F7.4,14X,F7.4//22X,
     216HEXIT BLADE ANGLE,10X,F8.4,13X,F8.4//30X,8HSOLIDITY,11X,
     3F7.4,14X,F7.4//15X,23HTRAILING EDGE THICKNESS,12X,F6.3,15X,F6.3)
2118 FORMAT(/71H **** R*THETA ITERATION LOOP NOT SATISFIED   COMPUTATIO
     1N CONTINUES ****/)
2119 FORMAT(////33X,4H*** ,12X,26HFINAL STATOR BLADE PROFILE,13X,3H***/
     133X,58H*** COORDINATES NORMALIZED WITH RESPECT TO BLADE CHORD ***/
     2)
2120 FORMAT(////33X,4H*** ,13X,25HFINAL ROTOR BLADE PROFILE,13X,3H***/
     133X,58H*** COORDINATES NORMALIZED WITH RESPECT TO BLADE CHORD ***/
     2)
2121 FORMAT(30X,7HPERCENT,10X,9HPITCHLINE,10X,4HMEAN,10X,5HBLADE,10X,
     15HBLADE/29X,10HMERIDIONAL,9X,6HRADIUS,9X,10HCAMBERLINE,6X,7HSURFAC
     2E,8X,7HSURFACE/30X,8HDISTANCE,25X,10HCOORDINATE,5X,10HCOORDINATE,
     35X,10HCOORDINATE/)
2122 FORMAT(31X,F5.3,12X,F6.3,10X,F7.4,8X,F7.4,8X,F7.4)
2123 FORMAT(//21X,11HBLADE CHORD,6X,14HBLADE SOLIDITY,6X,16HBLADE CAMBE
     1RLINE,6X,13HBLADE STAGGER,6X,12HBLADE NUMBER/22X,8H(INCHES),28X,15
     *HLENGTH (INCHES),
     211X,5HANGLE/)
2124 FORMAT(23X,F7.4,11X,F8.4,13X,F8.4,13X,F6.2,14X,I3)
2125 FORMAT(/// 23X,' CALCULATIONS FOR GENERATION OF STATOR BLADE ROW
     1AERODYNAMIC PERFORMANCE LOSSES'/23X,' ----------------------------
     2-------------------------------------------')
2126 FORMAT(/// 23X,' CALCULATIONS FOR GENERATION OF ROTOR BLADE ROW A
     1ERODYNAMIC PERFORMANCE LOSSES'/23X,' -----------------------------
     2-----------------------------------------')
2127 FORMAT(//43X,38H*** STEWART MIXING LOSS PARAMETERS ***/ )
2128 FORMAT(32X,40HTOTAL MOMENTUM THICKNESS (DIMENSIONLESS),14X,F6.4/
     132X,44HTOTAL DISPLACEMENT THICKNESS (DIMENSIONLESS),10X,F6.4/
     232X,41HCASCADE EXIT (MIXED) CRITICAL MACH NUMBER,13X,F6.4/
     332X,38HPROFILE (FRICTION) TOTAL PRESSURE LOSS,16X,F6.4)
2129 FORMAT(///75H*** BLADE LOADING ITERATION LOOP NOT SATISFIED    COM
     1PUTATION CONTINUES ***///)
2132 FORMAT(////44X,39HFINAL CALCULATIONS FOR STAGE EFFICIENCY/44X,
     139H---------------------------------------)
2133 FORMAT(///35X,48HSTAGE ADIABATIC EFFICIENCY CALCULATED FROM BLADE/
     135X,52HBOUNDARY LAYER AND SECONDARY FLOW LOSSES .........  ,F6.4)
2134 FORMAT(///32X,62H*** WARNING ***  STAGE EFFICIENCY ITERATION FAILE
     1D TO CONVERGE)
2140 FORMAT(//38X,39HOVERALL BLADE REACTION (R=1-VIN/VOUT) =,5X,F9.3/
     138X,44HPRESSURE SURFACE DIFFUSION (DP=1-VMIN/VIN) =,F9.3/38X,44HSU
     2CTION SURFACE DIFFUSION (DS=1-VOUT/VMAX) =,F9.3/)
2141 FORMAT(//44X,26HSTATOR INLET ANGLE ...... ,F9.3//44X,26HSTATOR EX
     1IT ANGLE ....... ,F9.3//44X,26HROTOR INLET ANGLE ........ ,F9.3//
```

```
     244X,26HROTOR EXIT ANGLE ........ ,F9.3//44X,26HROTOR EXIT SWIRL AN
     3GLE ....,F9.3)
2142 FORMAT(///////41X,37HEFFICIENCY ITERATION CONVERGED AFTER ,I2,
     17H PASSES)
2143 FORMAT(/27X,75HNOTE ...  BASIC LOADING DISTRIBUTION COULD NOT SATI
     1SFY SOLIDITY REQUIREMENT/27X,56HFOR OPTIMUM ZWEIFEL COEFFICIENT ..
     2..  ZWEIFEL CHANGED TO,F5.2)
2144 FORMAT(/46X,33H*** CASCADE LOSS COEFFICIENTS ***//40X,24HPROFILE L
     1OSS COEFFICIENT,15X,F6.4/40X,31HSECONDARY FLOW LOSS COEFFICIENT,8X
     2,F6.4/40X,30HTOTAL CASCADE LOSS COEFFICIENT,9X,F6.4///29X,58HNOTE
     3..... CASCADE GEOMETRY OPTIMIZED AT REYNOLDS NUMBER =,E9.2)
2145 FORMAT(//35X,52HSTAGE EFFICIENCY DECREMENT FOR ROTOR CLEARANCE ...
     1   ,F6.3///35X,52HFINAL STAGE TOTAL-TOTAL EFFICIENCY .............
     2.   ,F6.4)
2146 FORMAT(37X,45HSTAGE WORK COEFFICIENT BASED ON MEAN RADIUS .,F7.3//
     137X,45HSTAGE WORK COEFFICIENT BASED ON HUB RADIUS ..,F7.3//37X,
     245HTURBINE TOTAL-TOTAL PRESSURE RATIO ..........,F7.3/)
2200 FORMAT(////10X,87H** WARNING **   INPUT STATOR EXIT ANGLE IS TOO L
     1ARGE TO SATISFY CONTINUITY REQUIREMENTS//26X,17HANGLE CHANGED TO ,
     2F6.2,1X,7HDEGREES)
2201 FORMAT(/////// 9X,12HSTATOR INLET,6X,11HSTATOR EXIT,6X,14HSTATOR Z
     1WEIFEL,6X,13HROTOR ZWEIFEL,6X,12HSTATOR CHORD,6X,11HROTOR CHORD/10
     *X,
     210HFLOW ANGLE,7X,10HFLOW ANGLE,8X,11HCOEFFICIENT,9X,11HCOEFFICIENT
     3,9X,8H(INCHES),9X,8H(INCHES)/)
2202 FORMAT(12X,F6.2,12X,F5.2,13X,F5.3,15X,F5.3,14X,F5.3,11X,F5.3//)
2203 FORMAT(///45X,22HPROGRAM DEFAULT VALUES//31X,54HSTATOR EXIT FLOW A
     1NGLE .......... CALCULATED FROM WORK/65X,19HAND FLOW CONDITIONS/
     231X,37HSTATOR ZWEIFEL COEFFICIENT ...... 0.8 //31X,37HROTOR ZWEIFE
     3L COEFFICIENT ....... 0.8//31X,54HSTATOR CHORD ..................
     4. OPTIMIZED ON MINIMUM/65X,24HCASCADE LOSS COEFFICIENT//31X,54HROT
     5OR CHORD ..................... OPTIMIZED ON MINIMUM/65X,24HCASCADE
     6 LOSS COEFFICIENT)
2204 FORMAT(/////10X,11HSTATOR L.E.,8X,10HROTOR L.E.,8X,9HALLOWABLE,8X,
     110HROTOR EXIT,8X,17HBLADE PLOT OPTION,8X,10HROTOR EXIT/11X,9HTHICK
     2NESS,9X,9HTHICKNESS,8X,11HDISK STRESS,7X,10HAXIAL MACH,12X,11H0 =
     3NO PLOT,10X,11HSWIRL ANGLE/12X,8H(INCHES),10X,8H(INCHES),11X,5H(PS
     4I),12X,6HNUMBER,14X,8H1 = PLOT//13X,F5.3,13X,F5.3,12X,F7.0,11X,
     5F5.3,19X,I1,18X,F6.2/)
2210 FORMAT(//23X,65HNOTE .... MAXIMUM ALLOWABLE STATOR ANGLE FOR INPUT
     1 CONDITIONS IS ,F5.2,8H DEGREES)
2220 FORMAT(//35X,52HFINAL STAGE TOTAL-STATIC EFFICIENCY .............
     1..,F6.4///35X,52HFINAL STAGE RATING EFFICIENCY ..................
     2...,F6.4)
2221 FORMAT(//8X,' NOTE ..... PREDICTED SUCTION SURFACE BOUNDARY LAYER
     1 TRANSITION AT',F5.1,' PERCENT OF CAMBER LENGTH'/19X,' PREDICTED
     2PRESSURE SURFACE BOUNDARY LAYER TRANSITION AT',F4.1,'  PERCENT OF
     3CAMBER LENGTH')
2230 FORMAT(//15X,85HTHE FOLLOWING IS A LIST OF POSSIBLE CONFIGURATIONS
     1 FOR THE INPUT CONDITIONS SPECIFIED/15X,85H--------------------
     2--------------------------------------------------------------////
     *)
2231 FORMAT(2X,4HPASS,3X,7HETA T-T,3X,7HETA T-S,3X,5HU HUB,3X,5HU TIP,
     13X,10HROTOR EXIT,3X,10HROTOR EXIT,3X,12HBLADE STRESS,3X,11HDISK ST
     2RESS,3X,10HROTOR LIFE/29X,5H(FPS),3X,5H(FPS),3X,10HHUB RADIUS,3X,1
     *0HTIP RADIUS,6X,
     35H(PSI),10X,5H(PSI),7X,7H(HOURS)/46X,8H(INCHES),5X,8H(INCHES)///)
2232 FORMAT( X,I2,4X,F6.4,4X,F6.4,4X,F5.0,3X,F5.0,5X,F6.3,7X,F6.3,8X,
     1F7.0,7X,F7.0,5X,E10.4)
2233 FORMAT(////5X,106HTHE FOLLOWING IS AN AERODYNAMICALLY OPTIMIZED ST
     1AGE CHOSEN FROM THE POSSIBLE FLOWPATH CONFIGURATIONS ABOVE//)
2234 FORMAT(//55X,11HSTRESS DATA/55X,11H-----------///35X,45HALLOWABLE
     1AVERAGE DISK STRESS (INPUT) .......,F8.0,4H PSI//35X,45HCOMPUTED A
     2VERAGE DISK STRESS ................,F8.0,4H PSI//35X,45HCOMPUTED R
     3OOT BLADE STRESS ..................,F8.0,4H PSI/)
2235 FORMAT(///20X,82HWARNING ** NO SOLUTION WHICH SATISFIES THE SPECIF
```

```
     1IED DISK STRESS HAS BEEN FOUND **///)
2236  FORMAT(///15X,33HNOTE ... OF 21 SOLUTIONS OBTAINED,I3,55H ARE (IS)
     1 WITHIN THE RANGE OF THE SPECIFIED DISK STRESS//)
2237  FORMAT(20X,81HNOTE ..... PROGRAM PREDICTS STATOR (MEANLINE) CHOKIN
     1G FOR THE CONDITIONS OF PASS ,I2/)
2238  FORMAT(20X,81HNOTE ...... PROGRAM PREDICTS ROTOR (MEANLINE) CHOKIN
     1G FOR THE CONDITIONS OF PASS ,I2/)
2239  FORMAT(//1X,' CONTINUITY CANNOT BE SATISFIED AT THE STATOR EXIT
     1FOR THE ROTOR EXIT SWIRL CONDITIONS SPECIFIED ... SOLUTION TERMINA
     2TES')
 2240 FORMAT(59X,5HSTAGE/59X,5H-----///37X,45HSTAGE WORK COEFFICIENT BAS
     1ED ON MEAN RADIUS .,F7.3//37X,45HSTAGE WORK COEFFICIENT BASED ON H
     2UB RADIUS ..,F7.3//37X,45HTURBINE TOTAL-TOTAL PRESSURE RATIO .....
     3.....,F7.3/)
2241  FORMAT(////55X,11HSTRESS DATA/55X,11H-----------///35X,45HCOMPUTED
     1 AVERAGE DISK STRESS ................,F8.0,4H PSI//35X,45HCOMPUTED
     2 BLADE ROOT STRESS ..................,F8.0,4H PSI/)
2242  FORMAT(//20X,35HNOTES ON FLOW ANGLE INPUT .........//25X,79H(1) ST
     1ATOR EXIT FLOW ANGLE AND ROTOR EXIT SWIRL CANNOT BE SIMULTANEOUSLY
     2 INPUT./29X,53HIF BOTH ARE INPUT, ONLY THE ROTOR EXIT SWIRL IS USE
     3D.//25X,82H(2) IF NEITHER ANGLE IS INPUT, STATOR EXIT ANGLE IS CAL
     4CULATED ASSUMING ZERO ROTOR/29X,10HEXIT SWIRL//25X,84H(3) IF STATO
     5R EXIT ANGLE IS INPUT, SET ROTOR SWIRL = ZERO (SWIRL WILL BE CALCU
     6LATED)/)
2243  FORMAT(//20X,96HADDITIONAL NOTE ..... IF FLOWPATH GEOMETRY IS INPU
     1T, ALLOWABLE DISK STRESS MUST BE INPUT AS ZERO/95X,4H----/)
2244  FORMAT(   20X,72HEACH CONFIGURATION IS CONSTRAINED BY THE FOLLOWIN
     1G (CONSTANT) PARAMETERS///35X,3HRPM/35X,9HMASS FLOW/35X,44HTURBINE
     2 INLET TOTAL TEMPERATURE AND PRESSURE/35X,16HWORK REQUIREMENT/35X,
     315HROTOR CLEARANCE/35X,25HROTOR EXIT AXIAL MACH NO./35X,16HROTOR E
     4XIT SWIRL/35X,37HSTATOR AND ROTOR ZWEIFEL COEFFICIENTS/////)
2245  FORMAT(/////36X,13HDISK MATERIAL,8X,14HBLADE MATERIAL,8X,17HDISK R
     1IM MATERIAL/34X,17HDENSITY (LBS/FT3),5X,17HDENSITY (LBS/FT3),6X,
     217HDENSITY (LBS/FT3)//40X,F5.1,16X,F5.1,19X,F5.1/)
  999 STOP
      END
      SUBROUTINE RCHOKE(VU3,VX3,G,R,T1,CON,UCHOKE)
      DIMENSION ALS(2),ARS(2),DIF1(2),DIF2(2)
      ACR=ACRIT(G,R,T1)
      A=100.
      S=100.
      DEL=100.
      K=0
20    ALS(1)=S
      K=K+1
      IF(K.GE.100) GO TO 1400
      VU2=CON/S+VU3
      T2PP=T1*(1.-(G-1.)/(G+1.)*((S/ACR)**2)*(2.*(VU2/ACR)/(S/ACR)-1.))
      ACR3=ACRIT(G,R,T2PP)
      ARS(1)=VU3+SQRT(ACR3**2-VX3**2)
      SS=S+DEL
      ALS(2)=SS
      VU2=CON/SS+VU3
      T2PP=T1*(1.-(G-1.)/(G+1.)*((SS/ACR)**2)*(2.*(VU2/ACR)/(SS/ACR)-1.)
     1)
      ACR3=ACRIT(G,R,T2PP)
      ARS(2)=VU3+SQRT(ACR3**2-VX3**2)
      DIF1(1)=ABS(ALS(1)-ARS(1))
      DIF1(2)=ABS(ALS(2)-ARS(2))
      DIF2(1)=ALS(1)-ARS(1)
      DIF2(2)=ALS(2)-ARS(2)
      IF(DIF1(1).LE.5.0) GO TO 1000
      IF(DIF1(2).LE.5.0) GO TO 1001
      Q=DIF2(1)*DIF2(2)
      IF(Q.LT.0.0) GO TO 200
      IF(DIF1(2).GT.DIF1(1)) GO TO 100
```

```
      S=S+A*1.0
      GO TO 20
200   DEL=DEL/2.
      A=A/2.
      GO TO 20
100   DEL=-DEL
      A=-A
      GO TO 20
1000  UCHOKE=ALS(1)
      GO TO 1200
1001  UCHOKE=ALS(2)
      GO TO 1200
1400  UCHOKE=ALS(1)
      WRITE(6,1100)
1100  FORMAT(//72H*** ROTOR CHOKE ITERATION LOOP NOT SATISFIED   COMPUTA
     1TION CONTINUES ***//)
1200  CONTINUE
      RETURN
      END
      SUBROUTINE DIST(VIN,VOUT,DS,X,VSUC,VPRES,DUSUC,DUPRES,EXTRM,
     1VRATIO)
      REACT=1.-(VIN/VOUT)**2
      REAC=1.-VIN/VOUT
      G=X-0.5
      ALMAX=0.5+EXTRM*REACT
      VMAX=VOUT/(1.-DS)
      IF(DS.LT.0.0) GO TO 100
      VCL=VOUT*((REAC/2.)*(SIN(3.14159*G)-1.)+1.)
      IF(X.GT.ALMAX)GO TO 10
      VSUC=(VIN-VMAX)*((X/ALMAX)**2)-2.*(VIN-VMAX)*(X/ALMAX)+VIN
      DUSUC=2.*X/(ALMAX**2)*(VIN-VMAX)-2.*(VIN-VMAX)/ALMAX
      GO TO 20
   10 VSUC=VOUT+(VOUT-VMAX)/((ALMAX-1.)**2)*(X**2-2.*ALMAX*(X-1.)-1.)
      DUSUC=(VOUT-VMAX)/((ALMAX-1.)**2)*(2.*X-2.*ALMAX)
   20 VPRES=VCL-VRATIO*(VSUC-VCL)
      DUPRES=3.14159*VOUT*(VRATIO+1.)/2.*REAC*COS(3.14159*G)-VRATIO*
     1DUSUC
      GO TO 40
  100 VCL=(VOUT-VIN)*X+VIN
      A1=(VMAX-VOUT)/(ALMAX*(ALMAX-1.))-(VOUT-VIN)/ALMAX
      A2=(VOUT-VIN)*(ALMAX+1.)/ALMAX-(VMAX-VOUT)/(ALMAX*(ALMAX-1.))
      VSUC=A1*X*X+A2*X+VIN
      DUSUC=2.*A1*X+A2
      VPRES=2.*VCL-VSUC
      DUPRES=2.*(VOUT-VIN)-DUSUC
   40 RETURN
      END
      SUBROUTINE DRANGE(G,VIN,VOUT,EXTRM,DSTART,DCHNGE)
      REACT=1.-(VIN/VOUT)**2
      XMAX=0.5+EXTRM*REACT
      VMIN=(VOUT-VIN)*XMAX+VIN+0.01
      VMAX=SQRT((G+1.)/(G-1.))-0.01
      D1=1.-VOUT/VMAX
      D2=1.-VOUT/VMIN
      DCHNGE=ABS((D1-D2)/10.)
      DSTART=(ABS(D1-D2))*0.3+D2
      RETURN
      END
      FUNCTION VELIT(W,T,G1,G2,ALP,AREA ,P,RHO,ACR)
      DIMENSION ALS(2),ARS(2),DIF1(2),DIF2(2)
      CONST=W*SQRT(T/518.7)/(COS(ALP)*AREA/144.*(P/14.696)*RHO*ACR)
      A=0.1
      S=0.5
      DEL=0.1
      K=0
20    ALS(1)=S
```

```
      K=K+1
      IF(K.GE.100) GO TO 1400
      ARS(1)=CONST/((1.-G1*(S**2.))**G2)
      ALS(2)=S+DEL
      ARS(2)=CONST/((1.-G1*((S+DEL)**2.))**G2)
      DIF1(1)=ABS(ALS(1)-ARS(1))
      DIF1(2)=ABS(ALS(2)-ARS(2))
      DIF2(1)=ALS(1)-ARS(1)
      DIF2(2)=ALS(2)-ARS(2)
      IF(DIF1(1).LE.0.001) GO TO 1000
      IF(DIF1(2).LE.0.001) GO TO 1001
      G=DIF2(1)*DIF2(2)
      IF(G.LT.0.0) GO TO 200
      IF(DIF1(2).GT.DIF1(1)) GO TO 100
      S=S+A*1.0
      GO TO 20
200   DEL=DEL/2.
      A=A/2.
      GO TO 20
100   DEL=-DEL
      A=-A
      GO TO 20
1000  VELIT=ALS(1)
      GO TO 1200
1001  VELIT=ALS(2)
      GO TO 1200
1400  VELIT=ALS(1)
      WRITE(6,1100)
1100  FORMAT(///81H*** BLADE EXIT VELOCITY ITERATION LOOP NOT SATISFIED
     1   COMPUTATION CONTINUES ***///)
1200  CONTINUE
      RETURN
      END
      SUBROUTINE VNEG(VIN,VOUT,EXTRM,DS,RATIO)
      DIMENSION ALS(2),ARS(2),DIF1(2),DIF2(2)
      IF(DS.LT.0.0) GO TO 1500
      REACT=1.-(VIN/VOUT)**2
      REAC=1.-VIN/VOUT
      ALMAX=0.5+EXTRM*REACT
      VMAX=VOUT/(1.-DS)
      CONST=3.14159*(ALMAX**2)*VOUT*REAC/(2.*(VIN-VMAX))
      A=0.1
      S=0.001
      DEL=0.1
      K=0
   20 ALS(1)=S
      K=K+1
      IF(K.GE.100) GO TO 1400
      ARS(1)=CONST*COS(3.14159*(S-0.5))+ALMAX
      ALS(2)=S+DEL
      ARS(2)=CONST*COS(3.14159*(S+DEL-0.5))+ALMAX
      DIF1(1)=ABS(ALS(1)-ARS(1))
      DIF1(2)=ABS(ALS(2)-ARS(2))
      DIF2(1)=ALS(1)-ARS(1)
      DIF2(2)=ALS(2)-ARS(2)
      IF(DIF1(1).LE.0.001) GO TO 1000
      IF(DIF1(2).LE.0.001) GO TO 1001
      G=DIF2(1)*DIF2(2)
      IF(G.LT.0.0) GO TO 200
      IF(DIF1(2).GT.DIF1(1)) GO TO 100
      S=S+A*1.0
      GO TO 20
200   DEL=DEL/2.
      A=A/2.
      GO TO 20
100   DEL=-DEL
```

```
      A=-A
      GO TO 20
 1000 XMIN=ALS(1)
      GO TO 1200
 1001 XMIN=ALS(2)
      GO TO 1200
 1400 XMIN=ALS(1)
      WRITE(6,1100)
 1100 FORMAT(///91H*** BLADE PRESSURE SURFACE LOADING ITERATION LOOP NOT
     1 SATISFIED   COMPUTATION CONTINUES ***///)
 1200 VCL=VOUT*((REAC/2.)*(SIN(3.14159*(XMIN-0.5))-1.)+1.)
      VSUC=(VIN-VMAX)*((XMIN/ALMAX)**2)-2.*(VIN-VMAX)*(XMIN/ALMAX)+VIN
      VPRES=2.*VCL-VSUC
      IF(VPRES.GT.0.0) GO TO 1500
      RATIO=(VCL-0.01)/(VCL-VPRES)
      GO TO 1600
 1500 RATIO=1.0
 1600 RETURN
      END
      SUBROUTINE ALIFE(BS,TEM,TIME)
      DIMENSION S(13),X(13)
C     DATA IS FOR IN-100 MATERIAL
      DATA S/10600.,13500.,17000.,21700.,27000.,32500.,38500.,45000.
     151500.,58500.,66000.,74000.,84000./
      DATA X/52.,51.,50.,49.,48.,47.,46.,45.,44.,43.,42.,41.,40./
      IF(BS.LE.10600.) GO TO 10
      IF(BS.GE.84000.) GO TO 20
      K=1
      KK=2
40    IF(BS.GE.S(K).AND.BS.LE.S(KK)) GO TO 30
      K=K+1
      KK=KK+1
      GO TO 40
10    PARAM=(52.-51.)/(10600.-13500.)*(BS-13500.)+51.
      GO TO 50
20    PARAM=(40.-41.)/(84000.-74000.)*(BS-74000.)+41.
      GO TO 50
30    PARAM=(X(KK)-X(K))/(S(KK)-S(K))*(BS-S(K))+X(K)
50    G=1000.*PARAM/TEM
      IF(G.GE.30.) TIME=10.E10
      IF(G.LT.30.) TIME=10.**(G-20.)
      RETURN
      END
      FUNCTION SIMP2 (F,A,DELX,N)
C     INTEGRATION OF TABULAR FUNCTION,F, BY SIMPSON'S RULE, WHERE
C           U
C     A=LOWER LIMIT, DELX=LENGTH OF SUBINTERVAL, N=NUMBER OF SUBINTERVAL
C     IF N IS LESS THAN 2, SIMP2 IS SET TO 0
C     N MAY BE ODD OR EVEN
      DIMENSION F(51)
23    IF(N-2) 14,17,17
14    SIMP2=0.0
      RETURN
17    IF((N/2)*2-N) 11,12,14
12    K=N/2
      ASSIGN 19 TO M
      GO TO 13
11    K=(N-1)/2
      ASSIGN 18 TO M
13    SUMA=0.0
      DO 15 J=1,K
15    SUMA=SUMA+F(2*J)
      SUMB=0.0
22    IF(K-1) 14,20,21
21    DO 16 J=2,K
16    SUMB=SUMB+F(2*J-1)
```

```
20    SIMP2=(1.3333333*SUMA+.66666667*SUMB+.33333333*F(2*K+1)+.33333333*
     1F(1))*DELX
      GO TO M,(19,18)
18    SIMP2=SIMP2+DELX*(.41666667*F(2*K+2)+.66666667*F(2*K+1)
     1-.08333333*F(2*K))
19    RETURN
      END
      SUBROUTINE VISCO(T,V)
      C1=1.264E-5
      C2=0.600
      TREF=492.
      V=C1*((T/TREF)**C2)
      RETURN
      END
      SUBROUTINE HM(AJ,FORM)
      P=1./7.
      TOPSUM=0.0
      BOTSUM=0.0
      DO 10 J=1,10
      G=J-1
      TOPSUM=TOPSUM+(((2.*G+1.)*(AJ**G))/((2.*G+1.)*P+1.))
      BOTSUM=BOTSUM+((AJ**G)/(((2.*G+1.)*P+1.)*(2.*(G+1.)*P+1.)))
10    CONTINUE
      FORM=TOPSUM/BOTSUM
      RETURN
      END
      SUBROUTINE SDISK(RH,RT,CX,RHOD,RHOB,RHOA,S,SOL,A,STRESD,STRESB)
      RH=RH/12.
      RT=RT/12.
      CX=CX/12.
      A=A/144.
      STRESB=(2.51E-7)*RHOB*A*(S**2)
      STRESB=1.2*STRESB
      DELRA=0.5*CX
      BO=0.75*CX
      PHI=0.1745
      RM=(RH+RT)/2.
      Z=2.*3.14159*RM*SOL/CX
      RD=RH-DELRA
      BI=BO+2.*RD*TAN(PHI)
      SIG1=(3.942E-7)*RHOD*((S*RD)**2)*(BI/BO+3.)/(BI/BO+1.)
      TBAR=0.1*CX
      ABLD=TBAR*CX
      FB=STRESB/1.2*ABLD*144.
      RCG=RD+DELRA*(BO+2.*CX)/(3.*(BO+CX))
      VA=3.14159*RCG*(CX+BO)*DELRA
      FA=RHOA/(Z*32.174)*((2.*3.14159*S/60.)**2)*VA*RCG
      FT=FA+FB
      SIG2=Z*FT/(3.14159*RD*BO*(BI/BO+1.))
      SIG2=SIG2/144.
      STRESD=SIG1+SIG2
      RH=RH*12.
      RT=RT*12.
      CX=CX*12.
      A=A*144.
      RETURN
      END
      SUBROUTINE BLOCK(G,T,Z,BETAI,VI,BETAO,VO)
      DIMENSION DIF1(2),DIF2(2),ANGLE(2),VCR1(2),SS(2)
      G1=G-1.
      G2=G+1.
      RAD=3.14159/180.
      TARGT=BETAI
      A=RAD
      S=BETAI-5.*RAD
      DEL=RAD
```

```
      K=0
   20 DO 15 I=1,2
      SS(I)=S
      VACR1=ABS(VI/SIN(S))
      VCR1(I)=VACR1
      AFS1=G1/G2*(VACR1**2)
      VXCR1=VACR1*COS(S)
         =T/(Z*COS(S))
      C=((1.-AFS1 *(G2/(2.*G))+(1.-TET)*(VXCR1**2))/((1.-TET)*VXCR1)
      D=VI
      E=G*C/G2
      VXCR2=E-SQRT(E**2-1.+G1/G2*(D**2))
      ANGLE(I)=ATAN(D/VXCR2)
      VCR2=SQRT(VXCR2**2+D**2)
      IF(I.EQ.1) S=S+DEL
   15 CONTINUE
      K=K+1
      IF(K.GE.100) GOTO 1500
      DIF1(1)=ABS(ANGLE(1)-TARGT)
      DIF1(2)=ABS(ANGLE(2)-TARGT)
      DIF2(1)=ANGLE(1)-TARGT
      DIF2(2)=ANGLE(2)-TARGT
      IF(DIF1(1).LE.0.00001) GO TO 1000
      IF(DIF1(2).LE.0.00001) GO TO 1001
      Q=DIF2(1)*DIF2(2)
      IF(Q.LT.0.0) GOTO 200
      IF(DIF1(2).GT.DIF1(1)) GOTO 100
      GO TO 20
  200 S=S-DEL
      DEL=DEL/2.
      GO TO 20
  100 DEL=-DEL
      S=S+DEL
      GO TO 20
 1000 BETAO=SS(1)
      VO=VCR1(1)
      GO TO 1600
 1001 BETAO=SS(2)
      VO=VCR1(2)
      GOTO 1600
 1500 BETAO=SS(1)
      VO=VCR1(1)
      WRITE(6,1700)
 1700 FORMAT(///10X,47H*** BLOCKAGE CALCULATION FAILED TO CONVERGE ***)
 1600 RETURN
      END
      FUNCTION FIT(ZK)
      DIMENSION AK(34),ALAM(34)
      DATA ALAM/12.,11.,10.,9.,8.,7.8,7.6,7.4,7.2,7.052,7.,6.8,6.6,6.4,
     16.2,6.,5.,4.,3.,2.,1.,0.,-1.,-2.,-3.,-4.,-5.,-6.,-7.,-8.,-9.,-10.,
     2-11.,-12./
      DATA AK/0.0948,0.0941,0.0919,0.0882,0.0831,0.0819,0.0807,0.0794,
     10.0781,0.0770,0.0767,0.0752,0.0737,0.0721,0.0706,0.0689,0.0599,
     20.0497,0.0385,0.0264,0.0135,0.,-0.0140,-0.0284,-0.0429,-0.0575,
     3-0.0720,-0.0862,-0.0999,-0.1130,-0.1254,-0.1369,-0.1474,-0.1567/
      IF(ZK.GE.0.0948) GO TO 10
      IF(ZK.LE.-0.1567) GO TO 20
      K=1
      KK=2
40    IF(ZK.LE.AK(K).AND.ZK.GE.AK(KK)) GO TO 30
      K=K+1
      KK=KK+1
      GO TO 40
10    FIT=12.
      GO TO 50
20    FIT=-12.
```

```
      GO TO 50
30    FIT=(ALAM(KK)-ALAM(K))/(AK(KK)-AK(K))*(ZR-AK(K))+ALAM(K)
50    CONTINUE
      RETURN
      END
      FUNCTION RECRIT(ZL)
      DIMENSION RE(8),X(8)
      DATA X/8.,6.,4.,2.,0.,-2.,-4.,-6./
      DATA RE/11500.,9600.,5600.,2000.,645.,250.,140.,100./
      IF(ZL.GE.8.0) GO TO 10
      IF(ZL.LE.-6.0) GO TO 20
      K=1
      KK=2
40    IF(ZL.LE.X(K).AND.ZL.GE.X(KK)) GO TO 30
      K=K+1
      KK=KK+1
      GO TO 40
10    RECRIT=11500.
      GO TO 50
20    RECRIT=100./6.*ZL+200.
      GO TO 50
30    RECRIT=(RE(KK)-RE(K))/(X(KK)-X(K))*(ZL-X(K))+RE(K)
50    CONTINUE
      RETURN
      END
      SUBROUTINE AFLOW(W,T,P,VX,RHOSTD,ACRSTD,VUH,GAMMA,RH,WCAL,RT)
      DIMENSION R(51),FS(51)
      VMAX=SQRT(VX**2+VUH**2)
      AMAX=W*SQRT(T/518.7)/(P/14.696)/(RHOSTD*ACRSTD)/RHOV(GAMMA,VMAX)
     1*VMAX/VX
      RTMAX=SQRT(AMAX/3.14159+RH**2)
      DELR=(RTMAX-RH)/50.
      KOUNT=1
      RO=RH
      WO=0.0
      CONST=2.*3.14159*VX*RHOSTD*ACRSTD*(P/14.696)/SQRT(T/518.7)
230   DO 100 I=1,51
      AI=I-1
      R(I)=RO+AI*DELR
      V=SQRT(VX**2+(VUH*RH/R(I))**2)
      FS(I)=((1.-(GAMMA-1.)/(GAMMA+1.)*(V**2))**(1./(GAMMA-1.)))*R(I)
100   CONTINUE
      DO 200 J=1,50
      IF(J.GT.1) GO TO 125
      WCAL=CONST*(FS(1)+FS(2))*DELR/2.+WO
      GO TO 150
125   WCAL=CONST*SIMP2(FS,0.0,DELR,J)+WO
150   IF(ABS(W-WCAL).LT.0.001) GO TO 220
      IF(WCAL.LT.W) GO TO 200
      JJ=J-1
      WO=CONST*SIMP2(FS,0.0,DELR,JJ)+WO
      IF(JJ.EQ.1)WO=CONST*(FS(1)+FS(2))*DELR/2.+WO
      DELR=(R(J+1)-R(J))/50.
      RO=R(J)
      KOUNT=KOUNT+1
      IF(KOUNT.GE.5) GO TO 260
      GO TO 230
200   CONTINUE
260   WRITE(6,300)WCAL,W
300   FORMAT(//5X,82H *** WARNING ***    MASS FLOW ITERATION LOOP DID NOT
     1 CONVERGE ... CALCULATED FLOW =,F8.4,3X,13HACTUAL FLOW =,F8.4/)
220   RT=R(J+1)
      RETURN
      END
      FUNCTION RHOV(G,V)
      RHOV=((1.-((G-1.)/(G+1.))*(V**2))**(1./(G-1.)))*V
```

```
      RETURN
      END
      SUBROUTINE SMALST(ARRAY,LIMIT,MIN)
      DIMENSION ARRAY(200)
      SMALL=ARRAY(1)
      MIN=1
      DO 10 I=2,LIMIT
      IF(ARRAY(I).GT.SMALL)GO TO 10
      SMALL=ARRAY(I)
      MIN=I
 10   CONTINUE
      RETURN
      END
      FUNCTION ANGIT(W,T,G1,G2,VU,AREA ,P,RHO,ACR,NBLD)
      DIMENSION ALS(2),ARS(2),DIF1(2),DIF2(2)
      CONST=W*SQRT(T/518.7)/(VU*AREA/144.*(P/14.696)*RHO*ACR)
      A=0.0871553
      S=0.7853976
      ALPMIN=ASIN(VU)
      DEL=0.0871553
      IF(NBLD.EQ.1) DEL=(S-ALPMIN)/10.
      IF(NBLD.EQ.1) A=(S-ALPMIN)/10.
      K=0
 20   ALS(1)=COS(S)/SIN(S)
      K=K+1
      IF(K.GE.100) GO TO 1400
      ARS(1)=CONST/((1.-G1*((VU/SIN(S))**2))**G2)
      ALS(2)=COS(S+DEL)/SIN(S+DEL)
      ARS(2)=CONST/((1.-G1*((VU/SIN(S+DEL))**2))**G2)
      DIF1(1)=ABS(ALS(1)-ARS(1))
      DIF1(2)=ABS(ALS(2)-ARS(2))
      DIF2(1)=ALS(1)-ARS(1)
      DIF2(2)=ALS(2)-ARS(2)
      IF(DIF1(1).LE.0.002) GO TO 1000
      IF(DIF1(2).LE.0.002) GO TO 1001
      Q=DIF2(1)*DIF2(2)
      IF(Q.LT.0.0) GO TO 200
      IF(DIF1(2).GT.DIF1(1)) GO TO 100
      S=S+A*1.0
      GO TO 20
 200  DEL=DEL/2.
      A=A/2.
      GO TO 20
 100  DEL=-DEL
      A=-A
      GO TO 20
 1000 BNGIT=ALS(1)
      ANGIT=ATAN(1./BNGIT)
      GO TO 1200
 1001 BNGIT=ALS(2)
      ANGIT=ATAN(1./BNGIT)
      GO TO 1200
 1400 BNGIT=ALS(1)
      ANGIT=ATAN(1./BNGIT)
      WRITE(6,1500)
 1500 FORMAT(///15X,77H*** BLADE EXIT ANGLE ITERATION LOOP NOT SATISFIED
     1   COMPUTATION CONTINUES ***///)
 1200 CONTINUE
      RETURN
      END
      FUNCTION ACRIT(G,R,T)
      ACRIT=SQRT(2.0*G/(G+1.)*32.174*R*T)
      RETURN
      END
      SUBROUTINE FDISK(GAMMA,VEXIT,GAMM1,GAMM2,GAMM3,NPASS,KPASS,RGAS,
     1SPEED,P1P,T1P,RWORK,WFLOW,ALP1,RM1,RM2,RM3,H1,H2,H3,T2P,U2,UACR2,
```

```
     2U3,V1,VU1,ETA,P2P,T3P,P3P,PRTURB,ALP2,V2,VU2,VWRK2,VWRK3,UACR3,
     3VU3,TPTP2,T2PP,PDPP2,T32PP,T3PP,WU2,WUPP2,BETA2,WPP2,WU3,WUPP3,V3,
     4ALP3,VX3,WXPP3,WPP3,BETA3,P32PP,PLOS1,PLOS2,RH3,RT3,RTS,ACR1,ADP3,
     5H1A,H2A,H3A,VX2,WFACTM,WFACTH,UT3,STGACC,RBEST,T2PPH,ACR3)
      PASS=KPASS
      T2P=T1P
      TSTD=518.7
      ASTD=ACRIT(GAMMA,RGAS,TSTD)
      RHSTD=2116.22/(RGAS*TSTD)
      CP=(1./GAMM2)*RGAS/778.26
      ACR1=ACRIT(GAMMA,RGAS,T1P)
      T3P=T1P-RWORK/CP
      ACR3=ACRIT(GAMMA,RGAS,T3P)
      UMAX=ACR3
      VX3=VEXIT
      CON=25039.737*RWORK
      VX3D=VX3*ACR3
      V3=VX3/COS(ALP3)
      VU3=VX3*TAN(ALP3)
      VWRK3=VU3*ACR3
      IF(KPASS.GT.0) GO TO 10
      IF(RBEST.EQ.0.0) CALL RCHOKE(VWRK3,VX3D,GAMMA,RGAS,T1P,CON,UCHOKE)
      IF(UCHOKE.LT.ACR3) UMAX=UCHOKE
      IF(ALP1.LT.0.349) GO TO 100
      IF(ALP1.EQ.ALP3) GO TO 100
      IF(ALP3.GT.0.0) GO TO 100
      UFLAT=CON/(VX3D*(TAN(ALP1+0.140)-TAN(ALP3)))
      IF(UFLAT.LT.UMAX) UMAX=UFLAT
100   IF(RBEST.EQ.0.0)GO TO 20
      RM3=RBEST
      U3=RM3*3.14159*SPEED/30.
      GO TO 15
20    UMIN=(VWRK3+SQRT(VWRK3**2+2.*CON))/2.+10.
30    RMIN=UMIN/(3.14159*SPEED/30.)
      DEL=(UMAX-UMIN)/20.
      U3=UMIN
      RM3=RMIN
      GO TO 15
10    U3=UMIN+PASS*DEL
      RM3=U3/(3.14159*SPEED/30.)
15    SWPM=(U3**2)/(25036.62*RWORK)
      WFACTM=1./SWPM
      IF(ALP3.EQ.0.0) STGACC=1.-WFACTM/2.
      IF(NPASS.EQ.1)ETA=(0.92*SWPM)/(SWPM+0.0227)
      IF(NPASS.EQ.1)P2P=0.98*P1P
      P3P=P1P*((1.-(1.-T3P/T1P)/ETA)**(1./GAMM2))
      PRTURB=P1P/P3P
      UACR3=U3/ACR3
      AREA3=WFLOW*SQRT(T3P/TSTD)/(P3P/14.696)/(RHSTD*ASTD)/(RHOV(GAMMA,
     1V3)*COS(ALP3))
      H3=AREA3/(2.*3.14159*RM3)
      H3A=H3
      RH3=RM3-H3/2.
      IF(RBEST.GT.0.0) GO TO 25
      IF(KPASS.GT.0) GO TO 25
      IF(RH3.GE.0.083) GO TO 25
      UMIN=UMIN+10.
      GO TO 30
25    RT3=RH3+H3
      VWRK2=239111.88*RWORK/(SPEED*RM3)+VWRK3
      VU2=VWRK2/ACR1
      VX2D=VX3D
      VX2=VX2D/ACR1
      V2=SQRT(VU2**2+VX2**2)
      ALP2=ATAN(VU2/VX2)
      U2=U3
```

```
      UACR2=U2/ACR1
      RM2=RM3
      RH2=RH3
      WFACTH=WFACTM*((RM3/RH3)**2)
      UT3=U3*RT3/RM3
      VUH2=RM2*VU2/RH2
      CALL AFLOW(WFLOW,T2P,P2P,VX2,RHSTD,ASTD,VUH2,GAMMA,RH2,WCAL,RT2)
      H2A=RT2-RH2
      H2=WFLOW*SGRT(T1P/TSTD)/((RHOV(GAMMA,V2)*VX2/V2)*2.*3.14159*RM2*
     1P2P/14.696*RHSTD*ASTD)
      RTS=RT2
      AREA1=3.14159*(RT2**2-RH2**2)*144.
      BLP1=ABS(ALP1)
      V1=VELIT(WFLOW,T1P,GAMM1,GAMM3,BLP1,AREA1,P1P,RHSTD,ASTD)
      VU1=V1*SIN(ALP1)
      H1A=H2A
      RM1=RM2
      H1=WFLOW*SGRT(T1P/TSTD)/((RHOV(GAMMA,V1)*COS(ALP1))*2.*3.14159*
     1RM1*P1P/14.696*RHSTD*ASTD)
      TPTP2=1.-GAMM1*(UACR2**2)*(2.*VU2/UACR2-1.)
      T2PP=TPTP2*T2P
      UACRH2=RH2/RM2*UACR2
      TPTPH2=1.-GAMM1*(UACRH2**2)*(2.*VUH2/UACRH2-1.)
      T2PPH=TPTPH2*T2P
      PDPP2=TPTP2**(1./GAMM2)
      T32PP=1.-GAMM1*(UACR2**2)*(1./TPTP2)*(1.-((RM3/RM2)**2))
      T3PP=T32PP*T2PP
      ADP2=ACRIT(GAMMA,RGAS,T2PP)
      ADP3=ADP2*SGRT(T32PP)
      WU2=VWRK2-U2
      WUPP2=WU2/ADP2
      BETA2=ASIN((VU2-UACR2)/(SGRT(V2**2+UACR2**2-2.*VU2*UACR2)))
      WPP2=WUPP2/SIN(BETA2)
      WU3=VWRK3-U3
      WUPP3=WU3/ADP3
      WXPP3=VX3*ACR3/ADP3
      WPP3=SGRT(WXPP3**2+WUPP3**2)
      W3FPS=WPP3*ADP3
      W2FPS=WPP2*ADP2
      V2FPS=V2*ACR1
      V3FPS=V3*ACR3
      IF(ALP3.NE.0.0) STGACC=(W3FPS**2-W2FPS**2)/(V2FPS**2-V3FPS**2+
     1W3FPS**2-W2FPS**2)
      BETA3=ASIN(WUPP3/WPP3)
      IF(NPASS.EG.1)P32PP=T32PP**(1./GAMM2)
      IF(NPASS.EG.1)PLOS1=0.98
      IF(NPASS.EG.1)PLOS2=P32PP
      RETURN
      END
$
```